Deregulation of Oxidative Phosphorylation System and Energy Homeostasis in Alzheimer's Disease

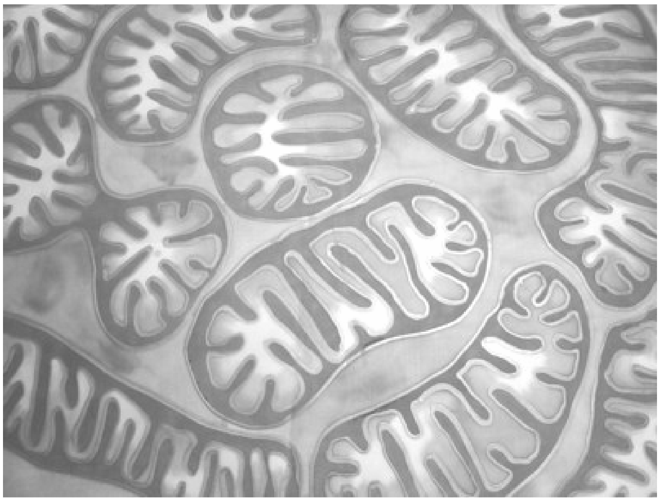

Inauguraldissertation

zur
Erlangung der Würde eines Doktors der Philosophie
vorgelegt der
Philosophisch-Naturwissenschaftlichen Fakultät
der Universität Basel

von

Virginie Rhein

aus Frankreich

Basel, 2009

Genehmigt von der Philosophisch-Naturwissenschaftlichen Fakultät

auf Antrag von	Prof. Dr. Anne Eckert
	Prof. Dr. Heinrich Reichert
	Prof. Dr. Ayikoe Guy Mensah-Nyagan

Basel, den 15. September 2009

Prof. Dr. Eberhard Parlow
Dekan der Philosophisch Naturwissenschaftlichen Fakultät

- TABLE OF CONTENTS -

ACKNOWLEDGEMENTS .... **I**

SUMMARY .... **III**

1. INTRODUCTION **1**

1.1. ALZHEIMER'S DISEASE 1
1.1.1. Clinical symptoms *1*
1.1.2. Neuropathological phenotype *2*
1.1.3. Epidemiology and genetics *3*
1.1.4. Cleavage pathway of APP and Aβ deposits *5*
1.1.5. Phosphorylation of tau and development of neurofibrillary lesions *8*
1.2. MITOCHONDRIA: A MATTER OF LIFE AND DEATH 11
1.2.1. Pivotal role of mitochondria within cells *11*
Mitochondrial structure 11
Mitochondrial respiratory capacity 12
Mitochondrial DNA 13
1.2.2. Mitochondria as sources and targets of reactive oxygen species *15*
1.2.3. Mitochondria-dependent apoptosis *17*
1.3. MITOCHONDRIAL DYSFUNCTION IN ALZHEIMER'S DISEASE 20
1.3.1. Link between Aβ toxicity and mitochondria *21*
1.3.2. Effects of tau protein on mitochondrial function and axonal transport *22*
1.3.3. Aβ and tau share mitochondria as a common target *24*
1.3.4. Transgenic mouse models *25*
1.3.5. Ginkgo biloba extract for the treatment of Alzheimer's disease *28*
1.4. REFERENCES 30

2. AMYLOID-BETA AND TAU SYNERGISTICALLY IMPAIR THE OXIDATIVE PHOSPHORYLATION SYSTEM IN TRIPLE TRANSGENIC ALZHEIMER'S DISEASE MICE **46**

3. AMYLOID-BETA LEADS TO IMPAIRED CELLULAR RESPIRATION, ENERGY PRODUCTION AND MITOCHONDRIAL ELECTRON CHAIN COMPLEX ACTIVITIES IN HUMAN NEUROBLASTOMA CELLS **74**

4. GINKGO BILOBA EXTRACT AMELIORATES OXIDATIVE PHOSPHORYLATION PERFORMANCE AND RESCUES AB-INDUCED FAILURE **92**

5. CONCLUSION **113**

ABBREVIATIONS **118**

CURRICULUM VITAE **121**

PUBLICATIONS **122**

Acknowledgements

This present thesis was performed at the Neurobiology Laboratory for Brain Aging and Mental Health of the Psychiatric University Clinics of Basel (UPK), under the supervision of Prof. Dr. Anne Eckert.

Zunächst möchte ich mich bei meiner Dissertationsleiterin, Frau Prof. Dr. Anne Eckert, dafür bedanken, dass sie mir ermöglicht hat, meine Promotion in ihrem Team durchzuführen, in welchem sie stets wissenschaftliche Exzellenz mit einer angenehmen Arbeitsatmosphäre zu verbinden wusste. Ich bedanke mich bei ihr für ihre guten Ratschläge, für die Zeit, die sie mir gewidmet hat, und dafür, dass sie während meiner Promotion immer ein offenes Ohr für mich hatte. Ich bin ihr sehr dankbar für ihre Großzügigkeit, mir ermöglicht zu haben an zahlreichen internationalen Kongressen teilzunehmen und für die abwechslungsreiche Zusammenarbeit, durch die ich vielfältige neue Kompetenzen erwerben dürfte.

My thanks also go to Prof. Dr. Heinrich Reichert who accepted to be my Faculty responsible and to Prof. Dr. Ayikoe Guy Mensah-Nyagan for making himself available as a co-referee. I would like to express my gratitude to Prof. Dr. Ayikoe Guy Mensah-Nyagan who always believed in my scientific skills and advised me as a PhD student to Prof. Dr. Anne Eckert. I also wish to acknowledge Prof. Dr. Matthias Hamburger for his participation in my dissertation.

I would like to express all my sympathy to Ginette Baysang and Fides Meier who were during these four years my two mainstays at the lab. I will never forget our sojourn in Schröcken. Thanks for these fantastic memories! My warmest thanks go to the “ladies” of the lab, Karen Schmitt, Maria Giese, Lucia Pagani, Kathrin Schulz, Britta Gompper and Doreen Anders. K and M, you made it easier when stress and strain went high! Thanks for being there, for being you! I am also grateful to the UPK Basel (Medical Director: Dr. Franz Müller-Spahn) for generously providing the infrastructure and the facilities.

I am indebted to our collaborators Prof. Jurgen Gotz, Dr. Christian Czech, Dr. Ozmen Laurence, Dr. Stefan Drose, Prof. Eberle and Dr. Lindinger as well as their respective group for their generous support.

I wish to thank all my friends for their understanding about my standard "I can not, sorry, I do not have any time." I have a particular thought to Virginie Haffner and her family, Francisca Meyer, Alexandra Oudot and Florence Clavaguera.

A Mamie pour sa tendresse,

A mes grands-parents toujours dans mon cœur,

A tous les membres de ma famille qui m'ont soutenu,

A mes parents, coachs personnels,
Merci pour votre indéfectible soutien et foi en moi. Cette thèse ce n'est pas la mienne, c'est la nôtre.

Summary

Alzheimer's disease (AD) is the most frequent form of dementia among the elderly affecting dozens of million people worldwide. Post-mortem, the disease is characterized by two main neuropathological hallmarks: extracellular amyloid plaques and intracellular neurofibrillary tangles (NFTs). Amyloid plaques are composed of the amyloid-beta (Aβ) protein, derived from its amyloid precursor protein (APP). NFTs are formed from paired helical filaments composed of hyperphosphorylated tau, a microtubule-associated-protein. Besides these well-characterized features, a growing body of evidence supports mitochondrial dysfunctions as part of the spectrum of chronic oxidative stress occurring in AD. This energy deficit may contribute finally to synaptic abnormality and neuronal degeneration observed in selected brain areas of AD patients. Nevertheless, the specific mechanisms leading to mitochondrial failure as well as the role of Aβ or/and tau within this process are only partly understood.

The purpose of the thesis was therefore to elucidate the role of mitochondria in the pathogenesis of AD. Specifically the thesis was designed to determine **(1)** the synergistic effects of Aβ-tau interplay, **(2)** the impact of soluble Aβ forms and **(3)** effects of *Ginkgo biloba* extract (GBE) on mitochondria in several models of AD.

(1) While many studies reported effects of amyloid plaques on energy metabolism, the role of tau pathology was until recently unknown. In a previous study, our group has been the first to show that tau was also able to induce mitochondrial dysfunction and raise reactive oxygen species (ROS) levels in brains of P301L mutant tau transgenic pR5 mice (pR5). Moreover, we found an increased mitochondrial vulnerability of pR5 cortical cells towards Aβ *in vitro*. Based on these findings, we hypothesized that Aβ and tau might share toxicity at the mitochondrial level. To reveal proof *in vivo*, we investigated the brains of wild-type control mice and three transgenic mouse models. Transgenic pR5 mice express P301L mutant tau found in the frontotemporal dementia with Parkinsonism linked to chromosome 17 (FTDP-17), a dementia related to AD. These mice model the tangle pathology of AD but lack Aβ plaques. Furthermore, they show a hippocampus- and amygdala-dependent behavioural impairment related to AD. APP152 double-transgenic mice co-express the N141I mutant form of PS2 together with the APP^{Swe} mutant found in familial cases of AD (FAD). These mice model the Aβ plaques pathology, but fail to form NFTs. In addition, the mice display age-

related cognitive deficits associated with discrete brain Aβ deposition and inflammation. Finally, we crossed the two strains to generate ^{triple}AD mice. In addition to be a robust model mimicing both plaques and tangles, this new transgenic line presents both amyloidosis and NFTs formation in an age-dependent manner. The progression of biochemical changes and histopathological features in the mice is reminiscent of the course of AD pathogenesis. The mice develop behavioral deficits before detection of protein aggregates correlating with the early mitochondrial dysfunction hypothesis proposed in AD. We applied the optimized quantitative mass-tag labelling proteomic technique, iTRAQ and nanoLC-ESI MS/MS mass spectrometry, followed by sophisticated high-resolution assays for metabolic and energetic functions. We demonstrated massive deregulation of 24 proteins of which one third were mitochondrial proteins mainly related to complexes I and IV of the mitochondrial respiratory system from the four strains of mice. Our functional analysis validated the proteomic approach by confirming the strongest defects of the respiratory capacity mainly at complexes I, IV and V in ^{triple}AD mice. Taken together, we demonstrated for the first time stringent mitochondrial respiratory capacity dysfunction and a failure to restore the energy metabolism in presence of both Aβ and tau.

(2) However, how these lesions and their proteinaceous components impair mitochondrial functions and ultimately lead to neuronal cell loss are unresolved so far. Intriguingly, some recent studies suggest that oligomeric Aβ species may be the main culprit, rather than fibrillar. This idea highlights the critical role of mitochondrial abnormalities in the biochemical pathway by which intracellular Aβ can lead to neuronal dysfunction in AD. To test this experimental paradigm, we examined in a second study the specific effects of soluble Aβ on mitochondrial function under physiological conditions. To this end, human neuroblastoma cells (SH-SY5Y) were stably transfected with cDNAs containing either a vector alone (control cells) or the entire coding region of human wild-type APP (APP695). APP cells led to a significantly increased Aβ secretion compared to control cells and mimiced relevant conditions for AD patients as Aβ levels were within a picomolar range. We established a novel high-resolution respiratory protocol to perform whole cell recording of total cellular respiration and mitochondrial metabolic states. To ripen our analyses, individual activity of mitochondrial respiratory enzymes (complex I to IV) and ATP levels were measured. We concluded that chronic exposure to soluble Aβ results (i) in serious impairment of mitochondrial respiratory machinery due to activity changes of complexes III and IV leading finally to (ii) a drop of ATP synthesis. This energy metabolism deficit may in turn accelerate/lead to cell death commonly observed in AD.

(3) Finally, we resumed the previous work by investigating the potential protective effect of standardized GBE (LI 1370) on Aβ-induced mitochondrial failure. Mainly, the antioxidant properties of GBE have been proposed as dietary strategies for many years in age-related cognitive disorders including AD. We showed for the first time that under physiological conditions GBE improves metabolic energy pathways by increasing the coupling state of mitochondria *per se*, but with specific benefit in APP cells exhibiting Aβ-induced mitochondrial failure. GBE effect on OXPHOS was even preserved in mitochondria after isolation from treated cells. The GBE-induced amelioration of oxygen consumption most likely arose from the modulation and respective normalization of the activity of mitochondrial complexes I, III and IV that are markedly disturbed in APP cells finally yielding a rise in ATP levels. Of note, these functional data were paralleled by an up-regulation of mitochondrial DNA in GBE-treated cells.

In summary, the present thesis took aim to highlight the key role of mitochondria in AD pathogenesis and the close inter-relationship of this organelle with the two main pathological features of the disease. First, we demonstrated main defects of mitochondrial respiratory capacity and the failure to restore energy homeostasis in mice with plaques and tangles. Although, a molecular link between Aβ and tau is still missing, these *in vivo* results consolidate the idea that a synergistic effect of tau and Aβ augments the pathological deterioration of mitochondria in AD by driving a vicious cycle. Secondly, we proved toxicity of soluble Aβ forms, recently defined as the toxic correlate within the Aβ cascade, on the mitochondrial function of vital cells. Finally, the critical role of mitochondria in early pathogenesis of AD may make them into a preferential target for treatment strategies such as antioxidants. Our work confirmed this idea and clearly showed stabilization and restoration of energy metabolism in APP cells treated with GBE. In view of the increasing interest in mitochondrial protection as treatment strategy in dementia, our findings of substantial protection of mitochondria by GBE against Aβ-induced dysfunction deserves further attention.

1. Introduction

1.1. Alzheimer’s disease

In 1907, the German psychiatrist and neuropathologist Alois Alzheimer published a report concerning “an unusual illness of the cerebral cortex”[11-13] that Emil Kraepelin subsequently named after him[14]. He described the case of a 51-year-old woman, Auguste D., who initially developed a delusional disorder followed by a rapid loss of short term memory. Post-mortem examination of her brain, using a silver staining method, revealed a cortical atrophy without evidence for focal degeneration and the presence of two histopathological modifications.

1.1.1. Clinical symptoms

One century later, Alzheimer’s disease (AD) has become the most common age-related neurodegenerative disorder affecting around 27 million people worldwide[15]. As the prototype of cortical dementias, AD develops prominent cognitive defects. The clinical scenario begins by episodic memory deficits with preserved alertness and motor function. The syndrome of mild cognitive impairment (MCI), characterized by a subtle decrease in short-term declarative memory with otherwise normal cognition, is often a harbinger of AD. Over time, gradual erosion of other cognitive abilities appear and lead to profound language, abstraction and orientation impairments[16]. Besides the cognitive deterioration, patients display dramatic neuropsychiatric symptoms as mood disturbances, delusions and hallucinations, personality changes and disorders of behavior (aggressiveness, depression, circadian disturbances)[17]. In contrast with cognitive symptomatology, the non-cognitive defects do not show a progressive course[2]. Patients who usually survive 7 to 10 years (range 2-20 years) after the onset of symptoms[18] typically died from medical complications (bronchitis or pneumonia)[19]. Despite manifest progresses in clinical diagnosis, brain biopsy is still required to confirm AD[20]. Characteristically, severe neuropathological changes occur in selective cognitive domains, particularly those related to memory and emotional behavioral such as the hippocampus, association cortices and subcortical structures including the amygdala and nucleus basalis of Meynert[21].

1.1.2. Neuropathological phenotype

The key neuropathological features of AD are abundant amounts of extracellular plaques composed of the amyloid-beta (Aβ) protein and intracellular neurofibrillary lesions formed of hyperphosphorylated tau, a microtubule-associated protein. Besides these histopathological characteristics described for the first time by Alzheimer that are still considered as the two main pathognomic features of AD, numerous other structural and functional alterations like energy dysfunction, oxidative stress[4, 22] and inflammatory responses[23-26] are associated with AD. The combined consequences of all the pathological changes lead to massive neuronal demise and synapse loss at specific brain regions involved in learning and memory[6] (Figure 1). Neurons that use glutamate or acetylcholine as neurotransmitters appear to be particularly affected, but cells that produce serotonin and norepinephrine are also damaged. At the time of death, the brain of a patient with AD may weigh one-third less than the brain of an age-matched, non-demented individual[27].

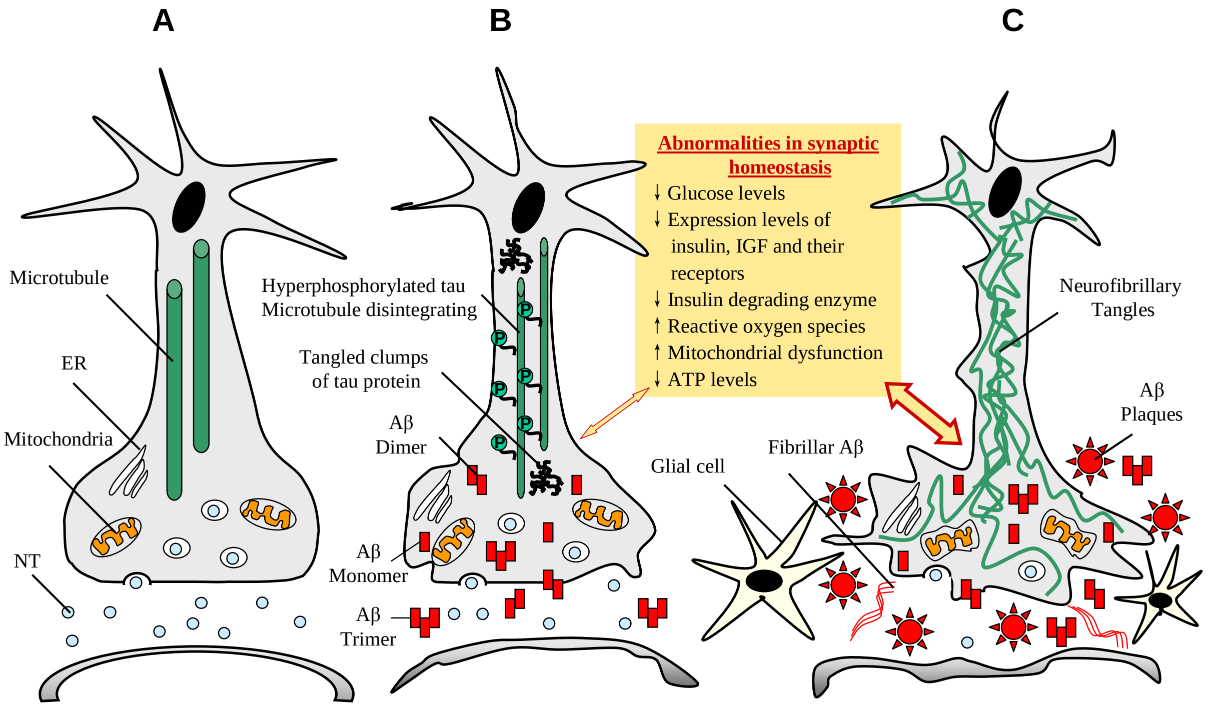
A
B
C
Microtubule
ER
Mitochondria
NT
Hyperphosphorylated tau
Microtubule disintegrating
Tangled clumps
of tau protein
Aβ
Dimer
Aβ
Monomer
Aβ
Trimer
Abnormalities in synaptic homeostasis
↓ Glucose levels
↓ Expression levels of insulin, IGF and their receptors
↓ Insulin degrading enzyme
↑ Reactive oxygen species
↑ Mitochondrial dysfunction
↓ ATP levels
Glial cell
Fibrillar Aβ
Neurofibrillary
Tangles
Aβ
Plaques
P

Figure 1. Histopathological modifications during progression of Alzheimer's disease. (A) Schematic representation of a normal healthy synapse. **(B)** At very early stages of Alzheimer's disease (AD), abnormal hyperphosphorylated tau protein and amyloid-beta peptide (Aβ) oligomers start to disturb the synaptic homeostasis including energy metabolism and molecular pathways (yellow box). **(C)** At late stages of the disease, neurofibrillary tangles and Aβ fibrils / plaques combined with glial changes and inflammation exacerbate these deficits finally leading to synaptic failure and neurodegeneration (from *Rhein et Eckert*, 2007[4]).

1.1.3. Epidemiology and genetics

AD is a devastating neurodegenerative disorder. As proof, the statistics attributable to the disease are vertiginous. AD is the most common cause of dementia comprising 50-70% of all cases[7] and affecting nearly 2% of the population in industrialized countries. Age is the greatest known risk factor for AD with an incidence of 25–50% in people aged 85 or older[28]. The number of patients is expected to increase threefold within the next 50 years[29] as a result of demographic changes and rising life expectancy. In 2050, 50% of people worldwide aged 85 or older may be affected by the disease if no suitable cure is found[30]. Today, AD is the fifth leading cause of death in people aged 65 and older, and most patients eventually need nursing home care.

While the complete etiological picture of AD remains still fragmentary, it is now widely accepted that, in addition to environmental conditions, genes play an essential role in predisposing to an early onset and/or modifying the progress of the disease. Twin studies support the notion that 70–80% of the risk to develop AD is determined by genetic factors[31]. However, genetically, AD is a complex and heterogeneous disease involving mutations and polymorphisms in multiple genes on several chromosomes and showing an age-related dichotomy. AD is therefore classified into two forms: the late sporadic AD (SAD) and the early familial AD (FAD). Importantly, other than the age of onset, the clinical and histopathological features cannot discriminate between the two AD forms.

SAD represents the vast majority of cases whose aging itself is the unique important risk factor known[32]. Until today, only the *apolipoprotein E (APOE*) gene located on chromosome 19q13.2 has been confirmed unanimously as a risk gene[33, 34]. Its ε4 allele increases the susceptibility to SAD whereas its ε2 allele confers protection against the late-onset of AD[35]. However, inheriting the ε4 allele of *APOE* is not sufficient to cause the disease. Numerous genetic factors of only minor to moderate effect are likely to play simultaneous and possibly interdependent roles, making the identification of novel genes gruelling. Nevertheless, the recent development of powerful and sophisticated genotyping approaches, like the high-density genome-wide association, may be promising tools to chararacterize other SAD susceptibility genes. For instance, the overexpression of the *growth factor receptor-bound protein associated binding-protein 2* (*GAB2)* gene, encoding a scaffolding protein involved in multiple signalling pathways, may modify SAD risk in APOE ε4 carriers[36]. Moreover, mutations of the *very low-density lipoprotein receptor* (*VLDL-R*) gene on chromosome 9, the *insulin-degrading enzyme* (*IDE*) gene on chromosome 10 as well as the *α2-macroglobulin* (*A2M*) gene and the *Low-density lipid receptor-related protein* (*LRP*) gene on chromosome 12 are also proposed as potential candidates for SAD genes[37, 38].

Besides cases arising sporadically, epidemiological studies indicate that about 30% of AD patients have a family history of disease in which at least one first-degree relative is affected, but only few of them have a clear autosomal dominant inheritance[39]. In point of fact, FAD which starts before 60 accounts for less than 1% of the total number of AD cases. Since the nineties, more than 20 pathogenic mutations in *amyloid precursor protein* (*APP)* gene[40-43] map to chromosome 21q21.3-21q22.05 have been identified and estimated for up to 5% of FAD (e.g. V717I 'London', K670D/M671L 'Swedish or APP^{Swe}') (Figure 2). Some APP mutations cause also cerebral amyloid angiopathy (CAA) described as amyloid deposits in walls of blood vessels of the central nervous system[44, 45]. CAA is present in over 80% of AD cases. Most FAD cases are caused by mutations in two other genes, *presenelin 1* (*PSEN1*) located on chromosome 14q24.3 and *presenelin 2* (*PSEN2*) on chromosome 1q31-q42[46, 47], of which over 130 have been identified. Remarkably, all of FAD mutations identified in these three genes result in the overproduction of Aβ, further providing evidence that Aβ plays a crucial role in the pathogenesis of the disease. In AD, no mutation has been identified in the gene encoding tau, *MAPT*. However, more than 30 exonic and intronic mutations in *MAPT,* map to chromosome 17q21.1, have been found in a familial dementia related to AD, the frontotemporal dementia with Parkinsonism linked to chromosome 17 (FTDP-17)[48-50]. The majority of these mutations (e.g. G272V, V337M, R406W and P301L) are located in the microtubule binding repeat region or close to it and reduce tau ability to promote microtubule assembly[51] and lead to tau aggregation into NFTs (Figure 2). Gallyas silver impregnation techniques are frequently employed to visualize NFTs in both AD and FTDP-17 brains[52]. Interestingly, in contrast to AD, there are almost no senile plaques in FTDP-17, suggesting that mutant tau is sufficiently potent to induce tau aggregation and does not need any enhancer such as Aβ. Importantly, these findings established that dysfunction of tau in itself can cause neurodegeneration and lead to dementia.

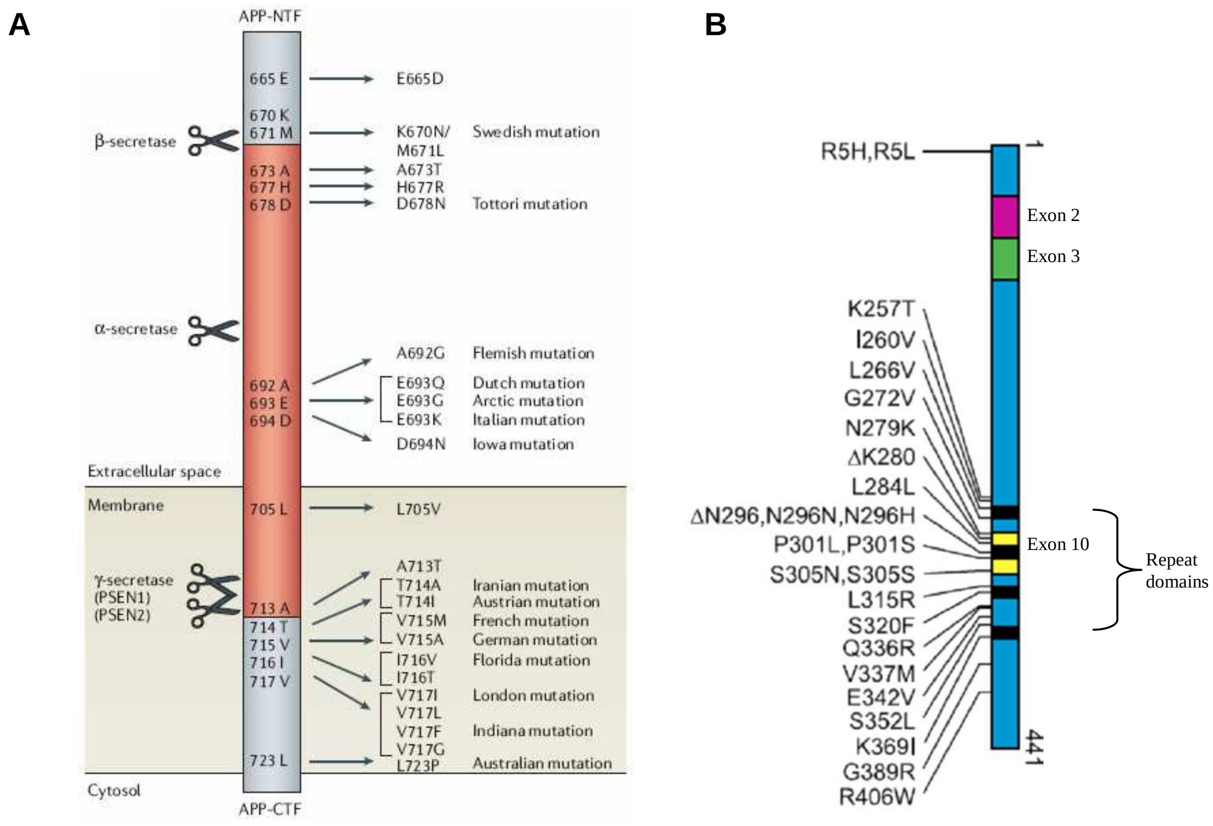
A
B
APP-NTF
665 E
E665D
670 K
671 M
K670N/
M671L
Swedish mutation
β-secretase
673 A
677 H
678 D
A673T
H677R
D678N
Tottori mutation
α-secretase
A692G
Flemish mutation
692 A
693 E
694 D
E693Q
E693G
E693K
Dutch mutation
Arctic mutation
Italian mutation
D694N
Iowa mutation
Extracellular space
Membrane
705 L
L705V
γ-secretase
(PSEN1)
(PSEN2)
713 A
714 T
715 V
716 I
717 V
A713T
T714A
T714I
V715M
V715A
I716V
I716T
V717I
V717L
V717F
V717G
Iranian mutation
Austrian mutation
French mutation
German mutation
Florida mutation
London mutation
Indiana mutation
723 L
L723P
Australian mutation
Cytosol
APP-CTF
R5H,R5L
1
Exon 2
Exon 3
K257T
I260V
L266V
G272V
N279K
ΔK280
L284L
ΔN296,N296N,N296H
P301L,P301S
S305N,S305S
L315R
S320F
Q336R
V337M
E342V
S352L
K369I
G389R
R406W
Exon 10
Repeat
domains
441

Figure 2. *APP* mutations associated with early-onset Alzheimer's disease (FAD) and *tau* mutations in frontotemporal dementia with parkinsonism linked to chromosome 17 (FTDP-17). (A) Most APP mutations are clustered in the close vicinity of secretase-cleavage sites, indicated by scissors, thereby influencing APP processing and are named after the nationality or location of the first family in which that specific mutation was demonstrated. The Aβ sequence is indicated in red (from *Van Dam and De Deyn*, 2006[2]). **(B)** Schematic diagram of the longest tau isoform (441 amino acids) with mutations in the coding region. Twenty missense mutations, two deletion mutations and three silent mutations are shown (adapted from *Goedert and Jakes*, 2005[10]).

1.1.4. Cleavage pathway of APP and Aβ deposits

The first histopathological hallmark, described by Alzheimer as a "peculiar substance" occurs as extracellular deposits. In the mid-1980s, it was discovered that the deposits consist of aggregates of small 40–42 amino acid polypeptide β-amyloid ($A\beta_{40}$ and $A\beta_{42}$) termed Aβ[53, 54]. Aβ deposits can either or not be surrounded by dystrophic neuritis, activated microglia and reactive astrocytes. The first case characterizes neuritic or senile plaques while the second refers to as "diffuse" plaques. Importantly, amyloid plaques do not occur simply in these two extreme forms (diffuse and neuritic) but rather as a continuum associated with varying degrees of surrounding neuritic and glial alterations. In addition, assault of Aβ peptide on endothelial cell walls may form lesions in case of excessive deposits and cause CAA which can present as intracranial haemorrhage[55]. Although, several studies have staged the progression of Aβ deposits in brain of AD patients, these studies findings are still a controversial issue[9, 56-58]. It is widely accepted that the distribution pattern and packing density of Aβ deposits turn out to be of limited significance for differentiation of neuropathological stages. The dispersion of neuritic plaques varied largely not only within architectonic units but also from one individual to another.

APP is a cellular ubiquitous glycoprotein whose amount varied according to the developmental and physiological state of cells. Although incompletely understood, increasing evidence suggests a role of APP in regulating neuronal survival, neurite outgrowth, synaptic plasticity and cell adhesion[59]. Structurally, APP is a single transmembrane receptor like protein, from 695 to 770 amino acids, with a large extracellular glycosylated amino-terminus (Nt), a shorter cytoplasmic carboxy-terminus (Ct) and is partly embedded up to its Aβ fragment in the plasma membrane, the lumenal side of endoplasmic reticulum, Golgi and mitochondrial membranes[60-62] (Figure 3). APP can be cleaved by associated proteases termed α-, β- and γ-secretases. Three enzymes, all belonging to the ADAM family (a disintegrin- and metalloproteinase-family enzyme): ADAM9, ADAM10 and ADAM17 (or tumour necrosis factor converting enzyme)[63] have been identified with α-secretase activity. The activity of β-secretase has been attributed to a single protein, BACE 1[64], whereas γ-secretase activity depends on four components, presenilin, nicastrin, anterior pharynx-defective 1 (APH1) and presenilin enhancer 2 (PEN-2)[65]. In the prevalent non-amyloidogenic pathway, cleavage of APP by α-secretase releases αAPPs and leaves an 83-amino-acid Ct APP fragment (C83). Following cleavage of C83 by γ-secretase produces a short fragment termed p3[66] and the Aβ intracellular cytoplasmic domain (AICD)[6]. Importantly, cleavage by α-secretase occurs within the Aβ region, thereby precluding formation of Aβ[7]. The alternative amyloidogenic processing involves sequential cleavages by BACE 1 and γ-secretase and leads to Aβ and AICD generation[6]. The initial proteolysis is mediated by β-secretase at a position located 99 amino acids from the Ct. This cut results in the release of βAPPs into the extracellular space, and leaves the 99-amino-acid Ct stub (C99) within the membrane, with the newly generated Nt corresponding to the first amino acid of Aβ. Subsequent cleavage of this fragment (between residues 38 and 43) by γ-secretase dictates the length of Aβ peptide (Figure 3). In healthy individuals, most of the full-length Aβ peptide normally produced by brain cells throughout life is $A\beta_{40}$, whereas a small proportion (approximately 10%) is $A\beta_{42}$[53, 54]. In AD, both Aβ variants may form oligomeric aggregates that are thought to represent the “primary toxic correlate” and eventually deposits as plaques.

Aβ_{42} is more hydrophobic[67] and consequently more prone to fibril formation and neurotoxity than the shorter form[68]. Recent evidence even suggests that Aβ_{40} may prevent Aβ_{42} from aggregating and forming plaques[69]. Aβ_{42} is the predominant compound in neuritic plaques[70] which are therefore mainly built of insoluble amyloid fibrils up. On the opposite, diffuse plaques exist mostly in a nonfibrillar form termed “preamyloid”[71, 72].

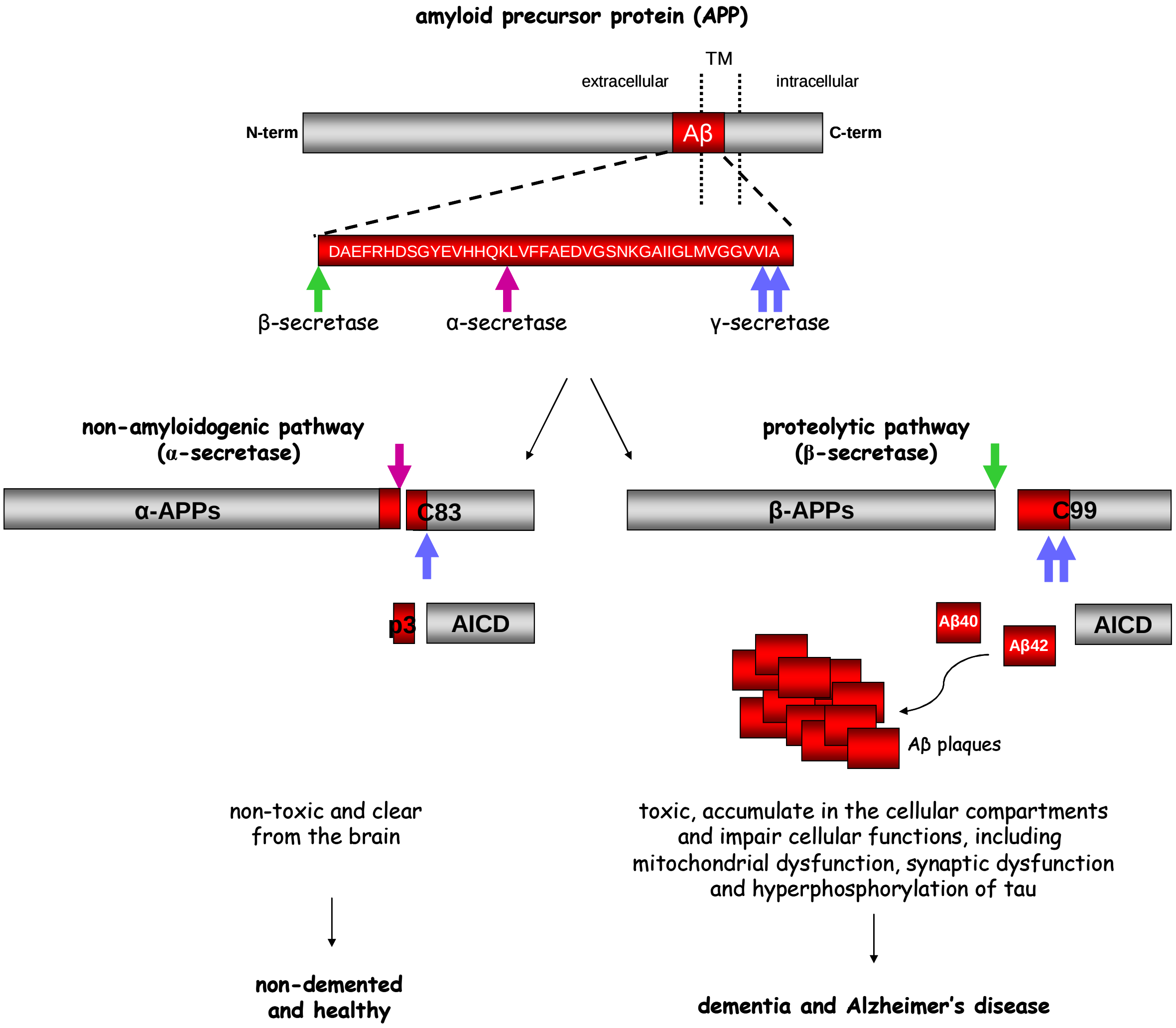
amyloid precursor protein (APP)
TM
extracellular
intracellular
N-term
Aβ
C-term
DAEFRHDSGYEVHHQKLVFFAEDVGSNKGAIIGLMVGGVVIA
β-secretase
α-secretase
γ-secretase
non-amyloidogenic pathway
(α-secretase)
proteolytic pathway
(β-secretase)
α-APPs
C83
β-APPs
C99
p3
AICD
Aβ40
Aβ42
AICD
Aβ plaques
non-toxic and clear
from the brain
toxic, accumulate in the cellular compartments
and impair cellular functions, including
mitochondrial dysfunction, synaptic dysfunction
and hyperphosphorylation of tau
non-demented
and healthy
dementia and Alzheimer's disease

Figure 3. APP and its metabolites. The amyloid-β (Aβ) peptide is derived by proteolytic cleavage from the amyloid precursor protein (APP). The most frequent enzymatic cleavage is mediated by α-secretase (purple arrow), occuring within the Aβ domain, thereby preventing the generation and release of Aβ. Two fragments are released, the larger ectodomain (α-APPs) and the smaller carboxy-terminal fragment (C83). Furthermore, C83 can also undergo an additional cleavage mediated by γ-secretase (blue arrow) to generate p3 and the Aβ intracellular cytoplasmic domain (AICD). APP molecules that are not cleaved by the non-amyloidogenic pathway become a substrate for β-secretase (green arrow) releasing an ectodomain (β-APPs), and retaining the last 99 amino acids of APP (C99) within the membrane. C99 is subsequently cleaved by γ-secretase complex (blue arrows), which predominantly produces A$\beta_{1\text{–}40}$, and the more amyloidogenic A$\beta_{1\text{–}42}$ at a ratio of 10:1, as well as AICD.

1.1.5. Phosphorylation of tau and development of neurofibrillary lesions

Alzheimer observed in the brain of his original patient a second lesion which co-occurs with Aβ plaques. But unlike Aβ deposits, these protein aggregates were present intraneuronally. In the late 1980s, it was discovered that they are composed of abnormally hyperphosphorylated microtubule-associated protein tau[73-75].

Structurally, human tau proteins consist of a heterogeneous mixture of six isoforms ranging from 50 to 70kDa and from 352 to 441 residues[76, 77] (Figure 4A). Tau is very hydrophilic and adopts natively an unfolded conformation with rare α-helices and β-sheets[78-80]. It contains a Nt acidic region, a middle basic and proline-rich region, and a Ct region with three (3R) or four (4R) microtubule binding repeats[81]. The isoforms derived by alternative mRNA splicing[82, 83] from a single gene (16 exons) located on chromosome 17. They differ in the presence of 3R or 4R constituted of 31 or 32 amino acids encoded by the exon 10 (E10), and the presence of one, two or none Nt inserts of 29 amino-acids (N1/N2) encoded by the exon 2 and/or 3 (E2/E3). In general, tau with 4R binds to microtubules more tightly than tau presenting 3R[84-86]. Tau is predominantly located in neuronal axons and if it could be partially enriched in soma, it is in contrast almost totally absent in dendrites[87, 88]. Small amounts of tau are also found in oligodendrocytes and astrocytes[89, 90]. Its main biological function is to promote the assembly and stabilization of the microtubular network[91, 92], essential for normal axonal transport[93]. In addition, tau may be a communication interface between mitochondria[94], cytoskeletal elements[95-97], and plasma membrane[98, 99] and play a role in signal transduction interacting with many phosphatases and kinases[100-103]. Tau is termed a phosphoprotein owing to its large number of potential phosphorylation sites, almost 20% of the molecule[104]. This distinctiveness is due to the high frequency of serine and threonine residues and its open structure affording access to many kinases[105]. Importantly, the majority of phosphorylation sites is clustered in flanking regions of the microtubule binding domain[76]. As a consequence, phosphorylation is a key mechanism that regulates tau's interaction with tubulin and other proteins[106, 107].

Under pathological conditions as in AD, tau exhibits abnormally hyperphosphorylation which means that it is phosphorylated to a higher degree at physiological sites, and at additional "pathological" sites[93] (Figure 4B). The phosphorylation level of tau in AD brains was shown to be three- to four-fold higher than that in normal human brains[108]. Recent data highlighted several kinases in the phosphorylating process like glycogen synthase kinase-3β (GSK-3β), cyclin-dependent kinase 5 (cdk5), extracellular signal-regulated kinase 2 (ERK2), protein kinase A and C, calcium-calmodulin dependent protein kinase II (CaMKII), and mitogen-associated protein affinity-regulating kinases (MARK)[109, 110]. In addition, tau undergoes conformational changes which likely assist in the differential phosphorylation[111]. The phosphorylation especially of microtubule-binding repeat domains[112, 113] combined with conformational changes result in the detachment of tau from microtubules and its aggregation in the form of two cytosolic pro-fibrillar structures[114]: the paired helical filaments (PHFs) and the straight filaments. The presence of additional proteins like microtubule-associated protein 1 and 2 (MAP1, MAP2) and Pin1[99] to the six tau isoforms widely-accepted as main compounds of pro-filaments is still controversial[73, 115]. PHFs are composed of two strands of filaments twisted one around another with a periodicity of 80nm and a width varying from 8 to 20nm[116]. Straight filaments lack this helical periodicity[117]. Although, the structural basis explaining differences between a twisted and a straight filament remains unresolved, some authors propose a role of the β-sheet secondary structure forming motifs at the beginning of R3 and R4 domain[118]. Consequently, tau fibers may consist of protofibrils made up of juxtaposed β-sheets pairs. Ultimately, PHFs as a major variant and straight filaments as a minor variant[119] compose the neurofibrillary lesions in AD. They are revealed by electron microscopy as neurofibrillary tangles (NFTs) in cell bodies and apical dendrites, as neuropil threads in distal dendrites, and associated with some senile plaques in abnormal neurites. Neurons with NFTs degenerate and die, leaving within the neuropil a residual “ghost tangle” and glial cells[24]. If the Aβ plaques colonise rather synchronously predilection specific sites in the brain of AD patients, NFTs develop and spread in a predictable manner across the brain providing the basis for distinguishing six stages of disease progression: the transentorhinal Braak stages I-II represent clinically silent cases, the limbic stages III-IV correspond to incipient AD, and the neocortical stages V-VI are associated to fully developed AD (Figure 4C).

A fascinating question still in debate is the mechanism(s) by which abnormal hyperphosphorylation of tau protein can lead initially to polymerisation into protofibrils (PHFs and straight filaments) and subsequently into the neurofibrillary lesions. Some hypotheses point up the role of other proteins as heparin sulphate and advanced glycosylation end-products[120]. Tau undergoes pathological posttranslational modifications such as truncation[121], glycosylation[122], glycation[123], ubiquitination[124], polyamination[125] and nitration[126] that may modify its conformational properties and consecutively its physiological function and its ability to aggregate.

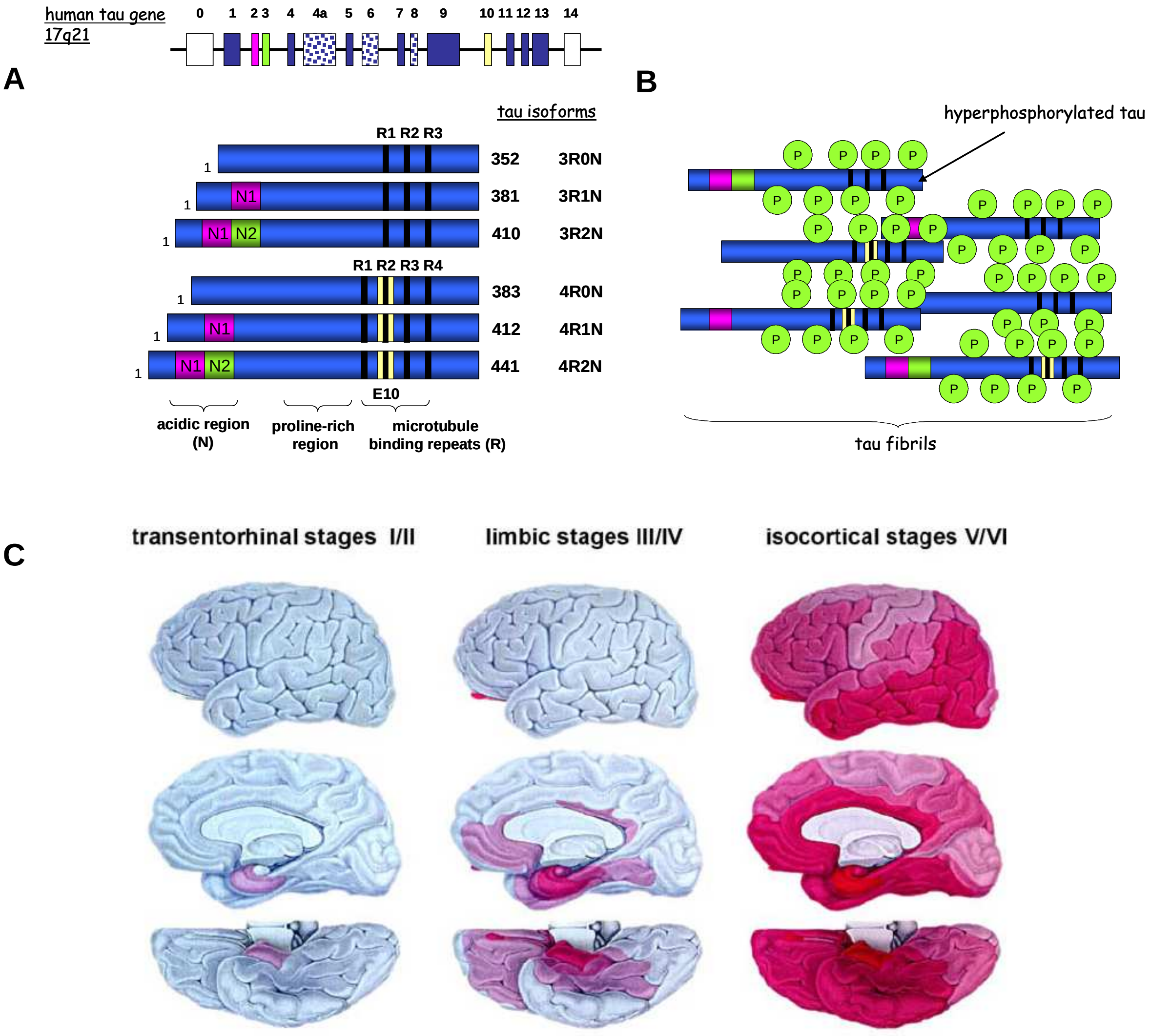
A
human tau gene
17q21
0 1 2 3 4 4a 5 6 7 8 9 10 11 12 13 14
tau isoforms
R1 R2 R3
1
N1
N2
352 3R0N
381 3R1N
410 3R2N
R1 R2 R3 R4
383 4R0N
412 4R1N
441 4R2N
E10
acidic region (N)
proline-rich region
microtubule binding repeats (R)
B
hyperphosphorylated tau
P
tau fibrils
C
transentorhinal stages I/II
limbic stages III/IV
isocortical stages V/VI

Figure 4. From tau gene to spread of neurofibrillary lesions in the brain of AD patients. (A) Schematic representation of the human tau gene and the six tau isoforms expressed in adult human brain. The human tau gene contains 16 exons, including exon 0 (E0), which is part of the promoter. E4a, E6 and E8 (stippled boxes) are not transcribed in the human central nervous system. Alternative mRNA splicing of E2 (pink box), E3 (green box) and E10 (yellow box) produce the six tau isoforms ranging from 352 to 441 amino-acids. They differ in the presence of 1, 2 or none N-terminal inserts (N1, N2) encoded by E2 and E3 and the presence of 3 or 4 microtubule-binding repeat domains (R1 to R4, black bars) (adapted from *Lee et al*, 2001[3]). **(B)** Abnormally hyperphosphorylated tau aggregated into neurofibrillary lesions. **(C)** Neuropathological staging of AD according the development and spread of neurofibrillary lesions across the brain. Stages I/II correspond to clinical silent cases, stages III/IV represent the start of first clinical symptoms, and stages V/VI are associated to severe dementia (from *Braak and Braak*, 1991[9]).

1.2. Mitochondria: a matter of life and death

Mitochondria are essential organelles for cell survival. They are the “powerhouses of cells”, providing energy supply by oxidative reactions from nutritional sources[127]. This energy, stored in the form of ATP, is subsequently used for a large repertoire of functions like intracellular calcium homeostasis[128], cell cycle regulation, thermogenesis and synaptic plasticity[129]. However, as the Pandora’s Box, mitochondria are full of potentially harmful proteins and biochemical reaction centres. They may liberate a flood of toxic compounds such as reactive oxygen species (ROS) and participate to apoptotic signalling pathways[130].

1.2.1. Pivotal role of mitochondria within cells

Mitochondrial structure

Mitochondria are cytoplasmic organelles composed of a double lipid membrane which structures four compartments, distinct by composition and function. The porous outer membrane (OMM) encompasses the whole organelle. It contains cholesterol and many proteins like import complexes[62, 131] and voltage-dependant anion channels (VDAC) responsible for the free passage of low molecular weight substances (up to 5000Da) between the cytoplasm and the intermembrane space (IMS). In contrast to the permeable OMM, the inner membrane (IMM), rich in cardiolipin, provides a highly efficient barrier to the flow of small molecules and ions, including protons. This membrane is invaginated into numerous cristae which increase greatly its surface area. It houses the respiratory enzymes, the cofactor coenzyme Q (ubiquinone Q) and many mitochondrial carriers[132]. All these proteins are necessary for ATP production. Between the two membranes, IMS contains pro-apoptotic proteins like cytochrome c[133], apoptosis-inducing factor (AIF)[134], Smac/Diablo, Endo G and Htra2/Omi[135]. Finally, it is in the matrix, bordered by IMM, which take place different metabolic pathways including the tricarboxylic acid (TCA) cycle, also known as the Kreb's cycle and the beta-oxidation[130, 136]. The mitochondrial genome responsible for the limited genetic autonomy of mitochondria is also located in the matrix.

Mitochondrial respiratory capacity

Although mitochondria are sites of many biosynthetic and metabolic processes, ATP production is paramount. They generate more than 90% of our cellular energy by two closely coordinated metabolic processes: TCA and the oxidative phosphorylation system (OXPHOS).

TCA, composed of 8 enzymatic steps, is able to convert carbohydrates and free fatty acids into ATP. However, its major role consists to yield electrons in the form of reduced hydrogen carriers, the nicotine adenine dinucleotide (NADH) and the flavin adenine dinucleotide ($FADH_2$). These 2 compounds, also produced in the cytosol and shuttled into mitochondria, enter subsequently as coenzymes into OXPHOS also called the mitochondrial respiratory machinery[137] (Figure 5A).

OXPHOS is made up of the electron transport chain (ETC) formed of more than 85 proteins and assembled in four enzymes (complex I to IV) as well as the F1F0-ATP synthase corresponding to the last complex (complex V). Complex I (NADH:ubiquinone oxidoreductase), complex III (ubiquinone:cytochrome c oxidoreductase) and complex IV (cytochrome c oxidase or COX)[138] are located in IMM as integral proteins whereas complex II (succinate dehydrogenase) which catalyses one of the TCA steps is attached to the inner surface of IMM. These five enzymes are connected functionally by mobile electrons acceptors and donors: ubiquinone and cytochrome c. In addition to flavins and nicotinamides, they utilize cytochromes, iron-sulfur clusters and copper centres to transfer electrons in a series of oxidation reduction steps (Figure 5A). Briefly, electrons from NADH and $FADH_2$ feed into complex I and II respectively. Ubiquinone Q carries electrons from both complexes to complex III and cytochrome c transports ultimately electrons from complex III to IV reducing the molecular oxygen (O_2) to water[139, 140]. As electrons are transferred along ETC, a fixed number of protons are pumped from the mitochondrial matrix into IMS, which establishes a proton electrochemical gradient (the proton motive force, Δ_P) across IMM[141]. Two components define Δ_P: a difference in the concentration of protons (ΔpH, alkaline inside) and a difference in the electrical potential (negative inside: $\Delta\psi$: −150 to −180 mV). The redox energy drives the synthesis of ATP from ADP and inorganic phosphate (Pi) by ATP synthase as protons are transported back from IMS into the mitochondrial matrix[138, 140, 142, 143]. ATP is then made available to the cell for various processes requiring energy. However, the consumption of NADH and $FADH_2$ and the pumping out of protons from the mitochondrial matrix on one hand are not perfectly coupled with proton re-entry and ATP synthesis on the other hand. The result is a proton leak mediated in part by specific inner membrane proteins, the uncoupling proteins (UCPs)[144-146] and dissipated as heat[147].

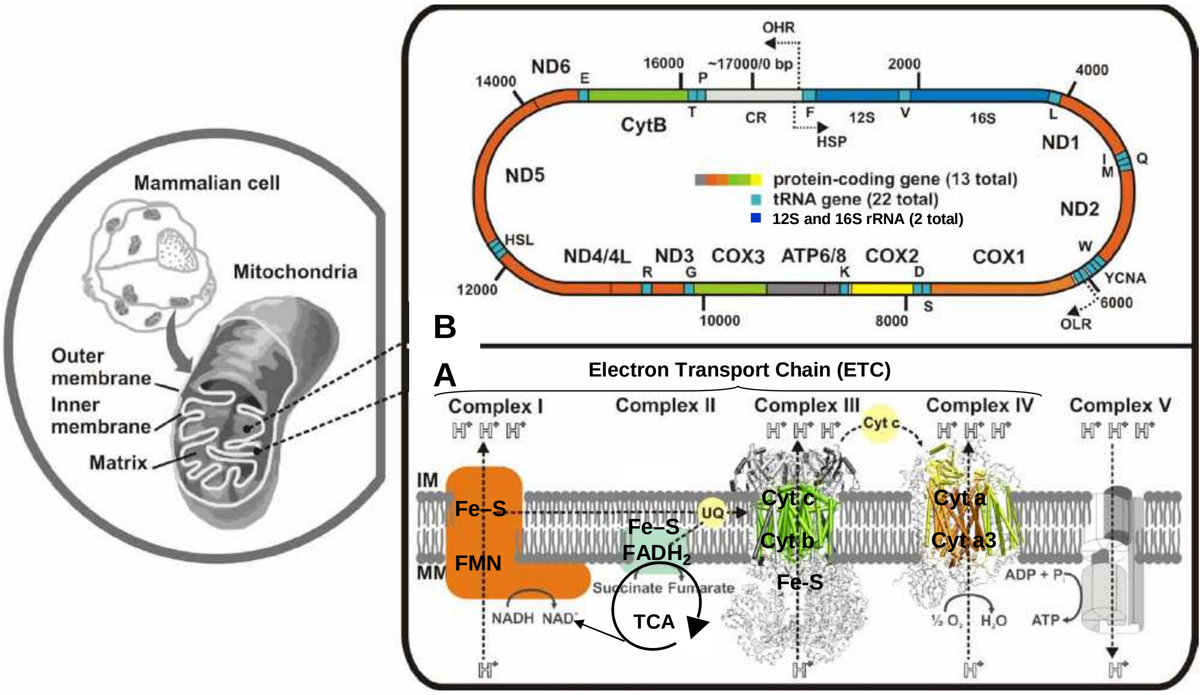
Mammalian cell
Mitochondria
Outer membrane
Inner membrane
Matrix
OHR
14000
ND6
E
16000
P
~17000/0 bp
2000
4000
T
CR
F
12S
V
16S
L
CytB
HSP
ND1
I
M
Q
ND5
protein-coding gene (13 total)
tRNA gene (22 total)
12S and 16S rRNA (2 total)
ND2
HSL
W
ND4/4L
ND3
COX3
ATP6/8
COX2
COX1
R
G
K
D
YCNA
12000
S
6000
10000
8000
OLR
B
A
Electron Transport Chain (ETC)
Complex I
Complex II
Complex III
Complex IV
Complex V
H+ H+ H+
Cyt c
IM
MM
Fe–S
FMN
Fe–S
FADH2
UQ
Cyt c
Cyt b
Fe-S
Cyt a
Cyt a3
ADP + Pi
ATP
½ O2
H2O
Succinate
Fumarate
TCA
NADH
NAD+
H+

Figure 5. The mammalian oxidative phosphorylation system (OXPHOS) and the mitochondrial genome. (A) Simplified view of the mitochondrial oxidative phosphorylation system (OXPHOS). Complexes I (NADH:ubiquinone oxidoreductase) and II (succinate dehydrogenase, belongs to the tricarboxylic acid cycle called TCA) receive electrons from NADH and $FADH_2$ respectively. Electrons are then driven from complexes by the mobile carrier molecules coenzyme Q/ubiquinone (UQ) and cytochrome c (Cyt c) to the final acceptor, molecular oxygen (O_2). Electron flow is coupled to proton movement across the inner membrane (IMM) in complexes I, III and IV. The resulting proton gradient is harvested by complex V to generate ATP. **(B)** Schematic representation of the mammalian mitochondrial genome (16,569 bp). Mitochondrial DNA encodes 22 tRNA genes (light-blue), two ribosomal RNA genes (dark-blue) and 13 genes encoding polypeptides of complex I (ND1-ND6), complex III (cytB), complex IV (COX1-3) and complex V (ATP6/8) (adapted from *da Fonseca et al*, 2008[8]).

Mitochondrial DNA

Current theory holds that mitochondria are descendants of aerobic bacteria that colonized an ancient prokaryote about 1.5 billion years ago[138, 148, 149]. This union may lead to the first eukaryotic cell capable of aerobic respiration, indispensable precursor to the evolution of current multicellular organisms[148]. This idea is supported by the fact that mitochondria are the only organelles in animal cells that possess their own genome. Each mitochondrion contains 2–10 copies of mitochondrial DNA (mtDNA) located in the matrix[150]. In every human cell except mature erythrocytes[151], 200 to 2000 mitochondria are found[152, 153]. The mtDNA copy number as well as the number of mitochondria per cell is exquisitely calibrated on the cell type and the cellular energy demand. The largest number of mitochondria is found in the most metabolically active tissues like muscles, liver and brain[154]. The latter consumes 20% of the total oxygen supply while it accounts for only 2% of the total body mass[155].

The mtDNA is a circular double-stranded molecule maternally heritated[156] (Figure 5B). The outer strand is a guanine-rich heavy strand and the inner strand is a cytosine-rich light strand. The mtDNA contains 37 genes (16,569 base pairs) and codes for 13 proteins which all belong to the five respiratory enzymes complexes. It consists in 7 of 46 subunits constituting complex I (ND1, 2, 3, 4, 4L, 5, and 6), 1 of 11 subunits of complex III (cytochrome b), 3 of 13 subunits of complex IV (COX1, COX2 and COX3), and 2 of 17 subunits of complex V (ATPase 6 and ATPase 8)[150]. In addition, the mitochondrial genome encodes the 12S and 16S ribosomal RNAs as well as 22 transfer RNAs[157] required for intramitochondrial protein synthesis. However, as only few mitochondrial proteins are encoded internally, the organelle is not liberated from the nuclear genes control. Complexes I, III and IV are encoded by both mtDNA and nuclear DNA (nDNA), while complex II is carried out exclusively by nDNA[158]. Furthermore, most of the proteins building mitochondria and these forming the mitochondrial machinery like metabolic enzymes, DNA and RNA polymerases, ribosomal proteins, and mtDNA regulatory factors (e.g. mitochondrial transcription factor A) are imported from the cytosol[159]. The import is mainly accomplished by membrane spanning, multi-subunit translocators of OMM and IMM.

Unlike nDNA, mtDNA is not protected by histones[160] making it more vulnerable to injury as oxidative stress[161] and its mutation rate is about 10-fold higher than this of nDNA[162], especially in tissues with a high ATP demand like the brain. To mitigate mutation risks, mitochondria develop an inheritance which greatly differs from the Mendelian mode of nDNA[163]. First, mitochondria are distributed to daughter cells more or less randomly during cell division. Most importantly, mitochondria divide mainly in response to cellular energy needs, independently of cell cycle. In other words, when a cell needs high energy, mitochondria grow and divide, and when the cell uses low energy, they are destroyed or become inactive. For example, the mitochondrial genome replicates regularly in postmitotic cells, about once per month[136] in order to maintain the mitochondrial function in neurons[164]. Finally, mitochondria continuously divide and fuse with each other, forming a veritable network. Although incompletely understood, the combined consequence of all the processes is mtDNA recombination and both normal and modified mitochondrial genes in a cell [136, 164]. The deleterious effects of mitochondrial mutations are reduced and the potential for the removal of modified mtDNA by autophagy increases. However, during ageing or in pathological case, these mechanisms may be altered and lead to mitochondrial alterations. Above a certain threshold ("threshold effect") they drive to respiratory and metabolic defects getting progressively worse. Since 1962 such impairments are associated with a wide range of severe human disorders regrouped under the name of mitochondrial diseases[165-167].

1.2.2. Mitochondria as sources and targets of reactive oxygen species

The fate of most electrons from NADH or $FADH_2$ driven in the respiratory chain is the reduction from O_2 to water at complex IV. Mitochondria consume approximately 85% of O_2 utilized by cells during ATP production[168]. However, this elegant system for energy production is not perfect. A small portion of electrons (up to 2%) escaping from ETC, mostly at complexes I and III[169, 170], react with O_2 and yield superoxide anion ($O_2^{-\cdot}$)[168, 171, 172], which can be converted into other ROS such as hydrogen peroxide (H_2O_2) and the highly reactive hydroxyl radical ($OH^{\cdot}$) through enzymatic and nonenzymatic reactions[173-175] (Figure 6). Although, ETC is the major source, radicals may be generated by peroxisomes as well as a variety of cytosolic enzymes systems (e.g. xanthine oxidase, mitochondrial monoamine oxidase (MAOA and MAOB), nitric oxide synthase (NOS), and NADPH oxidase)[176]. In addition, a number of external agents (e.g. toxins, chemotherapeutics and radiations) can trigger ROS[176].

Cells are endowed with robust endogenous antioxidant systems to counteract excessive ROS. $O_2^{-\cdot}$ is detoxified first to H_2O_2 by manganese superoxide dismutase (MnSOD) or copper/zinc superoxide dismutase (Cu/Zn SOD)[138] and then to water by glutathione peroxidase (GPX) or catalase (CAT)[177] (Figure 6). In addition to enzymes, low molecular weight antioxidants acting either indirectly as chelating agents or directly like the glutathione (GSH), NADPH and nutritional products (ascorbic acid, lipoic acid, polyphenols and carotenoids)[178, 179] regulate overall ROS levels to maintain physiological homeostasis. Interestingly, recent data suggest that neuronal UCPs proteins by regulating $\Delta\psi$[146] may reduce ROS production.

It is believed that ROS, in particular $O_2^{-\cdot}$ and H_2O_2, have roles as signalling molecules[180, 181] in physiological processes including defense against infection and coordination of inflammatory responses as well as synaptic plasticity, learning and memory[182]. However, when ROS production overwhelms endogenous antioxidant systems, they can lead to harmful effects on cellular compounds, inducing lipid peroxidation and proteins and DNA oxidation[183] (Figure 6). These injuries are collectively referred to as “oxidative stress”. Become the main target of ROS attacks is the price to pay by mitochondria for being the major source[178, 184-186]. The long polyunsaturated fatty acid chains of mitochondrial membranes are very susceptible to oxidation and may lead to the membrane depolarization and consecutively to mitochondrial impairments[169]. $O_2^{-\cdot}$, produced by complex I and III, damages the iron-sulfur cluster that resides in the active site of aconitase, a TCA enzyme[187]. Nitric oxide ($NO^\cdot$) produced by the mitochondrial nitric oxide synthase (mtNOS)[172] and also freely diffuses into mitochondria from the cytosol[177] reacts with $O_2^{-\cdot}$ to produce peroxynitrite ($ONOO^-$)[177]. This latter is a reactive molecule that can induce nitration of proteins on tyrosine residues and impair their function[188]. Unlike $ONOO^-$ which inactivates multiple mitochondrial enzymes, $NO^\cdot$ inhibits specifically and reversibly the complex IV activity by competitive binding on its oxygen site[189]. In parallel, mtDNA localized close to ROS production sites is vulnerable to oxidative damage as well. Oxidized guanosine levels are higher in mtDNA than in nDNA[162]. Taken together, oxidative damages of the mitochondrial compounds lead to a shutdown of energy production[166], which in turn, leads to a decrease of antioxidant defense (e.g. GSH) and the enhancement of ROS triggering the vicious cycle of oxidative stress, mitochondrial dysfunction and apoptosis. First states in the theory of aging[190, 191], the mitochondrial “vicious cycle” has been thereafter implicated in many degenerative diseases, most of them affecting the brain and muscles which are high energy consumers[192].

Of note, a major unsolved and still controversial issue is whether increased ROS production is a primary consequence of mitochondrial dysfunction or whether a primary defect in ROS scavenging activity is responsible for an abnormal respiratory function. This point is particularly challenging in many pathological cases in order to establish clear cause and effect relationship.

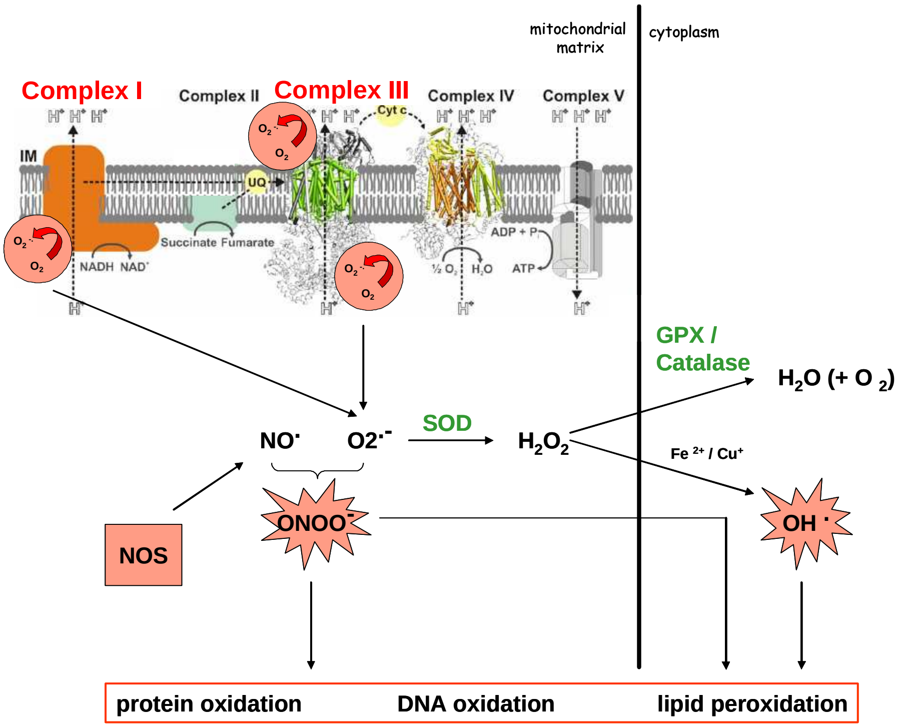
mitochondrial matrix
cytoplasm
Complex I
Complex II
Complex III
Complex IV
Complex V
IM
UQ
Cyt c
Succinate Fumarate
NADH NAD+
ADP + Pi
ATP
½ O2 H2O
O2·-
O2
GPX / Catalase
H2O (+ O 2)
NO·
O2·-
SOD
H2O2
Fe 2+ / Cu+
ONOO-
OH ·
NOS
protein oxidation
DNA oxidation
lipid peroxidation

Figure 6. Pathways of reactive oxygen species (ROS) formation and their enzymatic detoxification. Complexes I and III generate superoxide anion radical ($O_2^{\cdot-}$) during the electron transfer process. $O_2^{\cdot-}$ can interact with $NO^{\cdot}$, produced by nitric oxidase synthase (NOS), to generate peroxynitrite ($ONOO^-$). The enzymatic activity of mitochondrial manganese superoxide dismutase (SOD) converts $O_2^{\cdot-}$ to hydrogen peroxide (H_2O_2), which may then diffuse to the cytoplasmic compartment where glutathione peroxidase (GPX) and catalase convert H_2O_2 to H_2O. H_2O_2 can interact with Fe^{2+} or Cu^+ to generate hydroxyl radical ($OH^{\cdot}$), a highly reactive free radical, that can induce as well as $ONOO^-$, lipid peroxidation and oxidative damage to protein and DNA. Of, note, $NO^{\cdot}$ and its derivates (reactive nitrogen species or RNS) belong also to the group of ROS.

1.2.3. Mitochondria-dependent apoptosis

Although paradoxical with regards to their indispensable role on cell survival, mitochondria are also implicated in both widely recognized cellular demises namely the programmed cell death (apoptosis) and the accidental cell death (necrosis). During necrosis, cells are caught ‘‘off guard’’ by severe injuries and lead to nonselective cell damage. Conversely to necrosis, during apoptosis cells ‘‘decide’’ to die and activate molecular suicide cascades producing and mobilizing many proteins considered as executioners. While apoptosis plays an essential role in regulating growth and development, its misregulation may give rise to a series of pathological states[193]. Interestingly, it is not uncommon for one effector, such as oxidative stress to have the capacity to trigger a combination of apoptosis and necrosis[5]. For example, oxidative stress-dependent mitochondrial membrane permeabilization (MMP) may constitute a common event of both death modalities[5] and the exhaustion of ATP supply by apoptotic mechanisms may lead to necrosis[129].

Apoptosis results from two biochemical cascades, known as the extrinsic and mitochondrial pathways (Figure 7A and B). Mitochondrial apoptosis is caused by several conditions of intracellular stress, such as oxidative stress and Ca^{2+} overload. Holding many pro-apoptotic proteins, the structural and functional alterations of mitochondria have major impact on cellular viability[194, 195]. As mentioned previously (see paragraph 1.2.2), mitochondria are very vulnerable to oxidative stress which may lead to $\Delta\psi$ decrease[196], ETC impairment and ATP depletion[5, 189]. When these lethal signals predominate to pro-survival mechanisms attempted by the cell to cope the stress, mitochondrial membranes are permeabilized (MMP)[197]. This phase determines whether the cell will succumb to or survive the injury, and represents a “point of no return” in the mitochondrial cell death. Although still debated, the opening of the permeability transition pore complex, constituted of several transmembrane proteins, may break irreversibly $\Delta\psi$ down and induce MMP[5]. Bioenergetic and biosynthetic functions of mitochondria are consequently stopped and proteins like cytochrome c and AIF[198] regulated by pro- (bax, bak, bad, bim, bid) and anti-apoptotic proteins (bcl-2 and bcl-xl) of the Bcl-family[199] are released from IMS into the cytosol. The mechanism by which cytochrome c activates the apoptotic cascade remains to be fully elucidated. However, it seems to participate in the formation of a multiprotein complex called apoptosome. The complex activates initiator caspases (caspase 8 and 9) and transduces lethal signals by catalysing the proteolytic maturation of executioner caspases (caspase 3, 6 and 7) and pro-apoptotic factors (BH3-only protein BID). Finally, executioner caspases cleave numerous intracellular substrates contributing to the catabolic phase of cell death[195, 198] (Figure 7B).

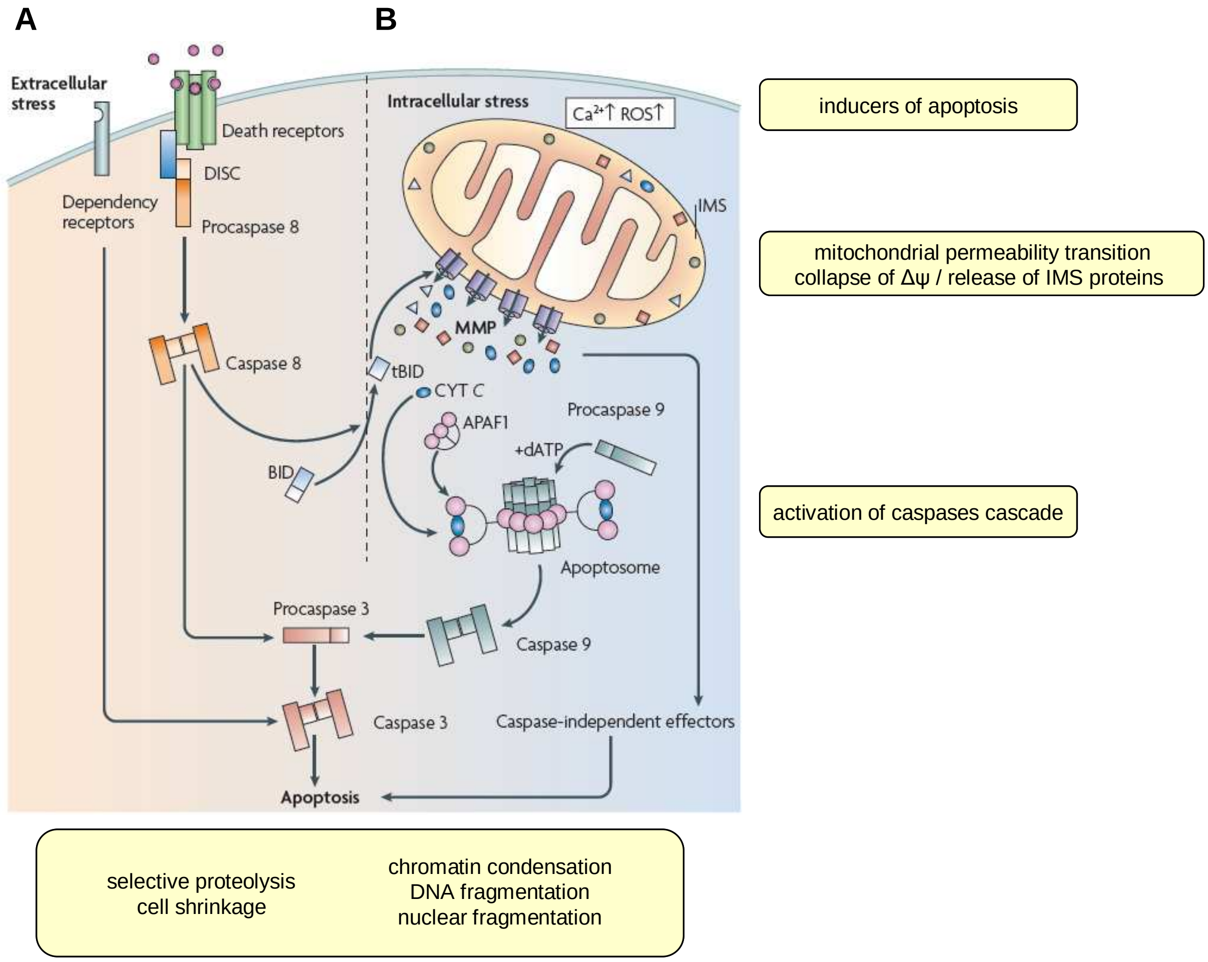
A
B
Extracellular stress
Death receptors
DISC
Dependency receptors
Procaspase 8
Caspase 8
BID
tBID
Intracellular stress
Ca²⁺↑ ROS↑
IMS
MMP
CYT C
APAF1
Procaspase 9
+dATP
Apoptosome
Procaspase 3
Caspase 9
Caspase 3
Caspase-independent effectors
Apoptosis
inducers of apoptosis
mitochondrial permeability transition
collapse of Δψ / release of IMS proteins
activation of caspases cascade
selective proteolysis
cell shrinkage
chromatin condensation
DNA fragmentation
nuclear fragmentation

Figure 7. The extrinsic and intrinsic (mitochondrial) pathways of apoptosis. (A) The extracellular apoptotic pathway is initiated at the plasma membrane by specific transmembrane receptors, whereas **(B)** the mitochondrial apoptosis is triggered by intracellular stimuli such as Ca^{2+} overload and overgeneration of reactive oxygen species (ROS). In both pathways, initiator caspases (caspase 8 and 9) are activated within specific supramolecular platforms and so can catalyse the proteolytic maturation of executioner caspases, such as caspase 3, which mediate (at least part of) the catabolic processes that characterize end-stage apoptosis. Mitochondrial membrane permeabilization (MMP) marks a point of no return in the mitochondrial pathway by activating both caspase-dependent and caspase-independent mechanisms that eventually execute cell death. For example, following MMP the mitochondrial intermembrane space (IMS) protein cytochrome *c* (CYT *C*) is released into the cytosol and interacts with the adaptor protein apoptotic peptidase activating factor 1 (APAF1) as well as with procaspase 9 to form the apoptosome. This results in the sequential activation of caspase 9 and executioner caspases, such as caspase 3, which lead to apoptotic features like cell shrinkage and DNA fragmentation. One of the major links between extrinsic and mitochondrial apoptosis is provided by the BCL-2 homology domain 3 (BH3)-only protein BID, which can promote MMP following caspase-8-mediated cleavage. dATP, deoxyadenosine triphosphate; DISC, death-inducing signalling complex; tBID, truncated BID (adapted from *Galluzzi et al*, 2009[5]).

1.3. Mitochondrial dysfunction in Alzheimer's disease

Although, our understanding of AD made tremendous strides in the last decades, its molecular pathogenesis is not clearly established yet, particularly the mechanisms occurring in the early phase of the disease. Interestingly, positron emission tomography (PET) measurements demonstrate reduced energy metabolism in affected brain regions of AD patients and suggest that cellular energy deficit may precede cognitive symptoms[200] (Figure 8). In line with this idea, oxidative stress and mitochondrial abnormalities are estimated to occur before the onset of Aβ aggregates, tau pathology, synaptic dysfunction and inflammation in AD brain[201-207]. Markers of proteins and mtDNA oxidative damages as well as lipid peroxidation products (e.g. malondialdehyde (MDA) and 4-hydroxynonenal (HNE))[208] have been found in cortical lesions of AD patients[62, 209, 210], cybrid cells[211] and transgenic mice[203, 212-214]. Increased free radical generation has also been observed in mitochondria from peripheral cells of AD patients like platelets, fibroblasts and lymphocytes[136, 192, 215]. Decreased activities of mitochondrial enzymes including pyruvate dehydrogenase, α-ketoglutarate dehydrogenase and COX have been reported[216, 217]. Finally, some authors propose that mitochondrial machinery impairments[218, 219] and axonal transport defects[220] may be directly responsible for the synaptic failure and the cell death observed in AD.

The causal factors of mitochondrial alterations in cells of AD patients have to be clarified, but may involve aging, AD-related proteins and oxidative stress leading to reduced synaptic/cellular energy availability and ultimately to cortical neurodegeneration. Moreover, the critical role of mitochondria on the early pathogenesis of AD makes them into a preferential target for treatment strategies including antioxidants such as *Ginkgo biloba* extract (GBE).

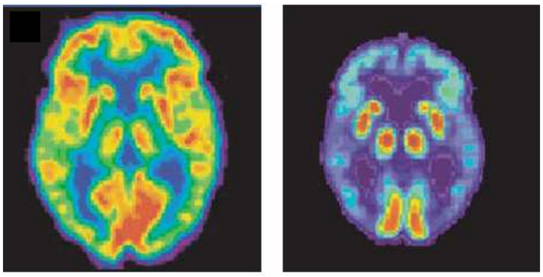
Normal brain AD brain

Figure 8. Major reductions in cellular energy metabolism in living AD patients. Positron emission tomography images show glucose uptake (red and yellow indicate high levels) in a normal control subject. AD patient exhibits large decreases in energy metabolism in the frontal cortex (top of brain) and temporal lobes (sides of the brain) (from *Mattson*, 2004[1]).

1.3.1. Link between Aβ toxicity and mitochondria

Ever since Aβ peptide was discovered, substantial research has focused on understanding its toxicity in brain of AD patients. Few years ago, it has been proposed that toxic species of Aβ intervening in molecular and biochemical abnormalities may be intracellular, oligomeric forms instead of extracellular, insoluble plaques[221, 222]. Aβ oligomers can inhibit long-term potentiation (LTP), a model system for synaptic plasticity and memory[223]. The presence of intracellular Aβ and synaptic alterations observed long before plaques formation in AD patients[224] and in several transgenic mouse models[225-227] have been acknowledged by the modification of the classical "amyloid cascade hypothesis"[6, 228] (Figure 9). Importantly, the "intracellular hypothesis" points up the role of mitochondria in the mechanism by which intracellular Aβ triggers synaptic failure and neurodegeneration[4, 229, 230] and correlates with studies recognizing energy metabolism deficiencies as earliest events in AD[231].

A time course investigation of Aβ and free radical production revealed that H_2O_2 formation correlates significantly with soluble Aβ but not insoluble Aβ, suggesting that in AD progression, soluble Aβ may enter mitochondria and induce ROS[214]. In accordance with this idea, some studies showed that oligomeric Aβ, with its sharp morphology, may have the ability to permeabilize cellular membranes and lipid bilayers thereby entering organelles, such as mitochondria[232, 233]. Recently, accumulation of Aβ inside mitochondria has been proved[62, 234-236] and associated to functional[237-240] as well as structural mitochondrial impairments[201] in several cellular and transgenic mouse models. Aβ can disrupt mitochondrial COX activity in a sequence- and conformer-dependent manner[234, 241]. An interaction between a mitochondrial matrix enzyme called the Aβ binding protein alcohol dehydrogenase (ABAD) and Aβ in AD brain and animal models[242] confirmed the Aβ intra-mitochondrial hypothesis. Aβ-ABAD complex impairs the binding of NAD to ABAD, changes mitochondrial membrane permeability[243] and reduces activities of respiratory enzymes[236] leading to mitochondrial failure. Finally, the interaction between Aβ and mitochondria may explain how Aβ induces apoptosis and caspase activation[236, 244, 245]. The way by which Aβ reaches mitochondria is still debated. Aβ may be internalized by cells, imported into mitochondria via the translocator outer membrane (TOM) complex and accumulated in cristae[61]. A second mechanism may implicate an intracellularly generation of Aβ[246-248]. Of note, some authors propose that Aβ precursor, APP, may block mitochondrial import channels preventing the import of nuclear-encoded COX (complex IV) subunits IV and Vb[213] which decreases its activity and increases ROS production[62].

Collectively, these studies suggest that Aβ enters mitochondria and interacts with mitochondrial proteins, disrupts ETC, generates ROS leading ultimately to the drop of ATP levels[154]. The presence of intracellular Aβ adds a further level of complexity to the mechanism of Aβ toxicity as this enables direct access to organelles that are vital for the function and viability of neurons.

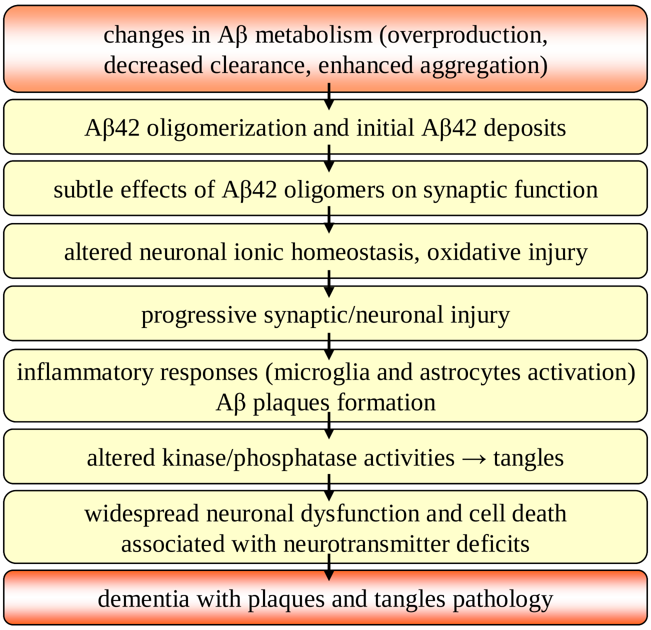
changes in Aβ metabolism (overproduction, decreased clearance, enhanced aggregation)
Aβ42 oligomerization and initial Aβ42 deposits
subtle effects of Aβ42 oligomers on synaptic function
altered neuronal ionic homeostasis, oxidative injury
progressive synaptic/neuronal injury
inflammatory responses (microglia and astrocytes activation) Aβ plaques formation
altered kinase/phosphatase activities → tangles
widespread neuronal dysfunction and cell death associated with neurotransmitter deficits
dementia with plaques and tangles pathology

Figure 9. The amyloid cascade hypothesis. The cascade is initiated by the generation of amyloid-β42 ($A\beta_{42}$). In AD familial early onset (FAD), $A\beta_{42}$ is overproduced owing to pathogenic mutations. In sporadic AD (SAD), various factors can contribute to an increased load of $A\beta_{42}$ oligomers and aggregates. Amyloid-β oligomers might directly injure the synapses and neurites of brain neurons, in addition to activating microglia and astrocytes. Tau pathology, which contributes substantially to the disease process through hyperphosphorylated tau and tangles, is triggered by $A\beta_{42}$ (adapted and modified from *Selkoe et al*, 2002[6]).

1.3.2. Effects of tau protein on mitochondrial function and axonal transport

For a long time, the “amyloid cascade hypothesis” claiming that in the pathogenic cascade of AD, Aβ is upstream of tau was an authority[249]. However, a recent theory declaring an Aβ-independent tau toxicity has seen the light[250]. The accumulation of NFTs occur in many neurodegenerative diseases referred to as “tauopathies”[251, 252] including AD. However, in contrast to AD, in many of these disorders, NFTs are abundant in the absence of overt Aβ plaques[3] suggesting a sufficient role of tau pathology to induce the neurodegeneration. Interestingly, oxidative stress and mitochondrial dysfunction have been proposed as key events within this tau pathology in these diseases including AD.

In AD, oxidative stress may lead to the phosphorylation of tau either by direct oxidative damages like HNE inducing tau conformational changes and NFTs formation[253, 254], or by deregulating proteins like ERK2 known to play a crucial role in the phosphorylating process[255]. In recent studies, it has been showed that misregulation of tau causes ATP depletion in synapses and enhancement of oxidative stress, long before tau detaches from microtubules and aggregates into NFTs[256-258]. Subsequent abnormal hyperphosphorylation of tau compromises the stability and function of microtubules which emphasizes the mitochondrial trafficking decrease and ATP starvation in nerve terminals[259] which may lead to neurotransmission impairments. Finally, NFTs formation leads to the progressive loss of axonal or dendritic transport[260]. Moreover, our group demonstrated mitochondrial dysfunction by proteomic and functional analyses[239] in a new tau transgenic mouse model[261]. The mice overexpressing the P301L mutant human tau protein exhibit an accumulation of hyperphosphorylated tau already at 3 months old and develop NFTs from 6 months old[261]. Mainly mitochondrial proteins, antioxidant enzymes and synaptic proteins were deregulated in the proteome pattern of P301L tau mice[239]. Functional analysis showed reduced complex I activity as well as impaired mitochondrial respiration and ATP synthesis with age. Mitochondrial dysfunction was associated with higher levels of ROS in aged transgenic mice. In addition, increased tau pathology revealed modified lipid peroxidation levels and up-regulation of antioxidant enzymes in response to oxidative stress[239]. For the first time, it has been proved that not only Aβ but also tau accumulation act on brain metabolism and oxidative conditions in AD.

Taken together, this evidence supports a role of Aβ-free tau pathology on mitochondrial and metabolic dysfunction. Tau toxicity may act indirectly by modifying microtubule stability, axonal transport and mitochondrial network. A second mechanism may be a direct inhibition of energy production by the rise of oxidative stress and impairment of respiratory enzymes as suggested by the accumulation of increasingly insoluble ATP synthase α-chain together with NFTs in AD brains whereas detergent soluble levels were reduced[262].

1.3.3. Aβ and tau share mitochondria as a common target

‘‘The genetics of Alzheimer’s disease favours a link to amyloid-beta but the clinical picture favours a link to tau neurofibrillary tangles.’’ M. Mesulam (International Conference on Alzheimer's Disease**,** 2008)

Although both Aβ and tau pathologies are common features in AD, it is still mysterious how they relate to each other. Some authors established that Aβ injections exaggerate a pre-existing tau pathology of several transgenic mouse models[261, 263-265]. Interestingly, recent evidence suggests that Aβ toxicity is also tau-dependent. Reducing endogenous tau levels prevented behavioral deficits as assessed in the Morris water maze, without altering Aβ levels[266]. Earlier findings in cultured hippocampal neurons derived from tau knockout and transgenic mice support the model that tau is required for Aβ-induced neurodegeneration[267]. Taken together, the studies illustrate a complex interplay between the two key proteins showing abnormal behavior in AD.

In parallel, increasing evidence suggests a role for mitochondrial alterations upstream of both Aβ and tau pathologies in AD. Moreover, close relationship between mitochondrial failure and Aβ on one hand, and tau on the other hand have been demonstrated (see paragraphs 1.3.1 and 1.3.2). Thereby, could be mitochondria the point of convergence of the two unquestionable pathologic hallmarks of the disease? Recent findings are in line with this hypothesis. Aβ aggregates and hyperphosphorylated tau may block the transport of mitochondria leading to energy deprivation at the synapse and neurodegeneration[257, 258]. Moreover, elevated tau may inhibit the transport of APP into axons and dendrites, causing impaired axonal transport suggesting a linkage between tau and APP[101, 268]. In addition, functional genomics encompassing transcriptomic and proteomic approaches[269-272] showed that Aβ treatment together with human tau over-expression in a cell culture model affected the regulation of genes controlling cell proliferation and synaptic elements in AD[273, 274].

In summary, these findings exemplify interactions between Aβ and tau at the mitochondria level, nevertheless many questions are still unresolved. How tau pathology mediates these changes and its role within the amyloid cascade remains unclear. The precise impacts of both lesions on mitochondrial respiratory machinery and energy homeostasis are still outstanding.

1.3.4. Transgenic mouse models

Understanding the molecular pathways by which the various pathological alterations including Aβ and tau, compromise neuronal integrity and lead to clinical symptoms has been a long-standing goal of AD research. Success in developing mouse models that mimic divers facets of the disease process has greatly facilitated this effort[2, 7, 35].

In 1995, Games and co-workers established the first Aβ plaque-forming mouse model by targeting high levels of the disease-linked V717F mutant form of APP in brain, using the platelet-derived growth factor (PDGF) mini-promoter for expression[275]. These PDAPP mice showed many of AD pathological features, including extensive deposition of extracellular amyloid plaques, astrocytosis and neuritic dystrophy[275]. Subsequently, a lot of APP-based transgenic models have been developed[276-280] and instrumental in addressing aspects of Aβ toxicity and age-dependent cognitive decline as well as testing therapies like vaccination trials[281, 282] (Figure 10A and B). The same year, Gotz and colleagues established the first tau transgenic mouse model, expressing the longest human brain tau isoform, without a pathogenic mutation and using the hThy1 promoter for neuronal expression[283]. Despite the lack of NFTs pathology, these mice modeled aspects of human AD, such as the somatodendritic localization of hyperphosphorylated tau and, therefore, represented an early "pre-NFTs" phenotype. Once the first pathogenic FTDP-17 mutations identified in the *MAPT* gene in 1998, several groups expressed them in mice. For example, the P301L tau-expressing pR5 mice develop aggregated forms of hyperphosphorylated tau and NFTs as well as neuronal loss[261, 284-286]. Moreover, these mice showed age-related behavioral impairment in amygdala- and hippocampus-dependent tasks which could be correlated with the aggregation pattern of the transgene[287, 288] (Figure 10A and B). Finally, the discovery of FAD mutations in the presenilin (PSEN) genes which influence APP processing, opened the path for *PSEN1* and *PSEN2* transgenic mouse models, and double-cross APP/PSEN models[35]. Recently, double[264, 289] and triple[225, 290, 291] transgenic mice combining Aβ and tau pathologies in one model have been generated (Figure 10A). The latest triple transgenic mouse line termed ^{triple}AD co-expresses mutated tau (P301L), PS2 (N141l) and APP^{Swe} (KM670/671NL). This model complements a first triple transgenic mouse model[292] harboring the PS1^{M146V} instead of the previous PS2 mutation. In this model with plaques and tangles, behavioural and neuronal symptoms of AD were already reported including synaptic dysfunction and LTP deficits[293]. However, a molecular link between Aβ and tau protein in AD pathology was still missing *in vivo*. Moreover, while recent findings indicated an interplay between PS1 and PS2 on mitochondrial functionality, more relevantly a specific role for PS2/γ-secretase on these organelles has been highlighted[294]. Finally, ^{triple}AD mice are the only known model to develop both tau and amyloid deposits in an age-dependent manner. NFTs pathology starts at 4 months old in contrast to other models developing substantial NFTs pathology very later, at 18-24 months old[292, 293]. The ^{triple}AD model is therefore particularly suited to study relationship between Aβ and tau in an age-related way. It has been shown, for example, that Aβ accumulation leads to the development of tau phosphorylation at a specific AD-epitope (Ser422). Although, the mice do not develop extensive neuronal loss or pronounced cognitive deficits, the progression of biochemical changes and histopathological features is reminiscent of the pathogenesis course observed in AD. Consequently, the model may be very useful for assessing therapeutic interventions addressing amyloidosis and/or Tau pathology. Importantly, behavioral deficits are present before detection of any protein aggregates which is especially meaningful considering the paradigm of the early mitochondrial dysfunction reported in AD.

It has been over a decade since the first AD transgenic mouse models have been reported. These models have enabled dramatic advances in our understanding of the pathogenic mechanism in AD and potential therapeutic approaches to tackling the inexorable clinical progression of the disease. Many of new therapeutic strategies have their foundation in transgenic animal work[2]. In this vein, the recent triple transgenic mice are not only promising in order to understand the complex interplay between Aβ and tau at the mitochondrial level *in vivo* but also to assist in the development of new treatments more adapted and efficient towards AD.

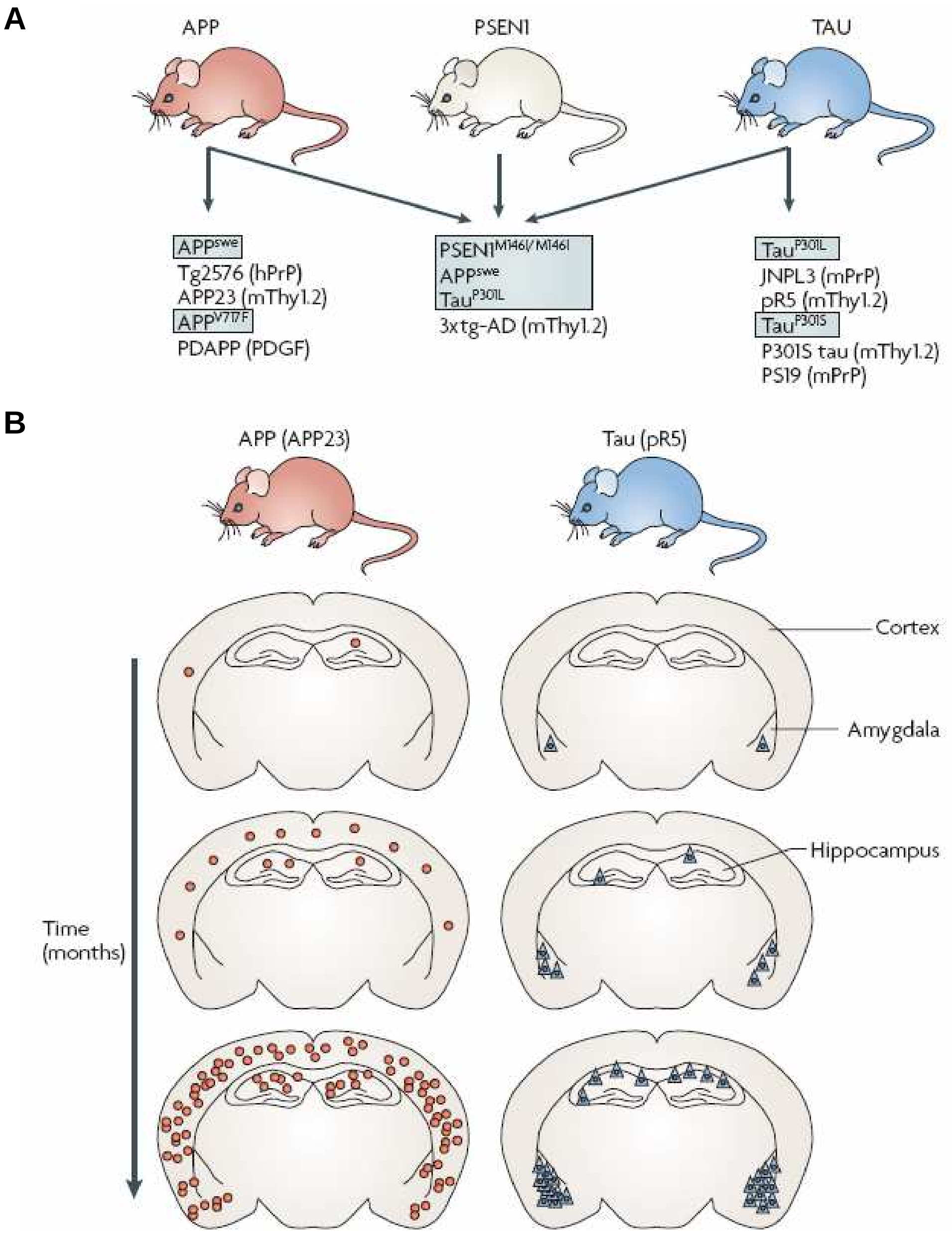
A
APP
PSEN1
TAU
APP^{swe}
Tg2576 (hPrP)
APP23 (mThy1.2)
APP^{V717F}
PDAPP (PDGF)
$PSEN1^{M146I/M146I}$
APP^{swe}
Tau^{P301L}
3xtg-AD (mThy1.2)
Tau^{P301L}
JNPL3 (mPrP)
pR5 (mThy1.2)
Tau^{P301S}
P301S tau (mThy1.2)
PS19 (mPrP)
B
APP (APP23)
Tau (pR5)
Cortex
Amygdala
Hippocampus
Time
(months)

Figure 10. Reproducing plaques and NFTs in transgenic mice. (A) Plaques are produced by expressing mutant amyloid precursor protein (APP), as found in patients with familial Alzheimer's disease (FAD), both with and without mutant *PSEN1*. Neurofibrillary tangles (NFTs) are produced by expressing mutant tau, as found in patients with frontotemporal dementia with Parkinsonism linked to chromosome 17 (FTDP-17). A few exemplary mutations are listed (grey boxes) together with their strain names and the promoters (in brackets) that were used for expression. **(B)** Progression of the pathology in APP23 and pR5 mice. NFTs formation in pR5 mice is initiated in the amygdala and eventually found in the hippocampus, whereas the cortex is virtually spared. Plaque formation in APP23 mice is prominent in the cortex and in the hippocampus. This reflects, to some extent, the situation in the brain of patients with AD, in which plaques and NFTs are anatomically separated (from *Gotz and Ittner*, 2008[7]).

1.3.5. Ginkgo biloba extract for the treatment of Alzheimer's disease

There is no cure for AD and the available treatments (e.g. acetyl cholinesterase inhibitors (tacrine, donepezil, rivastigmine and galantamine) and N-methyl-D-aspartate (NMDA) antagonist (memantine)) are only symptomatic. However, the increasing body of evidence implicating oxidative stress and mitochondrial dysfunction in the pathogenesis of AD raises the possibility of the beneficial use of antioxidants. The hypothesis is particularly promising owing to numerous free radical scavengers are known and many including *Ginkgo biloba* extract (GBE) have no major side effects. GBE is a valuable therapeutic drug for the treatment of memory impairment and dementia including AD. Double-blind, placebo-controlled studies showed the improvement of cognitive symptoms in the elderly and in AD patients[295-299].

Standardized GBE, obtained from dried green whole leaves of *Ginkgo biloba* tree with acetone/water mixture, is defined as dried extract (drug-extract ratio 35-67:1). Different standardized GBE are on the market, e.g. EGb 761 (Schwabe Firm, Germany, Tebokan® in Switzerland) and LI 1370 (Vifor Firm, Switzerland, Symfona®)[300]. The most studies refer to EGb 761 as yet. GBE consists in two major groups of substances, flavone glycosides (flavonoid fraction, 22-27%) and terpene lactones (terpenoid fraction, 5-7%). Ginkgolic acids are reduced to at most 5ppm[301]. The flavonoid fraction is primarily composed of quercetin, kaempferol and isorhamnetin glycosides, and the terpenoid fraction of ginkgolides A, B, C, J and M (2.8-3.4%) as well as bilobalide (2.6-3.2%)[302] (Figure 11). The chemical structure of flavonoids preferentially reacts with hydroxyl radicals[303] and chelate pro-oxidant transition heavy metal ions[304], which consequently inhibits the formation of new hydroxyl radicals. Ginkgolides are known to be platelet activating factor (PAF) antagonists, able to improve blood circulation[305] and cerebral insufficiency[306]. Although individual constituents have been found to be active in a variety of assays, mechanisms underlying GBE beneficial effects may reside in the synergistic action of all components.

Substantial *in vitro* and *in vivo* models demonstrated free radical scavenger activity and anti-apoptotic properties of GBE[302, 307-310]. In addition to its intracellular antioxidant properties, GBE may stabilize directly mitochondrial function. Our group showed that GBE improves $\Delta\psi$ and ATP levels, and protects mitochondrial respiratory complexes in stress models[311-313]. Of note, the ginkgolide J, the flavonoid fraction and the bilobalide were the most effective to stabilize Δψ in this study. These effects may lead to a decrease of ROS production and cell death processes. In accordance with this idea, the transcript level for an anti-apoptotic Bcl-2-like protein was elevated, whereas the transcript level for pro-apoptotic caspase 12 was decreased in PC12 cells treated with GBE[310, 314]. In addition, enhancement of tau mRNA expression in cortex of mice whose diets were supplemented with GBE has been observed[315]. Interestingly, recent studies suggest that GBE may develop an antiamyloidogenic property inhibiting amyloid fibrils formation either by a direct interaction with Aβ[316, 317] or by activating α-secretase pathway[318]. It is assumed that GBE anti-oxidative properties combined to its action on AD-related proteins may protect the brain against the cognitive dysfunction observed in the disease. Moreover, GBE may improve the neurotransmission[319] as well as the neuronal plasticity[304] and develop anti-inflammatory effects[320]. In several aging and stress animal models, GBE enhanced the cognition, spatial learning and explorative behavior[321-323]. Clinical studies including meta-analyses and double-blind trials supported also efficiency of GBE on cognitive defects, daily living and clinical global impression in dementia patients including AD[295-297, 324].

Although, many animal models reports and clinical studies propose neuroprotective effects of GBE[318, 325], cellular and molecular mechanisms, specially these relating to mitochondrial respiratory function, remain unknown. The elucidation of biochemical pathways by which GBE exercises its polyvalent protective effects may not only open new ways for the development of more efficacious therapies but also ripen our understanding of mitochondria role within AD pathological processes.

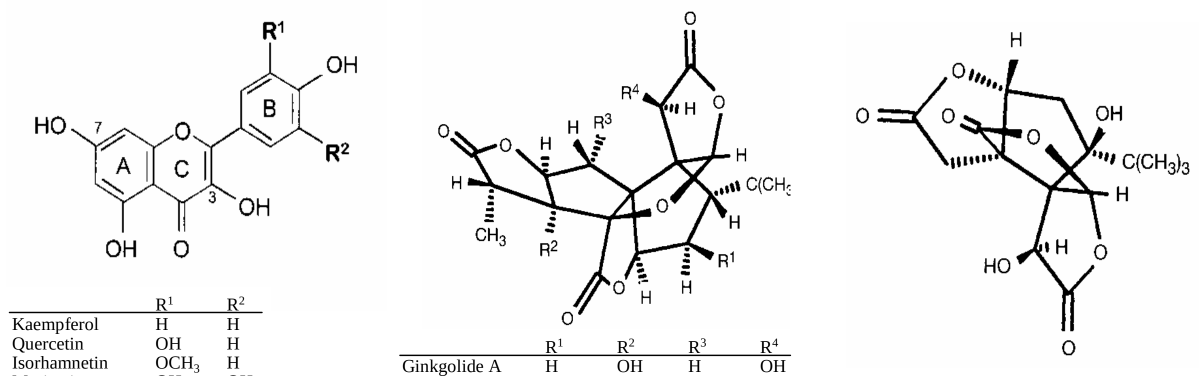

	R^1	R^2
Kaempferol	H	H
Quercetin	OH	H
Isorhamnetin	OCH_3	H
Myricetin	OH	OH

	R^1	R^2	R^3	R^4
Ginkgolide A	H	OH	H	OH
Ginkgolide B	H	OH	OH	OH
Ginkgolide C	OH	OH	OH	OH
Ginkgolide J	OH	OH	H	OH
Ginkgolide M	OH	H	OH	OH

Flavonoids **Ginkgolides** **Bilobalide**

Figure 11. Chemical structures of main constituents present in *Ginkgo Biloba* Extract (GBE). GBE consist in two major groups of substances: the flavonoid fraction (22-27%) composed of quercetin, kaempferol, isorhamnetin and myricetin, as well as the terpenoid fraction (5-7%) composed of ginkgolides A, B, C, J and M and bilobalide**.**

1.4. References

1. Mattson, M.P., *Pathways towards and away from Alzheimer's disease.* Nature, 2004. **430**(7000): p. 631-9.
2. Van Dam, D. and P.P. De Deyn, *Drug discovery in dementia: the role of rodent models.* Nat Rev Drug Discov, 2006. **5**(11): p. 956-70.
3. Lee, V.M., M. Goedert, and J.Q. Trojanowski, *Neurodegenerative tauopathies.* Annu Rev Neurosci, 2001. **24**: p. 1121-59.
4. Rhein, V. and A. Eckert, *Effects of Alzheimer's amyloid-beta and tau protein on mitochondrial function -- role of glucose metabolism and insulin signalling.* Arch Physiol Biochem, 2007. **113**(3): p. 131-41.
5. Galluzzi, L., K. Blomgren, and G. Kroemer, *Mitochondrial membrane permeabilization in neuronal injury.* Nat Rev Neurosci, 2009. **10**(7): p. 481-94.
6. Selkoe, D.J., *Alzheimer's disease is a synaptic failure.* Science, 2002. **298**(5594): p. 789-91.
7. Gotz, J. and L.M. Ittner, *Animal models of Alzheimer's disease and frontotemporal dementia.* Nat Rev Neurosci, 2008. **9**(7): p. 532-44.
8. da Fonseca, R.R., et al., *The adaptive evolution of the mammalian mitochondrial genome.* BMC Genomics, 2008. **9**: p. 119.
9. Braak, H. and E. Braak, *Neuropathological stageing of Alzheimer-related changes.* Acta Neuropathol, 1991. **82**(4): p. 239-59.
10. Goedert, M. and R. Jakes, *Mutations causing neurodegenerative tauopathies.* Biochim Biophys Acta, 2005. **1739**(2-3): p. 240-50.
11. Alzheimer, A., All. Z. Psychiatr., 1907. **64**: p. 146.
12. Alzheimer, A., Z. Ges. Neurol. Psychiat., 1911. **4**: p. 356.
13. Kraepelin, E., *Psychiatrie, Ein Lehrbuch fur Studierende und Arzte. II. Band (Barth Verlag, Leipzig).* 1910.
14. Alzheimer, A., et al., *An English translation of Alzheimer's 1907 paper, "Uber eine eigenartige Erkankung der Hirnrinde".* Clin Anat, 1995. **8**(6): p. 429-31.
15. Brookmeyer, R., Johnson, E., Ziegler-Graham, K., Arrighi HM, *Forecasting the global burden of Alzheimer's disease.* Alzheimers dement, 2007. **3**: p. 186-191.
16. McKhann, G., et al., *Clinical diagnosis of Alzheimer's disease: report of the NINCDS-ADRDA Work Group under the auspices of Department of Health and Human Services Task Force on Alzheimer's Disease.* Neurology, 1984. **34**(7): p. 939-44.
17. Chung, J.A. and J.L. Cummings, *Neurobehavioral and neuropsychiatric symptoms in Alzheimer's disease: characteristics and treatment.* Neurol Clin, 2000. **18**(4): p. 829-46.
18. Pallas, M. and A. Camins, *Molecular and biochemical features in Alzheimer's disease.* Curr Pharm Des, 2006. **12**(33): p. 4389-408.
19. Selkoe, D.J., *Alzheimer disease: mechanistic understanding predicts novel therapies.* Ann Intern Med., 2004. **140**(8): p. 627-38.
20. Terry, R.D., *Alzheimer's disease and the aging brain.* J Geriatr Psychiatry Neurol, 2006. **19**(3): p. 125-8.
21. Arnold, S.E., et al., *The topographical and neuroanatomical distribution of neurofibrillary tangles and neuritic plaques in the cerebral cortex of patients with Alzheimer's disease.* Cereb Cortex, 1991. **1**(1): p. 103-16.
22. Chagnon, P., et al., *Distribution of brain cytochrome oxidase activity in various neurodegenerative diseases.* Neuroreport, 1995. **6**(5): p. 711-5.

23. Rozemuller, J.M., P. Eikelenboom, and F.C. Stam, *Role of microglia in plaque formation in senile dementia of the Alzheimer type. An immunohistochemical study.* Virchows Arch B Cell Pathol Incl Mol Pathol, 1986. **51**(3): p. 247-54.
24. Wyss-Coray, T., *Inflammation in Alzheimer disease: driving force, bystander or beneficial response?* Nat Med, 2006. **12**(9): p. 1005-15.
25. Markesbery, W.R., *Oxidative stress hypothesis in Alzheimer's disease.* Free Radic Biol Med, 1997. **23**(1): p. 134-47.
26. McGeer, P.L., J. Rogers, and E.G. McGeer, *Inflammation, anti-inflammatory agents and Alzheimer disease: the last 12 years.* J Alzheimers Dis, 2006. **9**(3 Suppl): p. 271-6.
27. LaFerla, F.M., K.N. Green, and S. Oddo, *Intracellular amyloid-beta in Alzheimer's disease.* Nat Rev Neurosci., 2007. **8**(7): p. 499-509.
28. Giacobini, E., *Cholinesterase inhibitors stabilize Alzheimer's disease.* Ann N Y Acad Sci, 2000. **920**: p. 321-7.
29. Zilka, N., M. Korenova, and M. Novak, *Misfolded tau protein and disease modifying pathways in transgenic rodent models of human tauopathies.* Acta Neuropathol, 2009.
30. Reddy, P.H. and S. McWeeney, *Mapping cellular transcriptosomes in autopsied Alzheimer's disease subjects and relevant animal models.* Neurobiol Aging, 2006. **27**(8): p. 1060-77.
31. Gatz, M., et al., *Heritability for Alzheimer's disease: the study of dementia in Swedish twins.* J Gerontol A Biol Sci Med Sci, 1997. **52**(2): p. M117-25.
32. Tanzi, R.E., *A genetic dichotomy model for the inheritance of Alzheimer's disease and common age-related disorders.* J Clin Invest, 1999. **104**(9): p. 1175-9.
33. Rocchi, A., et al., *Causative and susceptibility genes for Alzheimer's disease: a review.* Brain Res Bull, 2003. **61**(1): p. 1-24.
34. Bertram, L. and R.E. Tanzi, *The genetic epidemiology of neurodegenerative disease.* J Clin Invest, 2005. **115**(6): p. 1449-57.
35. McGowan, E., J. Eriksen, and M. Hutton, *A decade of modeling Alzheimer's disease in transgenic mice.* Trends Genet, 2006. **22**(5): p. 281-9.
36. Reiman, E.M., et al., *GAB2 alleles modify Alzheimer's risk in APOE epsilon4 carriers.* Neuron, 2007. **54**(5): p. 713-20.
37. Tanzi, R.E. and L. Bertram, *New frontiers in Alzheimer's disease genetics.* Neuron., 2001. **32**(2): p. 181-4.
38. Blacker, D., et al., *Results of a high-resolution genome screen of 437 Alzheimer's disease families.* Hum Mol Genet, 2003. **12**(1): p. 23-32.
39. Delacourte, A., et al., *Nonoverlapping but synergetic tau and APP pathologies in sporadic Alzheimer's disease.* Neurology, 2002. **59**(3): p. 398-407.
40. Goate, A., et al., *Segregation of a missense mutation in the amyloid precursor protein gene with familial Alzheimer's disease.* Nature, 1991. **349**(6311): p. 704-6.
41. Murrell, J., et al., *A mutation in the amyloid precursor protein associated with hereditary Alzheimer's disease.* Science, 1991. **254**(5028): p. 97-9.
42. Mullan, M., et al., *A pathogenic mutation for probable Alzheimer's disease in the APP gene at the N-terminus of beta-amyloid.* Nat Genet, 1992. **1**(5): p. 345-7.
43. Nilsberth, C., et al., *The 'Arctic' APP mutation (E693G) causes Alzheimer's disease by enhanced Abeta protofibril formation.* Nat Neurosci, 2001. **4**(9): p. 887-93.
44. Ellis, R.J., et al., *Cerebral amyloid angiopathy in the brains of patients with Alzheimer's disease: the CERAD experience, Part XV.* Neurology, 1996. **46**(6): p. 1592-6.

45. Rovelet-Lecrux, A., et al., *APP locus duplication causes autosomal dominant early-onset Alzheimer disease with cerebral amyloid angiopathy.* Nat Genet, 2006. **38**(1): p. 24-6.
46. Sherrington, R., et al., *Cloning of a gene bearing missense mutations in early-onset familial Alzheimer's disease.* Nature, 1995. **375**(6534): p. 754-60.
47. Rogaev, E.I., et al., *Familial Alzheimer's disease in kindreds with missense mutations in a gene on chromosome 1 related to the Alzheimer's disease type 3 gene.* Nature, 1995. **376**(6543): p. 775-8.
48. Hutton, M., et al., *Association of missense and 5'-splice-site mutations in tau with the inherited dementia FTDP-17.* Nature, 1998. **393**(6686): p. 702-5.
49. Poorkaj, P., et al., *Tau is a candidate gene for chromosome 17 frontotemporal dementia.* Ann Neurol, 1998. **43**(6): p. 815-25.
50. Spillantini, M.G., et al., *Mutation in the tau gene in familial multiple system tauopathy with presenile dementia.* Proc Natl Acad Sci U S A, 1998. **95**(13): p. 7737-41.
51. Hasegawa, M., M.J. Smith, and M. Goedert, *Tau proteins with FTDP-17 mutations have a reduced ability to promote microtubule assembly.* FEBS Lett, 1998. **437**(3): p. 207-10.
52. Chen, F., et al., *Posttranslational modifications of tau--role in human tauopathies and modeling in transgenic animals.* Curr Drug Targets, 2004. **5**(6): p. 503-15.
53. Glenner, G.G. and C.W. Wong, *Alzheimer's disease: initial report of the purification and characterization of a novel cerebrovascular amyloid protein.* Biochem Biophys Res Commun, 1984. **120**(3): p. 885-90.
54. Masters, C.L., et al., *Amyloid plaque core protein in Alzheimer disease and Down syndrome.* Proc Natl Acad Sci U S A, 1985. **82**(12): p. 4245-9.
55. Rensink, A.A., et al., *Pathogenesis of cerebral amyloid angiopathy.* Brain Res Brain Res Rev, 2003. **43**(2): p. 207-23.
56. Thal, D.R., et al., *Phases of A beta-deposition in the human brain and its relevance for the development of AD.* Neurology, 2002. **58**(12): p. 1791-800.
57. Thal, D.R., et al., *Vascular pathology in Alzheimer disease: correlation of cerebral amyloid angiopathy and arteriosclerosis/lipohyalinosis with cognitive decline.* J Neuropathol Exp Neurol, 2003. **62**(12): p. 1287-301.
58. Thal, D.R., et al., *Cerebral amyloid angiopathy and its relationship to Alzheimer's disease.* Acta Neuropathol, 2008. **115**(6): p. 599-609.
59. Mattson, M.P., *Cellular actions of beta-amyloid precursor protein and its soluble and fibrillogenic derivatives.* Physiol Rev, 1997. **77**(4): p. 1081-132.
60. Anandatheerthavarada, H.K. and L. Devi, *Amyloid precursor protein and mitochondrial dysfunction in Alzheimer's disease.* Neuroscientist, 2007. **13**(6): p. 626-38.
61. Hansson Petersen, C.A., et al., *The amyloid beta-peptide is imported into mitochondria via the TOM import machinery and localized to mitochondrial cristae.* Proc Natl Acad Sci U S A, 2008. **105**(35): p. 13145-50.
62. Devi, L., et al., *Accumulation of amyloid precursor protein in the mitochondrial import channels of human Alzheimer's disease brain is associated with mitochondrial dysfunction.* J Neurosci., 2006. **26**(35): p. 9057-68.
63. Allinson, T.M., et al., *ADAMs family members as amyloid precursor protein alpha-secretases.* J Neurosci Res, 2003. **74**(3): p. 342-52.
64. Vassar, R., et al., *Beta-secretase cleavage of Alzheimer's amyloid precursor protein by the transmembrane aspartic protease BACE.* Science, 1999. **286**(5440): p. 735-41.
65. Edbauer, D., et al., *Reconstitution of gamma-secretase activity.* Nat Cell Biol, 2003. **5**(5): p. 486-8.

66. Haass, C., et al., *beta-Amyloid peptide and a 3-kDa fragment are derived by distinct cellular mechanisms.* J Biol Chem, 1993. **268**(5): p. 3021-4.
67. Iwatsubo, T., et al., *Visualization of A beta 42(43) and A beta 40 in senile plaques with end-specific A beta monoclonals: evidence that an initially deposited species is A beta 42(43).* Neuron, 1994. **13**(1): p. 45-53.
68. Jarrett, J.T., E.P. Berger, and P.T. Lansbury, Jr., *The carboxy terminus of the beta amyloid protein is critical for the seeding of amyloid formation: implications for the pathogenesis of Alzheimer's disease.* Biochemistry, 1993. **32**(18): p. 4693-7.
69. Yan, Y. and C. Wang, *Abeta40 protects non-toxic Abeta42 monomer from aggregation.* J Mol Biol, 2007. **369**(4): p. 909-16.
70. Younkin, S.G., *The role of A beta 42 in Alzheimer's disease.* J Physiol Paris, 1998. **92**(3-4): p. 289-92.
71. Yamaguchi, H., et al., *Diffuse type of senile plaques in the brains of Alzheimer-type dementia.* Acta Neuropathol, 1988. **77**(2): p. 113-9.
72. Tagliavini, F., et al., *Preamyloid deposits in the cerebral cortex of patients with Alzheimer's disease and nondemented individuals.* Neurosci Lett, 1988. **93**(2-3): p. 191-6.
73. Grundke-Iqbal, I., et al., *Abnormal phosphorylation of the microtubule-associated protein tau (tau) in Alzheimer cytoskeletal pathology.* Proc Natl Acad Sci U S A, 1986. **83**(13): p. 4913-7.
74. Ihara, Y., et al., *Phosphorylated tau protein is integrated into paired helical filaments in Alzheimer's disease.* J Biochem, 1986. **99**(6): p. 1807-10.
75. Kosik, K.S., C.L. Joachim, and D.J. Selkoe, *Microtubule-associated protein tau (tau) is a major antigenic component of paired helical filaments in Alzheimer disease.* Proc Natl Acad Sci U S A, 1986. **83**(11): p. 4044-8.
76. Buee, L., et al., *Tau protein isoforms, phosphorylation and role in neurodegenerative disorders.* Brain Res Brain Res Rev, 2000. **33**(1): p. 95-130.
77. Friedhoff, P., et al., *Structure of tau protein and assembly into paired helical filaments.* Biochim Biophys Acta, 2000. **1502**(1): p. 122-32.
78. Lichtenberg, B., et al., *Structure and elasticity of microtubule-associated protein tau.* Nature, 1988. **334**(6180): p. 359-62.
79. Schweers, O., et al., *Structural studies of tau protein and Alzheimer paired helical filaments show no evidence for beta-structure.* J Biol Chem, 1994. **269**(39): p. 24290-7.
80. Wille, H., et al., *Alzheimer-like paired helical filaments and antiparallel dimers formed from microtubule-associated protein tau in vitro.* J Cell Biol, 1992. **118**(3): p. 573-84.
81. Mandelkow, E.M. and E. Mandelkow, *Tau in Alzheimer's disease.* Trends Cell Biol, 1998. **8**(11): p. 425-7.
82. Himmler, A., et al., *Tau consists of a set of proteins with repeated C-terminal microtubule-binding domains and variable N-terminal domains.* Mol Cell Biol, 1989. **9**(4): p. 1381-8.
83. Goedert, M., et al., *Multiple isoforms of human microtubule-associated protein tau: sequences and localization in neurofibrillary tangles of Alzheimer's disease.* Neuron, 1989. **3**(4): p. 519-26.
84. Butner, K.A. and M.W. Kirschner, *Tau protein binds to microtubules through a flexible array of distributed weak sites.* J Cell Biol, 1991. **115**(3): p. 717-30.
85. Goode, B.L. and S.C. Feinstein, *Identification of a novel microtubule binding and assembly domain in the developmentally regulated inter-repeat region of tau.* J Cell Biol, 1994. **124**(5): p. 769-82.

86. Makrides, V., et al., *Evidence for two distinct binding sites for tau on microtubules.* Proc Natl Acad Sci U S A, 2004. **101**(17): p. 6746-51.
87. Binder, L.I., A. Frankfurter, and L.I. Rebhun, *The distribution of tau in the mammalian central nervous system.* J Cell Biol, 1985. **101**(4): p. 1371-8.
88. Kempf, M., et al., *Tau binds to the distal axon early in development of polarity in a microtubule- and microfilament-dependent manner.* J Neurosci, 1996. **16**(18): p. 5583-92.
89. Shin, R.W., et al., *Hydrated autoclave pretreatment enhances tau immunoreactivity in formalin-fixed normal and Alzheimer's disease brain tissues.* Lab Invest, 1991. **64**(5): p. 693-702.
90. LoPresti, P., et al., *Functional implications for the microtubule-associated protein tau: localization in oligodendrocytes.* Proc Natl Acad Sci U S A, 1995. **92**(22): p. 10369-73.
91. Weingarten, M.D., et al., *A protein factor essential for microtubule assembly.* Proc Natl Acad Sci U S A, 1975. **72**(5): p. 1858-62.
92. Drubin, D.G. and M.W. Kirschner, *Tau protein function in living cells.* J Cell Biol, 1986. **103**(6 Pt 2): p. 2739-46.
93. Goedert, M., et al., *Cloning and sequencing of the cDNA encoding a core protein of the paired helical filament of Alzheimer disease: identification as the microtubule-associated protein tau.* Proc Natl Acad Sci U S A, 1988. **85**(11): p. 4051-5.
94. Jancsik, V., et al., *Binding of microtubule-associated proteins (MAPs) to rat brain mitochondria: a comparative study of the binding of MAP2, its microtubule-binding and projection domains, and tau proteins.* Cell Motil Cytoskeleton, 1989. **14**(3): p. 372-81.
95. Sattilaro, R.F., W.L. Dentler, and E.L. LeCluyse, *Microtubule-associated proteins (MAPs) and the organization of actin filaments in vitro.* J Cell Biol, 1981. **90**(2): p. 467-73.
96. Griffith, L.M. and T.D. Pollard, *The interaction of actin filaments with microtubules and microtubule-associated proteins.* J Biol Chem, 1982. **257**(15): p. 9143-51.
97. Correas, I., R. Padilla, and J. Avila, *The tubulin-binding sequence of brain microtubule-associated proteins, tau and MAP-2, is also involved in actin binding.* Biochem J, 1990. **269**(1): p. 61-4.
98. Brandt, R., J. Leger, and G. Lee, *Interaction of tau with the neural plasma membrane mediated by tau's amino-terminal projection domain.* J Cell Biol, 1995. **131**(5): p. 1327-40.
99. Lau, L.F., et al., *Tau protein phosphorylation as a therapeutic target in Alzheimer's disease.* Curr Top Med Chem, 2002. **2**(4): p. 395-415.
100. Reszka, A.A., et al., *Association of mitogen-activated protein kinase with the microtubule cytoskeleton.* Proc Natl Acad Sci U S A, 1995. **92**(19): p. 8881-5.
101. Ebneth, A., et al., *Overexpression of tau protein inhibits kinesin-dependent trafficking of vesicles, mitochondria, and endoplasmic reticulum: implications for Alzheimer's disease.* J Cell Biol, 1998. **143**(3): p. 777-94.
102. Jenkins, S.M. and G.V. Johnson, *Tau complexes with phospholipase C-gamma in situ.* Neuroreport, 1998. **9**(1): p. 67-71.
103. Sontag, E., et al., *Molecular interactions among protein phosphatase 2A, tau, and microtubules. Implications for the regulation of tau phosphorylation and the development of tauopathies.* J Biol Chem, 1999. **274**(36): p. 25490-8.
104. Johnson, G.V. and W.H. Stoothoff, *Tau phosphorylation in neuronal cell function and dysfunction.* J Cell Sci, 2004. **117**(Pt 24): p. 5721-9.

105. Chen, F., et al., *Posttranslational modifications of tau - Role in human tauopathies and modeling in transgenic animals.* Curr Drug Targets, 2004. **5**(6): p. 503-15.
106. Reynolds, C.H., et al., *Phosphorylation regulates tau interactions with Src homology 3 domains of phosphatidylinositol 3-kinase, phospholipase Cgamma1, Grb2, and Src family kinases.* J Biol Chem, 2008. **283**(26): p. 18177-86.
107. Sadik, G., et al., *Phosphorylation of tau at Ser214 mediates its interaction with 14-3-3 protein: implications for the mechanism of tau aggregation.* J Neurochem, 2009. **108**(1): p. 33-43.
108. Ksiezak-Reding, H., W.K. Liu, and S.H. Yen, *Phosphate analysis and dephosphorylation of modified tau associated with paired helical filaments.* Brain Res, 1992. **597**(2): p. 209-19.
109. Muyllaert, D., et al., *Glycogen synthase kinase-3beta, or a link between amyloid and tau pathology?* Genes Brain Behav, 2008. **7 Suppl 1**: p. 57-66.
110. Ishiguro, K., et al., *Tau protein kinase I converts normal tau protein into A68-like component of paired helical filaments.* J Biol Chem, 1992. **267**(15): p. 10897-901.
111. Jicha, G.A., et al., *Alz-50 and MC-1, a new monoclonal antibody raised to paired helical filaments, recognize conformational epitopes on recombinant tau.* J Neurosci Res, 1997. **48**(2): p. 128-32.
112. Biernat, J., et al., *Phosphorylation of Ser262 strongly reduces binding of tau to microtubules: distinction between PHF-like immunoreactivity and microtubule binding.* Neuron, 1993. **11**(1): p. 153-63.
113. Bramblett, G.T., et al., *Abnormal tau phosphorylation at Ser396 in Alzheimer's disease recapitulates development and contributes to reduced microtubule binding.* Neuron, 1993. **10**(6): p. 1089-99.
114. Goedert, M., M.G. Spillantini, and S.W. Davies, *Filamentous nerve cell inclusions in neurodegenerative diseases.* Curr Opin Neurobiol, 1998. **8**(5): p. 619-32.
115. Goedert, M., et al., *Tau proteins of Alzheimer paired helical filaments: abnormal phosphorylation of all six brain isoforms.* Neuron, 1992. **8**(1): p. 159-68.
116. Crowther, R.A. and C.M. Wischik, *Image reconstruction of the Alzheimer paired helical filament.* Embo J, 1985. **4**(13B): p. 3661-5.
117. Crowther, R.A., *Straight and paired helical filaments in Alzheimer disease have a common structural unit.* Proc Natl Acad Sci U S A, 1991. **88**(6): p. 2288-92.
118. DeTure, M.A., L. Di Noto, and D.L. Purich, *In vitro assembly of Alzheimer-like filaments. How a small cluster of charged residues in Tau and MAP2 controls filament morphology.* J Biol Chem, 2002. **277**(38): p. 34755-9.
119. Kidd, M., *Paired helical filaments in electron microscopy of Alzheimer's disease.* Nature, 1963. **197**: p. 192-3.
120. Billingsley, M.L. and R.L. Kincaid, *Regulated phosphorylation and dephosphorylation of tau protein: effects on microtubule interaction, intracellular trafficking and neurodegeneration.* Biochem J, 1997. **323 (Pt 3)**: p. 577-91.
121. Novak, M., *Truncated tau protein as a new marker for Alzheimer's disease.* Acta Virol, 1994. **38**(3): p. 173-89.
122. Wang, J.Z., I. Grundke-Iqbal, and K. Iqbal, *Glycosylation of microtubule-associated protein tau: an abnormal posttranslational modification in Alzheimer's disease.* Nat Med, 1996. **2**(8): p. 871-5.
123. Yan, S.D., et al., *Glycated tau protein in Alzheimer disease: a mechanism for induction of oxidant stress.* Proc Natl Acad Sci U S A, 1994. **91**(16): p. 7787-91.
124. Bondareff, W., et al., *Molecular analysis of neurofibrillary degeneration in Alzheimer's disease. An immunohistochemical study.* Am J Pathol, 1990. **137**(3): p. 711-23.

125. Tucholski, J., J. Kuret, and G.V. Johnson, *Tau is modified by tissue transglutaminase in situ: possible functional and metabolic effects of polyamination.* J Neurochem, 1999. **73**(5): p. 1871-80.
126. Horiguchi, T., et al., *Nitration of tau protein is linked to neurodegeneration in tauopathies.* Am J Pathol, 2003. **163**(3): p. 1021-31.
127. Scheffler, I.E., *A century of mitochondrial research: achievements and perspectives.* Mitochondrion, 2001. **1**(1): p. 3-31.
128. Jacobson, J. and M.R. Duchen, *Interplay between mitochondria and cellular calcium signalling.* Mol Cell Biochem, 2004. **256-257**(1-2): p. 209-18.
129. Mattson, M.P., M. Gleichmann, and A. Cheng, *Mitochondria in neuroplasticity and neurological disorders.* Neuron, 2008. **60**(5): p. 748-66.
130. Sas, K., et al., *Mitochondria, metabolic disturbances, oxidative stress and the kynurenine system, with focus on neurodegenerative disorders.* J Neurol Sci, 2007. **257**(1-2): p. 221-39.
131. Roesch, K., et al., *Human deafness dystonia syndrome is caused by a defect in assembly of the DDP1/TIMM8a-TIMM13 complex.* Hum Mol Genet, 2002. **11**(5): p. 477-86.
132. Kunji, E.R., *The role and structure of mitochondrial carriers.* FEBS Lett, 2004. **564**(3): p. 239-44.
133. Liu, X., et al., *Induction of apoptotic program in cell-free extracts: requirement for dATP and cytochrome c.* Cell, 1996. **86**(1): p. 147-57.
134. Susin, S.A., et al., *Molecular characterization of mitochondrial apoptosis-inducing factor.* Nature, 1999. **397**(6718): p. 441-6.
135. Green, D.R. and G.I. Evan, *A matter of life and death.* Cancer Cell, 2002. **1**(1): p. 19-30.
136. Reddy, P.H., *Mitochondrial dysfunction in aging and Alzheimer's disease: strategies to protect neurons.* Antioxid Redox Signal, 2007. **9**(10): p. 1647-58.
137. Chance, B., H. Sies, and A. Boveris, *Hydroperoxide metabolism in mammalian organs.* Physiol Rev, 1979. **59**(3): p. 527-605.
138. Wallace, D.C., *A mitochondrial paradigm of metabolic and degenerative diseases, aging, and cancer: a dawn for evolutionary medicine.* Annu Rev Genet, 2005. **39**: p. 359-407.
139. Hunter, D.J., et al., *Angular dependences of perpendicular and parallel mode electron paramagnetic resonance of oxidized beef heart cytochrome c oxidase.* Biophys J, 2000. **78**(1): p. 439-50.
140. Brookes, P.S., et al., *Calcium, ATP, and ROS: a mitochondrial love-hate triangle.* Am J Physiol Cell Physiol, 2004. **287**(4): p. C817-33.
141. Nicholls, D.G., *Mitochondrial membrane potential and aging.* Aging Cell, 2004. **3**(1): p. 35-40.
142. Heales, S.J., et al., *Nitric oxide, mitochondria and neurological disease.* Biochim Biophys Acta, 1999. **1410**(2): p. 215-28.
143. Ghafourifar, P. and E. Cadenas, *Mitochondrial nitric oxide synthase.* Trends Pharmacol Sci, 2005. **26**(4): p. 190-5.
144. Krauss, S., C.Y. Zhang, and B.B. Lowell, *The mitochondrial uncoupling-protein homologues.* Nat Rev Mol Cell Biol, 2005. **6**(3): p. 248-61.
145. Graier, W.F., M. Trenker, and R. Malli, *Mitochondrial Ca2+, the secret behind the function of uncoupling proteins 2 and 3?* Cell Calcium, 2008. **44**(1): p. 36-50.
146. Andrews, Z.B., S. Diano, and T.L. Horvath, *Mitochondrial uncoupling proteins in the CNS: in support of function and survival.* Nat Rev Neurosci, 2005. **6**(11): p. 829-40.

147. Cannon, B. and J. Nedergaard, *Brown adipose tissue: function and physiological significance.* Physiol Rev, 2004. **84**(1): p. 277-359.
148. Spees, J.L., et al., *Mitochondrial transfer between cells can rescue aerobic respiration.* Proc Natl Acad Sci U S A, 2006. **103**(5): p. 1283-8.
149. DiMauro, S. and E.A. Schon, *Mitochondrial respiratory-chain diseases.* N Engl J Med, 2003. **348**(26): p. 2656-68.
150. Reddy, P.H. and M.F. Beal, *Are mitochondria critical in the pathogenesis of Alzheimer's disease?* Brain Res Brain Res Rev, 2005. **49**(3): p. 618-32.
151. Cohen, B.H. and D.R. Gold, *Mitochondrial cytopathy in adults: what we know so far.* Cleve Clin J Med, 2001. **68**(7): p. 625-6, 629-42.
152. Veltri, K.L., M. Espiritu, and G. Singh, *Distinct genomic copy number in mitochondria of different mammalian organs.* J Cell Physiol, 1990. **143**(1): p. 160-4.
153. Gray, M.W., *Origin and evolution of mitochondrial DNA.* Annu Rev Cell Biol, 1989. **5**: p. 25-50.
154. Reddy, P.H., *Mitochondrial medicine for aging and neurodegenerative diseases.* Neuromolecular Med, 2008. **10**(4): p. 291-315.
155. Papa, S., *Mitochondrial oxidative phosphorylation changes in the life span. Molecular aspects and physiopathological implications.* Biochim Biophys Acta, 1996. **1276**(2): p. 87-105.
156. Mandavilli, B.S., J.H. Santos, and B. Van Houten, *Mitochondrial DNA repair and aging.* Mutat Res, 2002. **509**(1-2): p. 127-51.
157. Anderson, S., et al., *Sequence and organization of the human mitochondrial genome.* Nature, 1981. **290**(5806): p. 457-65.
158. DiMauro, S., *Mitochondrial encephalomyopathies: what next?* J Inherit Metab Dis, 1996. **19**(4): p. 489-503.
159. Wallace, D.C., *The mitochondrial genome in human adaptive radiation and disease: on the road to therapeutics and performance enhancement.* Gene, 2005. **354**: p. 169-80.
160. Croteau, D.L. and V.A. Bohr, *Repair of oxidative damage to nuclear and mitochondrial DNA in mammalian cells.* J Biol Chem, 1997. **272**(41): p. 25409-12.
161. Yakes, F.M. and B. Van Houten, *Mitochondrial DNA damage is more extensive and persists longer than nuclear DNA damage in human cells following oxidative stress.* Proc Natl Acad Sci U S A, 1997. **94**(2): p. 514-9.
162. Celeste, A., et al., *H2AX haploinsufficiency modifies genomic stability and tumor susceptibility.* Cell, 2003. **114**(3): p. 371-83.
163. Krieger, C. and M.R. Duchen, *Mitochondria, Ca2+ and neurodegenerative disease.* Eur J Pharmacol, 2002. **447**(2-3): p. 177-88.
164. Chang, D.T. and I.J. Reynolds, *Mitochondrial trafficking and morphology in healthy and injured neurons.* Prog Neurobiol, 2006. **80**(5): p. 241-68.
165. Luft, R., et al., *A case of severe hypermetabolism of nonthyroid origin with a defect in the maintenance of mitochondrial respiratory control: a correlated clinical, biochemical, and morphological study.* J Clin Invest, 1962. **41**: p. 1776-804.
166. Wallace, D.C., *Mitochondrial diseases in man and mouse.* Science, 1999. **283**(5407): p. 1482-8.
167. DiMauro, S., *Mitochondrial diseases.* Biochim Biophys Acta, 2004. **1658**(1-2): p. 80-8.
168. Shigenaga, M.K., T.M. Hagen, and B.N. Ames, *Oxidative damage and mitochondrial decay in aging.* Proc Natl Acad Sci U S A, 1994. **91**(23): p. 10771-8.
169. Harper, M.E., et al., *Ageing, oxidative stress, and mitochondrial uncoupling.* Acta Physiol Scand, 2004. **182**(4): p. 321-31.

170. Adam-Vizi, V. and C. Chinopoulos, *Bioenergetics and the formation of mitochondrial reactive oxygen species.* Trends Pharmacol Sci, 2006. **27**(12): p. 639-45.
171. Evans, J.L., et al., *Oxidative stress and stress-activated signaling pathways: a unifying hypothesis of type 2 diabetes.* Endocr Rev, 2002. **23**(5): p. 599-622.
172. Carreras, M.C., et al., *Nitric oxide, complex I, and the modulation of mitochondrial reactive species in biology and disease.* Mol Aspects Med, 2004. **25**(1-2): p. 125-39.
173. Richter, C., J.W. Park, and B.N. Ames, *Normal oxidative damage to mitochondrial and nuclear DNA is extensive.* Proc Natl Acad Sci U S A, 1988. **85**(17): p. 6465-7.
174. Balaban, R.S., S. Nemoto, and T. Finkel, *Mitochondria, oxidants, and aging.* Cell, 2005. **120**(4): p. 483-95.
175. Vinogradov, A.D. and V.G. Grivennikova, *Generation of superoxide-radical by the NADH:ubiquinone oxidoreductase of heart mitochondria.* Biochemistry (Mosc), 2005. **70**(2): p. 120-7.
176. Finkel, T. and N.J. Holbrook, *Oxidants, oxidative stress and the biology of ageing.* Nature, 2000. **408**(6809): p. 239-47.
177. Green, K., M.D. Brand, and M.P. Murphy, *Prevention of mitochondrial oxidative damage as a therapeutic strategy in diabetes.* Diabetes., 2004. **53 Suppl 1**: p. S110-8.
178. Sies, H., *Strategies of antioxidant defense.* Eur J Biochem, 1993. **215**(2): p. 213-9.
179. Gilgun-Sherki, Y., E. Melamed, and D. Offen, *Oxidative stress induced-neurodegenerative diseases: the need for antioxidants that penetrate the blood brain barrier.* Neuropharmacology, 2001. **40**(8): p. 959-75.
180. Veal, E.A., A.M. Day, and B.A. Morgan, *Hydrogen peroxide sensing and signaling.* Mol Cell, 2007. **26**(1): p. 1-14.
181. Giorgio, M., et al., *Hydrogen peroxide: a metabolic by-product or a common mediator of ageing signals?* Nat Rev Mol Cell Biol, 2007. **8**(9): p. 722-8.
182. Kishida, K.T. and E. Klann, *Sources and targets of reactive oxygen species in synaptic plasticity and memory.* Antioxid Redox Signal, 2007. **9**(2): p. 233-44.
183. Gutteridge, J.M. and B. Halliwell, *Free radicals and antioxidants in the year 2000. A historical look to the future.* Ann N Y Acad Sci, 2000. **899**: p. 136-47.
184. Wei, Y.H., et al., *Oxidative damage and mutation to mitochondrial DNA and age-dependent decline of mitochondrial respiratory function.* Ann N Y Acad Sci, 1998. **854**: p. 155-70.
185. Duchen, M.R., *Mitochondria in health and disease: perspectives on a new mitochondrial biology.* Mol Aspects Med, 2004. **25**(4): p. 365-451.
186. James, A.M. and M.P. Murphy, *How mitochondrial damage affects cell function.* J Biomed Sci, 2002. **9**(6 Pt 1): p. 475-87.
187. Vasquez-Vivar, J., B. Kalyanaraman, and M.C. Kennedy, *Mitochondrial aconitase is a source of hydroxyl radical. An electron spin resonance investigation.* J Biol Chem, 2000. **275**(19): p. 14064-9.
188. Goldstein, S. and G. Merenyi, *The chemistry of peroxynitrite: implications for biological activity.* Methods Enzymol, 2008. **436**: p. 49-61.
189. Brown, G.C. and V. Borutaite, *Nitric oxide inhibition of mitochondrial respiration and its role in cell death.* Free Radic Biol Med, 2002. **33**(11): p. 1440-50.
190. Chan, D.C., *Mitochondria: dynamic organelles in disease, aging, and development.* Cell, 2006. **125**(7): p. 1241-52.
191. Trifunovic, A., *Mitochondrial DNA and ageing.* Biochim Biophys Acta, 2006. **1757**(5-6): p. 611-7.
192. Beal, M.F., *Mitochondria take center stage in aging and neurodegeneration.* Ann Neurol, 2005. **58**(4): p. 495-505.
193. Reed, J.C., *Mechanisms of apoptosis.* Am J Pathol, 2000. **157**(5): p. 1415-30.

194. Desagher, S. and J.C. Martinou, *Mitochondria as the central control point of apoptosis.* Trends Cell Biol, 2000. **10**(9): p. 369-77.

195. Green, D.R. and J.C. Reed, *Mitochondria and apoptosis.* Science, 1998. **281**(5381): p. 1309-12.

196. Wadia, J.S., et al., *Mitochondrial membrane potential and nuclear changes in apoptosis caused by serum and nerve growth factor withdrawal: time course and modification by (-)-deprenyl.* J Neurosci, 1998. **18**(3): p. 932-47.

197. Chandra, D., J.W. Liu, and D.G. Tang, *Early mitochondrial activation and cytochrome c up-regulation during apoptosis.* J Biol Chem, 2002. **277**(52): p. 50842-54.

198. Kroemer, G., L. Galluzzi, and C. Brenner, *Mitochondrial membrane permeabilization in cell death.* Physiol Rev, 2007. **87**(1): p. 99-163.

199. Reed, J.C., J.M. Jurgensmeier, and S. Matsuyama, *Bcl-2 family proteins and mitochondria.* Biochim Biophys Acta, 1998. **1366**(1-2): p. 127-37.

200. Mosconi, L., et al., *Hippocampal hypometabolism predicts cognitive decline from normal aging.* Neurobiol Aging, 2008. **29**(5): p. 676-92.

201. Hirai, K., et al., *Mitochondrial abnormalities in Alzheimer's disease.* J Neurosci., 2001. **21**(9): p. 3017-23.

202. Eckert, A., et al., *Mitochondrial dysfunction, apoptotic cell death, and Alzheimer's disease.* Biochem Pharmacol., 2003. **66**(8): p. 1627-34.

203. Keil, U., et al., *Amyloid beta-induced changes in nitric oxide production and mitochondrial activity lead to apoptosis.* J Biol Chem., 2004. **279**(48): p. 50310-20. Epub 2004 Sep 14.

204. Manczak, M., et al., *Differential expression of oxidative phosphorylation genes in patients with Alzheimer's disease: implications for early mitochondrial dysfunction and oxidative damage.* Neuromolecular Med, 2004. **5**(2): p. 147-62.

205. Nunomura, A., et al., *Involvement of oxidative stress in Alzheimer disease.* J Neuropathol Exp Neurol, 2006. **65**(7): p. 631-41.

206. Lin, M.T. and M.F. Beal, *Alzheimer's APP mangles mitochondria.* Nat Med., 2006. **12**(11): p. 1241-3.

207. Hauptmann, S., et al., *Mitochondrial dysfunction in sporadic and genetic Alzheimer's disease.* Exp Gerontol., 2006. **41**(7): p. 668-73. Epub 2006 May 4.

208. Schuessel, K., et al., *Impaired Cu/Zn-SOD activity contributes to increased oxidative damage in APP transgenic mice.* Neurobiol Dis., 2005. **18**(1): p. 89-99.

209. Smith, M.A., et al., *Oxidative damage in Alzheimer's.* Nature, 1996. **382**(6587): p. 120-1.

210. Bozner, P., et al., *The amyloid beta protein induces oxidative damage of mitochondrial DNA.* J Neuropathol Exp Neurol, 1997. **56**(12): p. 1356-62.

211. Swerdlow, R.H., et al., *Cybrids in Alzheimer's disease: a cellular model of the disease?* Neurology, 1997. **49**(4): p. 918-25.

212. Smith, M.A., et al., *Amyloid-beta deposition in Alzheimer transgenic mice is associated with oxidative stress.* J Neurochem, 1998. **70**(5): p. 2212-5.

213. Anandatheerthavarada, H.K., et al., *Mitochondrial targeting and a novel transmembrane arrest of Alzheimer's amyloid precursor protein impairs mitochondrial function in neuronal cells.* J Cell Biol, 2003. **161**(1): p. 41-54.

214. Manczak, M., et al., *Mitochondria are a direct site of A beta accumulation in Alzheimer's disease neurons: implications for free radical generation and oxidative damage in disease progression.* Hum Mol Genet., 2006. **15**(9): p. 1437-49. Epub 2006 Mar 21.

215. Leutner, S., et al., *Enhanced ROS-generation in lymphocytes from Alzheimer's patients.* Pharmacopsychiatry, 2005. **38**(6): p. 312-5.
216. Parker, W.D., Jr., C.M. Filley, and J.K. Parks, *Cytochrome oxidase deficiency in Alzheimer's disease.* Neurology, 1990. **40**(8): p. 1302-3.
217. Gibson, G.E., K.F. Sheu, and J.P. Blass, *Abnormalities of mitochondrial enzymes in Alzheimer disease.* J Neural Transm, 1998. **105**(8-9): p. 855-70.
218. Mungarro-Menchaca, X., et al., *beta-Amyloid peptide induces ultrastructural changes in synaptosomes and potentiates mitochondrial dysfunction in the presence of ryanodine.* J Neurosci Res, 2002. **68**(1): p. 89-96.
219. Gillardon, F., et al., *Proteomic and functional alterations in brain mitochondria from Tg2576 mice occur before amyloid plaque deposition.* Proteomics, 2007. **7**(4): p. 605-16.
220. Kann, O. and R. Kovacs, *Mitochondria and neuronal activity.* Am J Physiol Cell Physiol, 2007. **292**(2): p. C641-57.
221. Fernandez-Vizarra, P., et al., *Intra- and extracellular Abeta and PHF in clinically evaluated cases of Alzheimer's disease.* Histol Histopathol., 2004. **19**(3): p. 823-44.
222. Lustbader, J.W., et al., *ABAD directly links Abeta to mitochondrial toxicity in Alzheimer's disease.* Science., 2004. **304**(5669): p. 448-52.
223. Walsh, D.M., et al., *Naturally secreted oligomers of amyloid beta protein potently inhibit hippocampal long-term potentiation in vivo.* Nature, 2002. **416**(6880): p. 535-9.
224. Gouras, G.K., et al., *Intraneuronal Abeta42 accumulation in human brain.* Am J Pathol, 2000. **156**(1): p. 15-20.
225. Oddo, S., et al., *Triple-transgenic model of Alzheimer's disease with plaques and tangles: intracellular Abeta and synaptic dysfunction.* Neuron, 2003. **39**(3): p. 409-21.
226. Knobloch, M., et al., *Intracellular Abeta and cognitive deficits precede beta-amyloid deposition in transgenic arcAbeta mice.* Neurobiol Aging, 2007. **28**(9): p. 1297-306.
227. Oakley, H., et al., *Intraneuronal beta-amyloid aggregates, neurodegeneration, and neuron loss in transgenic mice with five familial Alzheimer's disease mutations: potential factors in amyloid plaque formation.* J Neurosci, 2006. **26**(40): p. 10129-40.
228. Selkoe, D.J., *Alzheimer's disease: genotypes, phenotypes, and treatments.* Science, 1997. **275**(5300): p. 630-1.
229. Leuner, K., et al., *Mitochondrial dysfunction: the first domino in brain aging and Alzheimer's disease?* Antioxid Redox Signal, 2007. **9**(10): p. 1659-75.
230. Eckert, A., et al., *Mitochondrial dysfunction, apoptotic cell death, and Alzheimer's disease.* Biochem Pharmacol, 2003. **66**(8): p. 1627-34.
231. Chagnon, P., et al., *Distribution of brain cytochrome oxidase activity in various neurodegenerative diseases.* Neuroreport., 1995. **6**(5): p. 711-5.
232. Glabe, C.G. and R. Kayed, *Common structure and toxic function of amyloid oligomers implies a common mechanism of pathogenesis.* Neurology, 2006. **66**(2 Suppl 1): p. S74-8.
233. Reddy, P.H. and M.F. Beal, *Amyloid beta, mitochondrial dysfunction and synaptic damage: implications for cognitive decline in aging and Alzheimer's disease.* Trends Mol Med, 2008. **14**(2): p. 45-53.
234. Crouch, P.J., et al., *Copper-dependent inhibition of human cytochrome c oxidase by a dimeric conformer of amyloid-beta1-42.* J Neurosci, 2005. **25**(3): p. 672-9.
235. Caspersen, C., et al., *Mitochondrial Abeta: a potential focal point for neuronal metabolic dysfunction in Alzheimer's disease.* Faseb J, 2005. **19**(14): p. 2040-1.
236. Lustbader, J.W., et al., *ABAD directly links Abeta to mitochondrial toxicity in Alzheimer's disease.* Science, 2004. **304**(5669): p. 448-52.

237. Keil, U., et al., *Amyloid beta-induced changes in nitric oxide production and mitochondrial activity lead to apoptosis.* J Biol Chem, 2004. **279**(48): p. 50310-20.
238. Eckert, A., et al., *Soluble beta-amyloid leads to mitochondrial defects in amyloid precursor protein and tau transgenic mice.* Neurodegener Dis, 2008. **5**(3-4): p. 157-9.
239. David, D.C., et al., *Proteomic and functional analyses reveal a mitochondrial dysfunction in P301L tau transgenic mice.* J Biol Chem., 2005. **280**(25): p. 23802-14. Epub 2005 Apr 14.
240. Eckert, A., et al., *Oligomeric and fibrillar species of beta-amyloid (A beta 42) both impair mitochondrial function in P301L tau transgenic mice.* J Mol Med, 2008. **86**(11): p. 1255-67.
241. Takuma, K., et al., *ABAD enhances Abeta-induced cell stress via mitochondrial dysfunction.* Faseb J, 2005. **19**(6): p. 597-8.
242. Chen, J.X. and S.D. Yan, *Amyloid-beta-induced mitochondrial dysfunction.* J Alzheimers Dis, 2007. **12**(2): p. 177-84.
243. Aleardi, A.M., et al., *Gradual alteration of mitochondrial structure and function by beta-amyloids: importance of membrane viscosity changes, energy deprivation, reactive oxygen species production, and cytochrome c release.* J Bioenerg Biomembr., 2005. **37**(4): p. 207-25.
244. White, A.R., et al., *Sublethal concentrations of prion peptide PrP106-126 or the amyloid beta peptide of Alzheimer's disease activates expression of proapoptotic markers in primary cortical neurons.* Neurobiol Dis, 2001. **8**(2): p. 299-316.
245. Ivins, K.J., E.T. Bui, and C.W. Cotman, *Beta-amyloid induces local neurite degeneration in cultured hippocampal neurons: evidence for neuritic apoptosis.* Neurobiol Dis, 1998. **5**(5): p. 365-78.
246. Casas, C., et al., *Massive CA1/2 neuronal loss with intraneuronal and N-terminal truncated Abeta42 accumulation in a novel Alzheimer transgenic model.* Am J Pathol, 2004. **165**(4): p. 1289-300.
247. Gomez-Ramos, P. and M. Asuncion Moran, *Ultrastructural localization of intraneuronal Abeta-peptide in Alzheimer disease brains.* J Alzheimers Dis, 2007. **11**(1): p. 53-9.
248. Wegiel, J., et al., *Intraneuronal Abeta immunoreactivity is not a predictor of brain amyloidosis-beta or neurofibrillary degeneration.* Acta Neuropathol, 2007. **113**(4): p. 389-402.
249. Hardy, J. and D.J. Selkoe, *The amyloid hypothesis of Alzheimer's disease: progress and problems on the road to therapeutics.* Science, 2002. **297**(5580): p. 353-6.
250. Fath, T., J. Eidenmuller, and R. Brandt, *Tau-mediated cytotoxicity in a pseudohyperphosphorylation model of Alzheimer's disease.* J Neurosci, 2002. **22**(22): p. 9733-41.
251. Giasson, B.I., V.M. Lee, and J.Q. Trojanowski, *Interactions of amyloidogenic proteins.* Neuromolecular Med, 2003. **4**(1-2): p. 49-58.
252. Kumar-Singh, S. and C. Van Broeckhoven, *Frontotemporal lobar degeneration: current concepts in the light of recent advances.* Brain Pathol, 2007. **17**(1): p. 104-14.
253. Takeda, A., et al., *In Alzheimer's disease, heme oxygenase is coincident with Alz50, an epitope of tau induced by 4-hydroxy-2-nonenal modification.* J Neurochem, 2000. **75**(3): p. 1234-41.
254. Liu, Q., et al., *Alzheimer-specific epitopes of tau represent lipid peroxidation-induced conformations.* Free Radic Biol Med, 2005. **38**(6): p. 746-54.
255. Perry, G., et al., *Activation of neuronal extracellular receptor kinase (ERK) in Alzheimer disease links oxidative stress to abnormal phosphorylation.* Neuroreport, 1999. **10**(11): p. 2411-5.

256. Mandelkow, E.M., et al., *MARK/PAR1 kinase is a regulator of microtubule-dependent transport in axons.* J Cell Biol, 2004. **167**(1): p. 99-110.

257. Gotz, J., L.M. Ittner, and S. Kins, *Do axonal defects in tau and amyloid precursor protein transgenic animals model axonopathy in Alzheimer's disease?* J Neurochem, 2006. **98**(4): p. 993-1006.

258. Thies, E. and E.M. Mandelkow, *Missorting of tau in neurons causes degeneration of synapses that can be rescued by the kinase MARK2/Par-1.* J Neurosci, 2007. **27**(11): p. 2896-907.

259. Alonso, A.D., et al., *Interaction of tau isoforms with Alzheimer's disease abnormally hyperphosphorylated tau and in vitro phosphorylation into the disease-like protein.* J Biol Chem, 2001. **276**(41): p. 37967-73.

260. Salehi, A., J.D. Delcroix, and W.C. Mobley, *Traffic at the intersection of neurotrophic factor signaling and neurodegeneration.* Trends Neurosci, 2003. **26**(2): p. 73-80.

261. Gotz, J., et al., *Formation of neurofibrillary tangles in P301l tau transgenic mice induced by Abeta 42 fibrils.* Science, 2001. **293**(5534): p. 1491-5.

262. Sergeant, N., et al., *Association of ATP synthase alpha-chain with neurofibrillary degeneration in Alzheimer's disease.* Neuroscience, 2003. **117**(2): p. 293-303.

263. Gotz, J., et al., *Amyloid-induced neurofibrillary tangle formation in Alzheimer's disease: insight from transgenic mouse and tissue-culture models.* Int J Dev Neurosci, 2004. **22**(7): p. 453-65.

264. Bolmont, T., et al., *Induction of tau pathology by intracerebral infusion of amyloid-beta -containing brain extract and by amyloid-beta deposition in APP x Tau transgenic mice.* Am J Pathol, 2007. **171**(6): p. 2012-20.

265. Clavaguera, F., et al., *Transmission and spreading of tauopathy in transgenic mouse brain.* Nat Cell Biol, 2009. **11**(7): p. 909-13.

266. Roberson, E.D., et al., *Reducing endogenous tau ameliorates amyloid beta-induced deficits in an Alzheimer's disease mouse model.* Science, 2007. **316**(5825): p. 750-4.

267. Rapoport, M., et al., *Tau is essential to beta -amyloid-induced neurotoxicity.* Proc Natl Acad Sci U S A, 2002. **99**(9): p. 6364-9.

268. Stamer, K., et al., *Tau blocks traffic of organelles, neurofilaments, and APP vesicles in neurons and enhances oxidative stress.* J Cell Biol, 2002. **156**(6): p. 1051-63.

269. Chen, F., et al., *Role for glyoxalase I in Alzheimer's disease.* Proc Natl Acad Sci U S A, 2004. **101**(20): p. 7687-92.

270. Hoerndli, F.J., et al., *Reference genes identified in SH-SY5Y cells using custom-made gene arrays with validation by quantitative polymerase chain reaction.* Anal Biochem, 2004. **335**(1): p. 30-41.

271. David, D., F. Hoerndli, and J. Gotz, *Functional Genomics meets neurodegenerative disorders Part I: Transcriptomic and proteomic technology.* Prog Neurobiol, 2005. **76**(3): p. 153-68.

272. Hoerndli, F., D. David, and J. Gotz, *Functional genomics meets neurodegenerative disorders. Part II: Application and data integration.* Prog Neurobiol, 2005. **76**(3): p. 169-88.

273. Arendt, T., *Synaptic plasticity and cell cycle activation in neurons are alternative effector pathways: the 'Dr. Jekyll and Mr. Hyde concept' of Alzheimer's disease or the yin and yang of neuroplasticity.* Prog Neurobiol, 2003. **71**(2-3): p. 83-248.

274. Hoerndli, F.J., et al., *Abeta treatment and P301L tau expression in an Alzheimer's disease tissue culture model act synergistically to promote aberrant cell cycle re-entry.* Eur J Neurosci., 2007. **26**(1): p. 60-72.

275. Games, D., et al., *Alzheimer-type neuropathology in transgenic mice overexpressing V717F beta-amyloid precursor protein [see comments]*. Nature, 1995. **373**(6514): p. 523-7.
276. Hsiao, K., et al., *Correlative memory deficits, Abeta elevation, and amyloid plaques in transgenic mice [see comments]*. Science, 1996. **274**(5284): p. 99-102.
277. Sturchler-Pierrat, C., et al., *Two amyloid precursor protein transgenic mouse models with Alzheimer disease-like pathology.* Proc Natl Acad Sci U S A, 1997. **94**(24): p. 13287-92.
278. Stalder, M., et al., *Association of microglia with amyloid plaques in brains of APP23 transgenic mice.* Am J Pathol, 1999. **154**(6): p. 1673-84.
279. Janus, C., et al., *A beta peptide immunization reduces behavioural impairment and plaques in a model of Alzheimer's disease.* Nature, 2000. **408**(6815): p. 979-82.
280. Mucke, L., et al., *High-level neuronal expression of abeta 1-42 in wild-type human amyloid protein precursor transgenic mice: synaptotoxicity without plaque formation.* J Neurosci, 2000. **20**(11): p. 4050-8.
281. Gotz, J., *Tau and transgenic animal models.* Brain Res Brain Res Rev, 2001. **35**(3): p. 266-86.
282. Gotz, J., et al., *Transgenic animal models of Alzheimer's disease and related disorders: Histopathology, behavior and therapy.* Mol Psychiatry, 2004. **9**: p. 664-683.
283. Gotz, J., et al., *Somatodendritic localization and hyperphosphorylation of tau protein in transgenic mice expressing the longest human brain tau isoform.* Embo J, 1995. **14**(7): p. 1304-13.
284. Gotz, J., et al., *Oligodendroglial tau filament formation in transgenic mice expressing G272V tau.* Eur J Neurosci, 2001. **13**(11): p. 2131-40.
285. Deters, N., L.M. Ittner, and J. Gotz, *Divergent phosphorylation pattern of tau in P301L tau transgenic mice.* Eur J Neurosci., 2008. **28**(1): p. 137-47.
286. Gotz, J., et al., *Tau filament formation in transgenic mice expressing P301L tau.* J Biol Chem, 2001. **276**(1): p. 529-34.
287. Pennanen, L., et al., *Accelerated extinction of conditioned taste aversion in P301L tau transgenic mice.* Neurobiol Dis, 2004. **15**(3): p. 500-9.
288. Pennanen, L., et al., *Impaired spatial reference memory and increased exploratory behavior in P301L tau transgenic mice.* Genes Brain Behav, 2006. **5**(5): p. 369-79.
289. Lewis, J., et al., *Enhanced neurofibrillary degeneration in transgenic mice expressing mutant tau and APP.* Science, 2001. **293**(5534): p. 1487-91.
290. Grueninger F, B.B., Czech C, Ballard TM, Frey JR, Weidensteiner C, von Kienlin M, Ozmen L, *Phosphorylation of Tau at S422 is enhanced by Abeta in TauPS2APP triple transgenic mice.* in press, 2009.
291. Boutajangout, A., et al., *Characterisation of cytoskeletal abnormalities in mice transgenic for wild-type human tau and familial Alzheimer's disease mutants of APP and presenilin-1.* Neurobiol Dis, 2004. **15**(1): p. 47-60.
292. Oddo, S., et al., *Amyloid deposition precedes tangle formation in a triple transgenic model of Alzheimer's disease.* Neurobiol Aging, 2003. **24**(8): p. 1063-70.
293. Gimenez-Llort, L., et al., *Modeling behavioral and neuronal symptoms of Alzheimer's disease in mice: a role for intraneuronal amyloid.* Neurosci Biobehav Rev, 2007. **31**(1): p. 125-47.
294. Behbahani, H., et al., *Differential role of Presenilin-1 and -2 on mitochondrial membrane potential and oxygen consumption in mouse embryonic fibroblasts.* J Neurosci Res, 2006. **84**(4): p. 891-902.

295. Kanowski, S., et al., *Proof of efficacy of the ginkgo biloba special extract EGb 761 in outpatients suffering from mild to moderate primary degenerative dementia of the Alzheimer type or multi-infarct dementia.* Pharmacopsychiatry, 1996. **29**(2): p. 47-56.

296. Le Bars, P.L., et al., *A placebo-controlled, double-blind, randomized trial of an extract of Ginkgo biloba for dementia. North American EGb Study Group.* Jama, 1997. **278**(16): p. 1327-32.

297. Napryeyenko, O. and I. Borzenko, *Ginkgo biloba special extract in dementia with neuropsychiatric features. A randomised, placebo-controlled, double-blind clinical trial.* Arzneimittelforschung, 2007. **57**(1): p. 4-11.

298. Yancheva, S., et al., *Ginkgo biloba extract EGb 761(R), donepezil or both combined in the treatment of Alzheimer's disease with neuropsychiatric features: a randomised, double-blind, exploratory trial.* Aging Ment Health, 2009. **13**(2): p. 183-90.

299. Mix, J.A. and W.D. Crews, Jr., *A double-blind, placebo-controlled, randomized trial of Ginkgo biloba extract EGb 761 in a sample of cognitively intact older adults: neuropsychological findings.* Hum Psychopharmacol, 2002. **17**(6): p. 267-77.

300. monograph, G.C.E., *Trockenextrakt (35-67:1) aus Ginkgo-Biloba-Blättern extrahiert mit Aceton-Wasser.* Bundesanzeiger, 1994. **46**: p. 7361-7362.

301. Curtis-Prior, P., D. Vere, and P. Fray, *Therapeutic value of Ginkgo biloba in reducing symptoms of decline in mental function.* J Pharm Pharmacol, 1999. **51**(5): p. 535-41.

302. DeFeudis, F.V. and K. Drieu, *Ginkgo biloba extract (EGb 761) and CNS functions: basic studies and clinical applications.* Curr Drug Targets, 2000. **1**(1): p. 25-58.

303. Zimmermann, M., et al., *Ginkgo biloba extract: from molecular mechanisms to the treatment of Alzhelmer's disease.* Cell Mol Biol (Noisy-le-grand), 2002. **48**(6): p. 613-23.

304. Gohil, K. and L. Packer, *Global gene expression analysis identifies cell and tissue specific actions of Ginkgo biloba extract, EGb 761.* Cell Mol Biol (Noisy-le-grand), 2002. **48**(6): p. 625-31.

305. Defeudis, F.V., *Bilobalide and neuroprotection.* Pharmacol Res, 2002. **46**(6): p. 565-8.

306. Smith, P.F., K. Maclennan, and C.L. Darlington, *The neuroprotective properties of the Ginkgo biloba leaf: a review of the possible relationship to platelet-activating factor (PAF).* J Ethnopharmacol, 1996. **50**(3): p. 131-9.

307. Lien, E.J., et al., *Quantitative structure-activity relationship analysis of phenolic antioxidants.* Free Radic Biol Med, 1999. **26**(3-4): p. 285-94.

308. Smith, J.V. and Y. Luo, *Elevation of oxidative free radicals in Alzheimer's disease models can be attenuated by Ginkgo biloba extract EGb 761.* J Alzheimers Dis, 2003. **5**(4): p. 287-300.

309. Schindowski, K., et al., *Age-related increase of oxidative stress-induced apoptosis in mice prevention by Ginkgo biloba extract (EGb761).* J Neural Transm, 2001. **108**(8-9): p. 969-78.

310. Smith, J.V., et al., *Anti-apoptotic properties of Ginkgo biloba extract EGb 761 in differentiated PC12 cells.* Cell Mol Biol (Noisy-le-grand), 2002. **48**(6): p. 699-707.

311. Eckert, A., et al., *Effects of EGb 761 Ginkgo biloba extract on mitochondrial function and oxidative stress.* Pharmacopsychiatry, 2003. **36 Suppl 1**: p. S15-23.

312. Eckert, A., et al., *Stabilization of Mitochondrial Membrane Potential and Improvement of Neuronal Energy Metabolism by Ginkgo Biloba Extract EGb 761.* Ann N Y Acad Sci., 2005. **1056**: p. 474-85.

313. Abdel-Kader, R., et al., *Stabilization of mitochondrial function by Ginkgo biloba extract (EGb 761).* Pharmacol Res, 2007. **56**(6): p. 493-502.

314. Luo, Y., et al., *Inhibition of amyloid-beta aggregation and caspase-3 activation by the Ginkgo biloba extract EGb761.* Proc Natl Acad Sci U S A, 2002. **99**(19): p. 12197-202.
315. Watanabe, C.M., et al., *The in vivo neuromodulatory effects of the herbal medicine ginkgo biloba.* Proc Natl Acad Sci U S A, 2001. **98**(12): p. 6577-80.
316. Bastianetto, S., et al., *The Ginkgo biloba extract (EGb 761) protects hippocampal neurons against cell death induced by beta-amyloid.* Eur J Neurosci, 2000. **12**(6): p. 1882-90.
317. Yao, Z., K. Drieu, and V. Papadopoulos, *The Ginkgo biloba extract EGb 761 rescues the PC12 neuronal cells from beta-amyloid-induced cell death by inhibiting the formation of beta-amyloid-derived diffusible neurotoxic ligands.* Brain Res, 2001. **889**(1-2): p. 181-90.
318. Colciaghi, F., et al., *Amyloid precursor protein metabolism is regulated toward alpha-secretase pathway by Ginkgo biloba extracts.* Neurobiol Dis, 2004. **16**(2): p. 454-60.
319. Ahlemeyer, B. and J. Krieglstein, *Neuroprotective effects of Ginkgo biloba extract.* Cell Mol Life Sci, 2003. **60**(9): p. 1779-92.
320. Oberpichler, H., et al., *PAF antagonist ginkgolide B reduces postischemic neuronal damage in rat brain hippocampus.* J Cereb Blood Flow Metab, 1990. **10**(1): p. 133-5.
321. Winter, E., *Effects of an extract of Ginkgo biloba on learning and memory in mice.* Pharmacol Biochem Behav, 1991. **38**(1): p. 109-14.
322. Winter, J.C., *The effects of an extract of Ginkgo biloba, EGb 761, on cognitive behavior and longevity in the rat.* Physiol Behav, 1998. **63**(3): p. 425-33.
323. Walesiuk, A. and J.J. Braszko, *Preventive action of Ginkgo biloba in stress- and corticosterone-induced impairment of spatial memory in rats.* Phytomedicine, 2009. **16**(1): p. 40-6.
324. Le Bars, P.L., M. Kieser, and K.Z. Itil, *A 26-week analysis of a double-blind, placebo-controlled trial of the ginkgo biloba extract EGb 761 in dementia.* Dement Geriatr Cogn Disord, 2000. **11**(4): p. 230-7.
325. Christen, Y., *Oxidative stress and Alzheimer disease.* Am J Clin Nutr, 2000. **71**(2): p. 621S-629S.

2. Amyloid-beta and tau synergistically impair the oxidative phosphorylation system in triple transgenic Alzheimer's disease mice

Virginie **Rhein**[*], Xiaomin Song[†], Andreas Wiesner[‡], Lars M. Ittner[‡], Ginette Baysang[*], Fides Meier[*], Laurence Ozmen[&], Horst Bluethmann[&], Stefan Dröse[¥], Ulrich Brandt[¥], Egemen Savaskan[*,$], Christian Czech[&], Jürgen Götz[‡,#], Anne Eckert[*]

[*]Neurobiology Laboratory for Brain Aging and Mental Health, Psychiatric University Clinics, University of Basel, 4025 Basel, Switzerland; [†]Australian Proteome Analysis Facility, Macquarie University, NSW, 2109, Australia; [‡]Alzheimer's & Parkinson's Disease Laboratory, Brain & Mind Research Institute, University of Sydney, 100 Mallett St, Camperdown, NSW 2050, Australia; [&]Hoffmann-La-Roche AG, Pharma Research, Neurosciences, 4070 Basel, Switzerland; [¥]Molecular Bioenergetics Group, Medical School, Cluster of Excellence Frankfurt "Macromolecular Complexes", Center for Membrane Proteomics, Johann Wolfgang Goethe-Universität, 60590 Frankfurt am Main, Germany; [$]Division of Psychiatric Research and Hospital for Psychogeriatric Medicine, University of Zurich, 8032 Zurich, Switzerland; [#]The Medical Foundation, University of Sydney, Camperdown, NSW 2050, Australia;

Under revision (Proceedings of the National Academy of Sciences of the United States of America)

ABSTRACT

Alzheimer's disease (AD) is characterized by β-amyloid (Aβ)-containing plaques, neurofibrillary tangles, as well as neuron and synapse loss. Tangle formation has been reproduced in P301L tau transgenic pR5 mice while $APP^{sw}PS2^{N141I}$ double-transgenic APP152 mice develop Aβ plaques. Cross-breeding generates triple transgenic (^{triple}AD) mice that combine both pathologies in one model. To determine functional consequences of the combined Aβ and tau pathologies, we performed a proteomic analysis followed by functional validation. Specifically, we obtained vesicular preparations from ^{triple}AD mice, the parental strains and non-transgenic mice, followed by the quantitative mass-tag labelling proteomic technique, iTRAQ, and mass spectrometry. Within 1275 quantified proteins, we found a massive deregulation of 24 proteins of which one third were mitochondrial proteins mainly related to complexes I and IV of the oxidative phosphorylation system (OXPHOS). Notably, deregulation of complex I was tau-dependent, while deregulation of complex IV was Aβ-dependent, both at the protein and activity levels. Synergistic effects of Aβ and tau were evident in 8-month-old ^{triple}AD mice as only they showed a reduction of the mitochondrial membrane potential at this early age. At the age of 12 months, the strongest defects on OXPHOS, synthesis of ATP and reactive oxygen species were exhibited in the ^{triple}AD mice, again emphasizing synergistic, age-associated effects of Aβ and tau in perishing mitochondria. Our study establishes a molecular link between Aβ and tau protein in AD pathology *in vivo* illustrating the potential of quantitative proteomics.

Abbreviations: Aβ, β-amyloid peptide; AD, Alzheimer's disease; APP, amyloid protein precursor; CS, citrate synthase; FTD, fronto-temporal dementia; GO, gene ontology; iTRAQ, isobaric tags for relative and absolute quantitation; LTP, long-term potentiation; MMP, mitochondrial membrane potential; NFT, neurofibrillary tangles; OXPHOS, oxidative phosphorylation system; ROS, reactive oxygen species; ^{triple}AD, triple transgenic Alzheimer's disease mice; wt, wild-type.

INTRODUCTION

Alzheimer's disease (AD) is a devastating neurodegenerative disorder affecting more than 15 million people worldwide (1). The key histopathological features are β-amyloid-containing plaques and microtubule-associated protein tau-containing neurofibrillary tangles (NFTs), along with neuronal and synapse loss in selected brain areas (2, 3). In determining the role of distinct proteins in these processes, traditionally, candidate-driven approaches have been pursued, linking neuronal dysfunction to the distribution of known proteins in healthy compared to degenerating neurons, or in transgenic compared to control brain. In comparison, proteomics offers a powerful non-biased approach as shown by us previously (4, 5).

APP152 (APP/PS2) double-transgenic mice model the Aβ plaque pathology of AD (6); they co-express the N141I mutant form of PS2 together with the APP^{sw} mutant found in familial cases of AD. The mice display age-related cognitive deficits associated with discrete brain Aβ deposition and inflammation (6). pR5 mice model the tangle pathology of AD (7-9). They express P301L mutant tau found in familial cases of frontotemporal dementia (FTD), a dementia related to AD. The pR5 mice show a hippocampus- and amygdala-dependent behavioural impairment related to AD (10). Crossing of pR5 and APP/PS2 mice produces ^{triple}AD mice, with tau and Aβ levels comparable to the parental strains (11).

Here, we performed a comparative, quantitative proteomic analysis of single-transgenic pR5, double-transgenic APP/PS2 and ^{triple}AD (pR5/APP/PS2) mice, as well as wild-type controls and found that one third of the deregulated proteins were mitochondrial. In evaluating our findings, we could establish mitochondrial dysfunction in ^{triple}AD mice, synergistically induced by tau and Aβ pathologies.

RESULTS

Comparative iTRAQ (isobaric tags for relative and absolute quantitation) mass-spectrometry. Crude vesicular fractions of forebrains obtained from 10 months-old single-transgenic pR5 mice, double-transgenic APP/PS2 mice, a cross of the two strains ($^{\text{triple}}$AD), and non-transgenic littermate controls were trypsin digested, and peptides labelled with iTRAQ. Then, these were separated by HPLC, using both reverse phase (RP) and strong cation exchange (SCX) columns, followed by nanoLC-ESI MS/MS mass spectrometry. Data processing identified 1598 proteins, 1539 of which were quantified; 1275 with more than two peptides. 24 proteins were found to be differentially expressed in $^{\text{triple}}$AD compared to the other samples (Table 1).

Deregulated proteins identified by iTRAQ. ProteinPilot requires a minimum of 40 counts of iTRAQ reporting ion intensities to calculate iTRAQ ratios. Proteins identified with iTRAQ tag ion intensities below this threshold were not quantified. In our study, about 90% of the identified proteins had iTRAQ ratios (SI Fig. 1A) and of these, about 80% were calculated from more than two peptides.

We tabulated iTRAQ ratios of all proteins using the $^{\text{triple}}$AD as denominator and iTRAQ ratios larger than 1.2 or smaller than 0.82 with a P-value smaller than 0.01 as threshold to identify deregulated proteins as listed in Table 1. A protein had to show the same deregulation trend in at least two of the three runs to be considered as deregulated. From our past experience iTRAQ ratios larger than 1.2 or smaller than 0.82 with a P-value smaller than 0.01 indicate protein differences of at least 1.5 fold.

Consistent with transgenic tau expression, the experimental data show that Tau is significantly up-regulated in pR5 mice and $^{\text{triple}}$AD mouse brain compared to wild-type and APP/PS2 mice. We performed an over-representation analysis using the Gene Ontology (GO) database to perform a functional characterization of the deregulated proteins and established a GO map as described (12). This revealed that one third of the proteins have functions in mitochondria, specifically complex I and IV (Table 1). In agreement, separation of mitochondrial complexes from cortical brain by two-dimensional resolution confirmed a similar deregulation of the 49 kDa subunit of complex I and subunits II and IV of complex IV (SI Fig. 1B). Therefore, we decided to assess $^{\text{triple}}$AD compared to pR5 and APP/PS2 mice for mitochondrial function.

Accession	**Name**	Wild-type **vs** tripleAD	pR5 **vs** tripleAD	APP/ PS2 **vs** tripleAD
ANXA5_MOUSE (P48036)	Annexin A5 (Annexin V) (Lipocortin V)	1.28		0.63
ANXA6_MOUSE (P14824)	Annexin A6 (Annexin VI) (Lipocortin VI)	1.46	2.2	
ARF3_MOUSE (P61205)	ADP-ribosylation factor 3			0.65
BASP_MOUSE (Q91XV3)	Brain acid soluble protein 1 (BASP1 protein)		1.51	
CALM_MOUSE (P62204)	Calmodulin (CaM)		0.78	0.65
COX2_MOUSE (P00405)	Cytochrome c oxidase subunit 2 (EC 1.9.3.1)		1.42	
COX41_MOUSE (P19783)	Cytochrome c oxidase subunit IV isoform 1, mitochondrial precursor (EC 1.9.3.1)	1.36	1.47	
COX5A_MOUSE (P12787)	Cytochrome c oxidase polypeptide Va, mitochondrial precursor (EC 1.9.3.1)	1.21	1.43	
COX5B_MOUSE (P19536)	Cytochrome c oxidase polypeptide Vb, mitochondrial precursor (EC 1.9.3.1)		1.33	
CX7A2_MOUSE (P48771)	Cytochrome c oxidase polypeptide VIIa-liver/heart, mitochondrial precursor (EC 1.9.3.1)		1.69	
HBA_MOUSE (P01942)	Hemoglobin alpha subunit	0.73	0.69	
HBB1_MOUSE (P02088)	Hemoglobin beta-1 subunit chain	0.69		0.6
MBP_MOUSE (P04370)	Myelin basic protein (MBP) (Myelin A1 protein)	1.32		1.22
NDKA_MOUSE (P15532)	Nucleoside diphosphate kinase A (EC 2.7.4.6)			0.56
NIDM_MOUSE (Q9DCS9)	NADH-ubiquinone oxidoreductase PDSW subunit (EC 1.6.5.3)		1.39	0.66
NUCM_MOUSE (Q91WD5)	NADH-ubiquinone oxidoreductase 49 kDa subunit, mitochondrial precursor (EC 1.6.5.3)			0.8
NUIM_MOUSE (Q8K3J1)	NADH-ubiquinone oxidoreductase 23 kDa subunit, mitochondrial precursor (EC 1.6.5.3)	1.22		
PHB_MOUSE (P67778)	Prohibitin (B-cell receptor associated protein 32) (BAP 32)			0.77
PPIA_MOUSE (P17742)	Peptidyl-prolyl cis-trans isomerase A (EC 5.2.1.8)			1.4
S12A2_MOUSE (P55012)	Solute carrier family 12 member 2 symporter)		1.49	
SYN2_MOUSE (Q64332)	Synapsin-2 (Synapsin II)		1.69	
TAU_MOUSE (P10637)	Microtubule-associated protein tau (Neurofibrillary tangle protein)	0.64		0.6
THY1_MOUSE (P01831)	Thy-1 membrane glycoprotein precursor	1.4	1.94	
VA0D_MOUSE (P51863)	Vacuolar ATP synthase subunit d	1.35	1.71	0.77

Table 1. Differentially expressed proteins observed by the iTRAQ experiment. Crossbreed mouse samples were compared to other types. Deregulated subunits of complex I and complex IV are highlighted in yellow.

^{Triple}AD mice exhibit strong defects in mitochondrial OXPHOS, complex activities, and energy homeostasis. A high-resolution respiratory system has been used to evaluate the capacity of the entire oxidative phosphorylation system (OXPHOS) of cerebral mitochondria from the four mouse strains (Fig. 1A). We determined flux control ratios to obtain information on metabolic states of respiration. The respiratory control ratio (RCR3/4) is an indicator of the state of coupling of mitochondria. State 3 is the rate of phosphorylating respiration in the presence of exogenous ADP, while state 4 is associated with proton leakage across the inner mitochondrial membrane in the absence of ADP. Our data demonstrate a pronounced decrease of RCR3/4 in mitochondria from APP/PS2 and ^{triple}AD compared to age-matched wild-type mice (Fig. 1B). When we examined the ETS/ROX (electron transport system/residual oxygen consumption) ratio which yields an index of the maximum oxygen consumption capacity relative to the magnitude of residual oxygen consumption, we found that it was also decreased in APP/PS2 and ^{triple}AD compared to age-matched wild-type mice (Fig. 1C). We have shown previously that respiration of mitochondria from pR5 mice is reduced compared to wild-type controls but not until the age of 24 months (4). In contrast, APP/PS2 mitochondria showed a decrease in OXPHOS compared to wild-type already at the age of 8 months (Fig. 1D). At this age, OXPHOS of brain mitochondria from $^{\text{triple}}$AD mice did not differ compared to that of age-matched APP/PS2 mitochondria (Fig. 1E), but it was significantly decreased in $^{\text{triple}}$AD mice at the age of 12 months (Fig. 1F-G). Taken together, with increasing age, the global failure of the mitochondrial respiratory capacity deteriorated the strongest in mitochondria from $^{\text{triple}}$AD mice, suggesting a synergistic destructive effect of tau and Aβ on mitochondria.

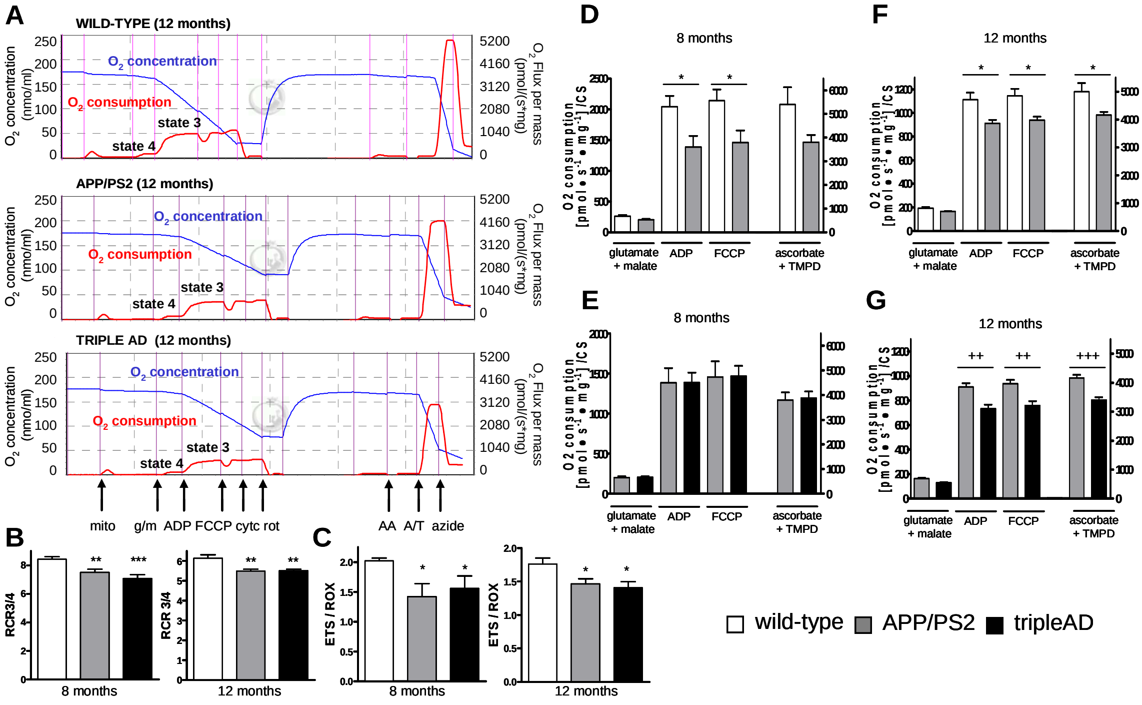

Fig.1. High-resolution respiratory system reveals a heightened defect in the mitochondrial OXPHOS from brains of $^{\text{triple}}$AD mice. Measurement of oxygen (O_2) flux and consumption in freshly isolated mitochondria from cortical brains of wild-type and age-matched APP/PS2 and $^{\text{triple}}$AD mice. After detection of endogenous respiration (mito), glutamate+malate (g/m) were added to induce state 4 respiration. ADP stimulated state 3 respiration. After determining coupled respiration, FCCP was added and the maximal respiratory capacity measured in the absence of a proton gradient. Cytochrome c (cyt c) demonstrated mitochondrial membrane integrity. To inhibit activities of complexes I - III, rotenone (rot) and antimycine A (AA) were added. Complex IV activity was stimulated by ascorbate/TMPD (A/T) before terminating mitochondrial respiration by adding sodium azide (azide). O_2 consumption was normalised to the corresponding citrate synthase (CS) activity. (A) Representative diagrams of O_2 flux and consumption in mitochondria from 12-months-old wild-type, APP/PS2 and $^{\text{triple}}$AD mice in response to titrated substrates and inhibitors of mitochondrial complexes. (B) RCR3/4 (state3/state4 ratio) representing the mitochondrial coupling state was reduced in 8- and 12-months-old APP/PS2 and $^{\text{triple}}$AD mice. (C) ETS/ROX ratio, which yields an index of the maximum oxygen consumption capacity of the electron transport system (ETS) relative to the magnitude of residual oxygen consumption (ROX), was reduced in 8- and 12-months-old APP/PS2 and $^{\text{triple}}$AD mice compared with age-matched wild-type mitochondria. (D) Two-way ANOVA revealed a significant effect of the transgene on the respiratory rates of mitochondria between 8-months-old wild-type and APP/PS2 mice ($p<0.001$). (E) No difference was observed in respiration between 8-months-old APP/PS2 and $^{\text{triple}}$AD mice. (F) At 12 months of age, respiration differed again significantly between wild-type and APP/PS2 ($p<0.001$) and (G) between APP/PS2 and $^{\text{triple}}$AD mice ($p<0.001$). A-G: *, $p<0.05$; **, $p<0.01$; ***, $p<0.001$ vs wild-type; $^{++}$, $p<0.01$; $^{+++}$, $p<0.001$ versus APP/PS2 (n = 7-12 animals/group).

Next, we used a direct measurement of the specific activity of complex I in freshly isolated brain mitochondria, i.e. NADH-ubiquinone oxidoreductase activity measured as NADH:DBQ activity that is then normalised to complex I content (NADH:HAR activity). At 8 months, complex I activity was only decreased in pR5 mice confirming our previous data about complex I deficiency in these mice (4) (Fig. 2A). At 12 months of age, all three transgenic mouse models exhibited a significant decrease of DBQ/HAR compared to wild-type mice (Fig. 2A). Interestingly, at the age of 12 months, content of complex I (measured by HAR activity) was increased in $^{\text{triple}}$AD mice suggesting a compensatory up-regulation in response to functional deficits of this complex (SI Fig. 3). Similarly, compared to APP/PS2 mice complex I proteins were found to be up-regulated (Table 1). Activity of citrate synthase (CS), a pace making enzyme in the first step of the Krebs cycle, thought to be proportional to the content of OXPHOS enzymes (13), was increased in 8-months-old APP/PS2 and $^{\text{triple}}$AD mice. At 12 months, the increase persisted only in cortical mitochondria from $^{\text{triple}}$AD mice suggesting a compensatory incapacity to restore a physiological state specifically in this mouse model that exhibits the strongest AD pathology of both plaques and tangles (Fig. 2B).

At the age of 8 months, APP/PS2 and $^{\text{triple}}$AD mice showed a significantly decreased complex IV activity (CIV/CS ratio) (Fig. 2C). This decrease became more marked at the age of 12 months, when the accumulation of defects in the single complexes as well as in the entire OXPHOS, respectively, could not be further compensated as shown by a drop in ATP levels in cortical brain cells from APP/PS2 and $^{\text{triple}}$AD mice, with the strongest decrease seen in the latter (Fig. 2D). This indicates a general disturbance of cellular energy homeostasis in the cortices of these mice. The effect was brain region-specific as no difference in ATP levels was observed in cerebellar cells from the same mice (SI Fig. 2).

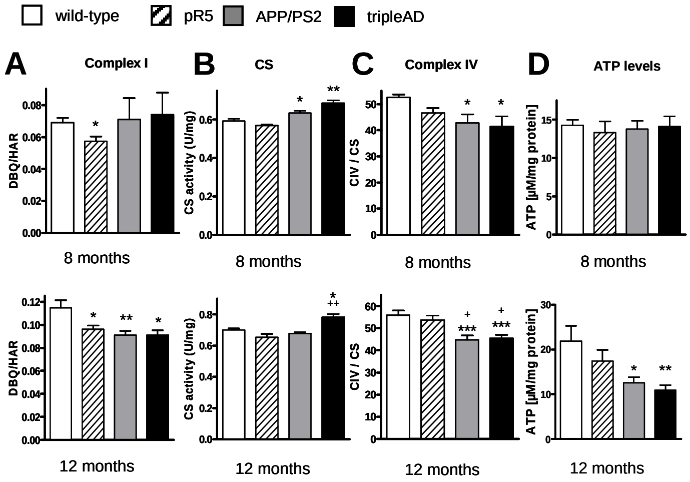

Fig.2. Impaired mitochondrial enzyme activities and decreased ATP levels in cortical brain cells from $^{\text{triple}}$AD mice. (A) Complex I activity (DBQ/HAR ratio) was decreased in 8-months-old pR5 mitochondria. At 12 months, all three transgenic mouse models presented a decrease in complex I activity. (B) Citrate synthase (CS) activity was increased in 8-months-old APP/PS2 and $^{\text{triple}}$AD mice. At 12 months, the increase persisted only in $^{\text{triple}}$AD mice. (C) Complex IV activity (CIV/CS ratio) was decreased in APP/PS2 and $^{\text{triple}}$AD mitochondria at 8 months of age. The decrease became more pronounced at the age of 12 months. (D) ATP levels were reduced in 12-months-old APP/PS2 and $^{\text{triple}}$ mice. A-D: *, $p<0.05$; **, $p<0.01$; ***, $p<0.001$ versus wild-type; $^{+}$, $p<0.05$ versus pR5 (n = 7-12 animals/group).

Aβ and hyperphosphorylated tau cause a decreased mitochondrial membrane potential (MMP). Based on our recent *in vitro* results that cortical brain cells from pR5 mice are particularly sensitive to synthetic Aβ insult (14, 15), we determined the mitochondrial membrane potential (MMP) that is widely considered as an indicator of mitochondrial functionality (16). Basal MMP was significantly and exclusively reduced in cortical cells from 8-months-old $^{\text{triple}}$AD mice. At 12 months, MMP was additionally reduced in cortical cells from APP/PS2 mice (Fig. 3A). Again, this effect was brain region-specific as it was not observed for the cerebellum (SI Fig. 4A).

Increased mitochondrial failure is accompanied by enhanced reactive oxygen species (ROS) production. Superoxide anion levels were enhanced in cortical brain cells of 12 months-old APP/PS2 mice and markedly increased in those of age-matched $^{\text{triple}}$AD mice (Fig. 3B). In addition, cytosolic ROS levels were enhanced in brain cells from APP/PS2 and $^{\text{triple}}$AD mice (Fig. 3C). These differences were only observed at an age of 12, and not 8 months (SI Fig. 4B and C), suggesting that at the older age, brain mitochondria are not capable of compensating their respiratory failure.

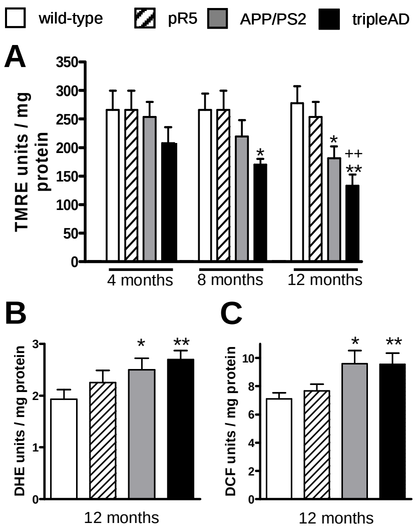

Fig.3. Reduced MMP and increased ROS levels in cortical brain cells from $^{\text{triple}}$AD mice. (A) MMP (TMRE fluorescence units/mg protein) was reduced in cortical cells from 8-months-old $^{\text{triple}}$AD mice. At the age of 12 months, MMP was also reduced in cells from APP/PS2 mice. (B) Levels of superoxide anion radicals (DHE fluorescence units/mg protein) and (C) cytosolic ROS (DCF fluorescence units/mg protein) were increased in cells from 12-months-old APP/PS2 and $^{\text{triple}}$AD mice. A-D: *, $p<0.05$; **, $p<0.01$; vs wild-type, $^{++}$ $p<0.01$ versus pR5 (n = 7-12 animals/group).

DISCUSSION

Energy deficiency and mitochondrial dysfunction have been recognized as a prominent, early event in AD, but the mechanisms leading to mitochondrial failure are not well understood (15, 17-25). Recently, we had shown *in vivo* that P301L mutant tau was capable of inducing mitochondrial dysfunction and increasing levels of ROS in pR5 mice (4). We had also found an increased mitochondrial vulnerability of pR5 cortical brain cells towards Aβ *in vitro* (4, 14). However, the relative contribution of tau and Aβ remained unclear as did possible synergistic effects. To address these, we investigated brains of pR5, APP/PS2 and $^{\text{triple}}$AD (pR5/APP/PS2) mice, the latter combining Aβ and tau pathologies.

In the present study we could clearly show that with increasing age, both Aβ and tau synergistically impair mitochondrial function and energy homeostasis *in vivo*. At 8 months of age, in agreement with previous data (4), complex I activity was only decreased in pR5, but not in APP/PS2 and $^{\text{triple}}$AD mice indicating a tau-specific sensitivity of complex I of OXPHOS. In contrast, CS activity, a pace making enzyme of the Krebs cycle, was increased in 8-months-old APP/PS2 and $^{\text{triple}}$AD mice. At this age, a robust cortical pathology of Aβ plaques and tau deposits is present (11). Since CS activity seems to be proportional to the content of enzymes of OXPHOS (13), the increased activity can be interpreted as compensatory mechanism of mitochondria in response to OXPHOS failure, a mechanism initiated in $^{\text{triple}}$AD mice already at the age of 4 months, when Aβ accumulation and abnormal tau phosphorylation (such as of epitope T231) become evident (11). Notably, at this early age, cortical brain cells from $^{\text{triple}}$AD mice exhibit already a tendency to reduced MMP suggesting that this is a very sensitive indicator of early mitochondrial failure. The decrease in MMP (that was not seen in the parental strains) further continued until $^{\text{triple}}$AD mice reached 8 months of age emphasizing a synergistic action of Aβ and tau. At 12 months, increased Aβ levels *per se* were able to reduce MMP, since a significant reduction was present also in APP/PS2 mice, but the reduction of MMP was more pronounced in $^{\text{triple}}$AD mice.

Complex IV activity was decreased in APP/PS2 and $^{\text{triple}}$ AD cortices at 8 months of age, but not in pR5, confirming related findings that it is mainly the Aβ pathology that affects complex IV activity, both *in vivo* and *in* vitro (23, 26, 27). In APP/PS2 compared to wild-type mice, an impairment of OXPHOS as detected by decreased oxygen consumption was seen at this age suggesting an earlier and stronger effect of the Aβ/APP pathway on this vulnerable mitochondrial system compared to tau, as oxygen consumption of pR5 mitochondria was reduced, but not until the mice reached 24 months of age (4). Similarly, both flux control ratios RCR3/4 and ETS/ROX which measure metabolic states of mitochondrial respiration were similarly decreased in APP/PS2 and ^{triple}AD mitochondria indicating an Aβ-induced increase of the uncoupling state of these organelles. The data indicate that Aβ affects mitochondrial function more extensively and at different levels of respiration and function than does tau which only shows an early effect on the activity of a single complex of OXPHOS, but evidently increases the vulnerability to Aβ toxicity *in vivo*. Notably, at 8 months, no change in cellular energy homeostasis or oxidative stress levels was evident suggesting an efficient compensatory machinery within brain cells at this age.

However, as the mice aged, impairment of OXPHOS and mitochondrial enzyme activities was aggravated, especially in the presence of both plaques and tangles. Indeed, despite compensatory mechanisms – increased complex I content and CS activity – the defects of complex I and IV became more marked at 12 months, indicating a failure to restore the bioenergetic homeostasis in ^{triple}AD mice as they age. Then, we also observed a difference in oxygen consumption between APP/PS2 and ^{triple}AD mice as well as a drop in ATP levels, with the strongest decrease found in ^{triple}AD again suggesting a synergistic action of the two lesions on mitochondria. These mitochondrial defects were associated with an increase of superoxide anion as well as cytosolic ROS levels in 12 month-old APP/PS2 and were most pronounced in ^{triple}AD mice suggesting that at this older age detoxifying mechanisms fail to balance increased ROS production which in turn might further damage mitochondrial OXPHOS.

In agreement with our functional data, iTRAQ MS identified three deregulated subunits of complex I in ^{triple}AD mice: NUCM, NUIM, and NIDM. NUCM likely has a central role within the catalytic core of mitochondrial complex I (28). Interestingly, NUCM and NIDM were up-regulated in ^{triple}AD brain, probably as a compensatory response to the functional failure of OXPHOS. These data nicely correspond with the detected increase in complex I content (detected by HAR activity). Inversely, NUIM, which is thought to participate in the electron transfer and proton pumping activities of complex I, is down-regulated in ^{triple}AD mice. Together, these findings emphasize that Aβ and tau synergistically impair complex I function with aging. On the contrary, changes in the expression of complex IV subunits seem to be mainly related to Aβ. Indeed, a down-regulation of several subunits of complex IV is essentially seen between pR5 and ^{triple}AD mice, but not between APP/PS2 and

^{triple}AD mice. Furthermore, our findings of a mitochondrial dysfunction in ^{triple}AD mice are supported by a significant deregulation of mitochondria-related proteins: Calmodulin, a small, ubiquitous Ca^{2+}-binding protein, and its putative target, the transmembrane proteolipid pore of the vacuolar or vesicular ATPase (V-ATPase V0) sector subunit a1, with calmodulin functioning in an ATPase V(0)-dependent manner at synapses (29). Interestingly, both proteins are deregulated in ^{triple}AD mice.

Our results are in line with recent studies associating Aβ and tau with oxidative stress (18, 19, 30, 31). Moreover, APP transport was shown to be impaired by elevated tau, suggesting a possible link of the two proteins (31, 32). Oligomeric Aβ can attach to tau (33) causing a rapid dissociation of tau from microtubules and a collapse of axonal structures leading initially to synaptic malfunction and ultimately, neuronal death (34). Interestingly, Aβ may not only be located to the cell surface but also directly interact with mitochondria (21) as it can be imported into mitochondria via the translocase of the outer membrane (TOM) machinery (35). A crucial role for mitochondria in AD is further underpinned by findings linking maternal inheritance of mitochondrial DNA to both predisposition of AD and glucose hypometabolism (36) that may reflect energy disturbances as found, e.g., in our ^{triple}AD model.

Together, our studies highlight the key role of mitochondria in AD pathogenesis, and the close inter-relationship of this organelle and the two main pathological features of the disease. This was obtained by combinatorial transgenesis, quantitative proteomics and functional assays. We show that disturbances in the respiratory and energy system of ^{triple}AD mice are due to: (i) a convergence of Aβ and tau on mitochondria, accelerating defects in respiratory capacity, and (ii) a main defect in mitochondrial complexes I and IV. Moreover, we found (iii) that age-related oxidative stress may exaggerate the dysfunctional energy metabolism in a vicious cycle, finally leading to cell death. Our data complement those obtained in a second ^{triple}TG mouse model (37, 38). They may contribute to a better understanding of these biochemical pathways and assist in the development of antioxidative treatments. Importantly, we could reveal defects of mitochondrial respiratory capacity and a failure to restore energy homeostasis in mice with plaques and tangles *in vivo* consolidating the idea that a synergistic effect of tau and Aβ augments the pathological deterioration of mitochondria.

MATERIALS AND METHODS

Mice used for the studies. Four strains of mice were investigated, single-transgenic pR5 (7), double-transgenic APP/PS2 (6), a crossbreeding ($^{\text{triple}}$AD) (11), and non-transgenic wild-type littermate controls. For the proteomic analysis, 6 female mice were sacrificed from each strain at 10 months of age, and forebrains dissected. For the functional studies, 7-12 female mice were sacrificed from each strain at the age of 2, 4, 8, 12 and 16 months in order to identify the age when functional changes start, and forebrains dissected (See SI Methods and Supplementary Table 1 for details).

Proteomic approach. Crude synaptosomal preparations of forebrains from freshly sacrificed mice were obtained for proteomic studies. The proteins were labelled using the iTRAQ technique and separated by both reverse phase and strong cation exchange HPLC. Data were acquired by NanoLC-ESI MS/MS mass spectrometry and submitted to ProteinPilot for processing (See SI Methods for all details).

Cellular analysis. Brain cells were obtained to determine mitochondrial function. The membrane potential of the inner mitochondrial membrane was measured using the dye tetramethylrhodamine ethyl ester (TMRE) (4). ATP content was determined using a bioluminescence photometer (ViaLightTM HT, Cambrex Bio Science) (14). The total amount of mitochondria was measured using the cell-permeable mitochondria-selective dye, MitoTracker Green FM (4). Finally, levels of ROS were measured using the fluorescent probe H2DCF-DA, and levels of superoxide anion radical using DHE (See SI Methods for all details).

Studies of isolated mitochondria. Mitochondria were isolated from mouse forebrains to investigate mitochondrial OXPHOS and respiratory capacity. Mitochondrial oxygen consumption was measured at 37°C using an Oroboros Oxygraph-2k system (4, 22). Several mitochondrial enzyme activities (complex I, complex IV and citrate synthase) were examined (13, 22) (See SI Methods for details).

Statistical Analysis. Data are represented as means ± S.E.M. For statistical comparison, Student’s t-test, One-way ANOVA followed by Tukey’s post hoc test or Two-way ANOVA followed by Bonferroni post tests were used. Only p values less than 0.05 were considered as statistically significant.

ACKNOWLEDGEMENTS

This research was supported by grants to A.E. from the Swiss National Science Foundation (SNF #310000-108223) and to J.G. from the University of Sydney, The Medical Foundation (University of Sydney), the NHMRC, the Judith Jane Mason & Harold Stannett Williams Memorial Foundation, the ARC and by the New South Wales Government through the Ministry for Science and Medical Research (BioFirst Grant). The iTRAQ experiment was facilitated by access to Australian Proteome Analysis Facility which is funded by an initiative of the Australian Government as part of the National Collaborative Research Infrastructure Strategy. We thank Chris Clarke for strong cation exchange and reverse phase fractionation.

REFERENCES

1. Gotz J, Streffer JR, David D, Schild A, Hoerndli F et al. (2004) Transgenic animal models of Alzheimer's disease and related disorders: histopathology, behavior and therapy. Mol Psychiatry 9:664-83.
2. Lee VM, Goedert M, Trojanowski JQ (2001) Neurodegenerative tauopathies. Annu Rev Neurosci 24:1121-59.
3. Gotz J, Ittner LM (2008) Animal models of Alzheimer's disease and frontotemporal dementia. Nat Rev Neurosci 9:532-44.
4. David DC, Hauptmann S, Scherping I, Schuessel K, Keil U et al. (2005) Proteomic and functional analyses reveal a mitochondrial dysfunction in P301L tau transgenic mice. J Biol Chem 280:23802-14. Epub 2005 Apr 14.
5. David DC, Ittner LM, Gehrig P, Nergenau D, Shepherd C et al. (2006) Beta-amyloid treatment of two complementary P301L tau-expressing Alzheimer's disease models reveals similar deregulated cellular processes. Proteomics 6:6566-77.
6. Richards JG, Higgins GA, Ouagazzal AM, Ozmen L, Kew JN et al. (2003) PS2APP transgenic mice, coexpressing hPS2mut and hAPPswe, show age-related cognitive deficits associated with discrete brain amyloid deposition and inflammation. J Neurosci 23:8989-9003.
7. Gotz J, Chen F, Barmettler R, Nitsch RM (2001) Tau filament formation in transgenic mice expressing P301L tau. J Biol Chem 276:529-34.
8. Gotz J, Chen F, van Dorpe J, Nitsch RM (2001) Formation of neurofibrillary tangles in P301l tau transgenic mice induced by Abeta 42 fibrils. Science 293:1491-5.
9. Deters N, Ittner LM, Gotz J (2008) Divergent phosphorylation pattern of tau in P301L tau transgenic mice. Eur J Neurosci 28:137-47.
10. Pennanen L, Wolfer DP, Nitsch RM, Gotz J (2006) Impaired spatial reference memory and increased exploratory behavior in P301L tau transgenic mice. Genes Brain Behav 5:369-79.
11. Grueninger F BB, Czech C, Ballard TM, Frey JR, Weidensteiner C et al. (2009) Phosphorylation of Tau at S422 is enhanced by Abeta in TauPS2APP triple transgenic mice. in press.
12. Sugino K, Hempel CM, Miller MN, Hattox AM, Shapiro P et al. (2006) Molecular taxonomy of major neuronal classes in the adult mouse forebrain. Nat Neurosci 9:99-107.
13. Aleardi AM, Benard G, Augereau O, Malgat M, Talbot JC et al. (2005) Gradual alteration of mitochondrial structure and function by beta-amyloids: importance of membrane viscosity changes, energy deprivation, reactive oxygen species production, and cytochrome c release. J Bioenerg Biomembr 37:207-25.
14. Eckert A, Hauptmann S, Scherping I, Meinhardt J, Rhein V et al. (2008) Oligomeric and fibrillar species of beta-amyloid (A beta 42) both impair mitochondrial function in P301L tau transgenic mice. J Mol Med 86:1255-67.
15. Eckert A, Hauptmann S, Scherping I, Rhein V, Muller-Spahn F et al. (2008) Soluble beta-amyloid leads to mitochondrial defects in amyloid precursor protein and tau transgenic mice. Neurodegener Dis 5:157-9.
16. Sompol P, Ittarat W, Tangpong J, Chen Y, Doubinskaia I et al. (2008) A neuronal model of Alzheimer's disease: an insight into the mechanisms of oxidative stress-mediated mitochondrial injury. Neuroscience 153:120-30.
17. Blass JP (2003) Cerebrometabolic abnormalities in Alzheimer's disease. Neurol Res 25:556-66.

18. Moreira PI, Santos MS, Oliveira CR, Shenk JC, Nunomura A et al. (2008) Alzheimer disease and the role of free radicals in the pathogenesis of the disease. CNS Neurol Disord Drug Targets 7:3-10.
19. Su B, Wang X, Nunomura A, Moreira PI, Lee HG et al. (2008) Oxidative stress signaling in Alzheimer's disease. Curr Alzheimer Res 5:525-32.
20. Gibson GE, Huang HM (2002) Oxidative processes in the brain and non-neuronal tissues as biomarkers of Alzheimer's disease. Front Biosci 7:d1007-15.
21. Lustbader JW, Cirilli M, Lin C, Xu HW, Takuma K et al. (2004) ABAD directly links Abeta to mitochondrial toxicity in Alzheimer's disease. Science 304:448-52.
22. Rhein V, Baysang G, Rao S, Meier F, Bonert A et al. (2009) Amyloid-beta Leads to Impaired Cellular Respiration, Energy Production and Mitochondrial Electron Chain Complex Activities in Human Neuroblastoma Cells. Cell Mol Neurobiol
23. Hauptmann S, Scherping I, Drose S, Brandt U, Schulz KL et al. (2008) Mitochondrial dysfunction: An early event in Alzheimer pathology accumulates with age in AD transgenic mice. Neurobiol Aging.
24. Moreira PI, Santos MS, Oliveira CR (2007) Alzheimer's disease: a lesson from mitochondrial dysfunction. Antioxid Redox Signal 9:1621-30.
25. Berchtold NC, Cribbs DH, Coleman PD, Rogers J, Head E et al. (2008) Gene expression changes in the course of normal brain aging are sexually dimorphic. Proc Natl Acad Sci U S A 105:15605-10.
26. Keil U, Bonert A, Marques CA, Scherping I, Weyermann J et al. (2004) Amyloid beta-induced changes in nitric oxide production and mitochondrial activity lead to apoptosis. J Biol Chem 279:50310-20.
27. Crouch PJ, Blake R, Duce JA, Ciccotosto GD, Li QX et al. (2005) Copper-dependent inhibition of human cytochrome c oxidase by a dimeric conformer of amyloid-beta1-42. J Neurosci 25:672-9.
28. Tocilescu MA, Fendel U, Zwicker K, Kerscher S, Brandt U (2007) Exploring the ubiquinone binding cavity of respiratory complex I. J Biol Chem 282:29514-20.
29. Zhang W, Wang D, Volk E, Bellen HJ, Hiesinger PR et al. (2008) V-ATPase V0 sector subunit a1 in neurons is a target of calmodulin. J Biol Chem 283:294-300.
30. Melov S, Adlard PA, Morten K, Johnson F, Golden TR et al. (2007) Mitochondrial oxidative stress causes hyperphosphorylation of tau. PLoS ONE 2:e536.
31. Mandelkow EM, Stamer K, Vogel R, Thies E, Mandelkow E (2003) Clogging of axons by tau, inhibition of axonal traffic and starvation of synapses. Neurobiol Aging 24:1079-85.
32. Ittner LM, Fath T, Ke YD, Bi M, van Eersel J et al. (2008) Parkinsonism and impaired axonal transport in a mouse model of frontotemporal dementia. Proc Natl Acad Sci U S A 105:15997-6002.
33. Guo JP, Arai T, Miklossy J, McGeer PL (2006) Abeta and tau form soluble complexes that may promote self aggregation of both into the insoluble forms observed in Alzheimer's disease. Proc Natl Acad Sci U S A 103:1953-8.
34. King ME, Kan HM, Baas PW, Erisir A, Glabe CG et al. (2006) Tau-dependent microtubule disassembly initiated by prefibrillar beta-amyloid. J Cell Biol 175:541-6.
35. Hansson Petersen CA, Alikhani N, Behbahani H, Wiehager B, Pavlov PF et al. (2008) The amyloid beta-peptide is imported into mitochondria via the TOM import machinery and localized to mitochondrial cristae. Proc Natl Acad Sci U S A 105:13145-50.
36. Mosconi L, Brys M, Switalski R, Mistur R, Glodzik L et al. (2007) Maternal family history of Alzheimer's disease predisposes to reduced brain glucose metabolism. Proc Natl Acad Sci U S A 104:19067-72.

37. Gimenez-Llort L, Blazquez G, Canete T, Johansson B, Oddo S et al. (2007) Modeling behavioral and neuronal symptoms of Alzheimer's disease in mice: a role for intraneuronal amyloid. Neurosci Biobehav Rev 31**:**125-47.
38. Oddo S, Caccamo A, Kitazawa M, Tseng BP, LaFerla FM (2003) Amyloid deposition precedes tangle formation in a triple transgenic model of Alzheimer's disease. Neurobiol Aging 24**:**1063-70.

SUPPLEMENTARY INFORMATION

SUPPLEMENTARY METHODS

Animals used for proteomic analysis. Four strains of mice were used in this analysis, single-transgenic pR5 (1, 2), double-transgenic APP/PS2 (3), a crossbreeding of the two strains (tripleAD) (4), and non-transgenic wild-type littermate controls. From each strain, 6 female mice were sacrificed at the age of 10 months, and the forebrain dissected. From each forebrain we obtained a ‘crude synaptosomal’ (vesicular) fraction, followed by lysis and determination of protein content using the D_C Protein Assay (BioRad #500-0116). For iTRAQ processing and labelling (see below), 33µg were obtained from three samples and mixed before analysis to reduce the impact of individual outliers. A mix from animals 1-3 (group 1) of each strain was used in the first run and of animals 4-6 (group 2) in the second. Three animals each from groups 1 and 2 were randomly chosen for the third run (Supplementary Table 1).

Animals used for analysis of mitochondrial function. Four strains of mice were used: pR5, APP/PS2, tripleAD, and non-transgenic wild-type littermate controls. From each strain, 7-12 female mice were sacrificed at the age of 2, 4, 8, 12 and 16 months in order to identify the age when functional changes start, and forebrains dissected.

Crude vesicular extraction and lysis. To prepare a crude vesicular extract from freshly sacrificed mice, forebrains were separated from brainstem and cerebellum. Forebrains were transferred into 5 ml pre-chilled preparation buffer (0.32 M Sucrose, 1 mM $NaHCO_3$, 1 mM $MgCl_2$, 0.5 mM $CaCl_2$) containing protease inhibitors (Complete, EDTA-free, Roche #11873580001). They were slowly and gently homogenised in a douncer, with 12 up and down strokes at 700 rpm. The lysate was then spun in a centrifuge at 1,400 g for 10 minutes at 4°C. The supernatant (S1) was saved and the pellet resuspended in 2 ml preparation buffer containing protease inhibitors. The suspension was homogenised further with 3 slow and gentle up and down strokes at 700 rpm and then spun in a centrifuge at 720 g for 10 minutes at 4°C. The pellet was discarded and the supernatant (S2) combined with supernatant S1. The lysate was then spun again in a centrifuge at 720 g for 10 minutes at 4°C and the pellet was discarded. Crude vesicles including synaptosomes were then pelleted at 13,800 g for 10 minutes at 4°C.

The crude synaptosomal preparation was resuspended in 500 µl RIPA buffer (50 mM Tris-HCl pH7.5, 1% (v/v) Triton X-100, 0.1 % (v/v) SDS, 15 mM sodium deoxycholate, 375 mM NaCl, 10 mM EGTA) containing Complete, EDTA-free protease inhibitors. Samples were homogenised by passing through a Terumo syringe needle (22Gx1 ½”) and subsequently incubated on ice for one hour. Lysates were then further passed through a Terumo Insulin syringe (29Gx ½”) and centrifuged at 22,000 g for 10 minutes at 4°C. The pellet was discarded and the supernatant used for further analysis.

Protein digestion and iTRAQ labelling. Preparation and labelling was conducted according to the iTRAQ manual (Applied Biosystems). In short, 100 µg of protein was acetone-precipitated and resuspended in 20 µl of dissolution buffer (0.5 M triethylammonium bicarbonate) containing 0.1 % (v/v) SDS. The sample was then reduced by adding TCEP (tris-(2-carboxyethyl) phosphine) to a concentration of 50 mM and incubated at 60°C for 1 hour. Subsequently, the sample was treated with 200 mM MMTS (methyl methanethiosulfate) for alkylation/cysteine blocking for 10 minutes at room temperature. The protein sample was then treated with 4 µg trypsin (Trypsin Gold, Promega) per 100 µg protein at 37°C for 16 to 24 hour. Labelling of the samples with iTRAQ labels was done at room temperature for one hour. Supplementary Table 1 shows the iTRAQ labels and the corresponding samples. In each iTRAQ run, the different samples were mixed after labelling and dried in SpeedyVac. The dried samples were then stored at -20ºC before 2-dimensional HPLC peptide separation and data acquisition.

First dimensional HPLC for peptide fractionation. To investigate the effect of the first dimensional HPLC peptide separation, we used both reverse phase (RP) and strong cation exchange (SCX) to fractionate peptides. RP HPLC was used for Run1; SCX HPLC was used for Run2; RP HPLC and SCX HPLC were both used in parallel for Run3 and this run identified most proteins. The collected fractions from the first dimensional HPLC were dried in SpeedyVac and then stored at -20°C before nanoLC-ESI MS/MS data acquisition.

SCX HPLC: An Agilent 1100 quaternary HPLC pump with a PolyLC PolySulfoethyl A (200mm x 2.1mm x 5µm, 200A) column was used for strong cation exchange chromatography sample clean up and fractionation. Buffer A was 5 mM Phosphate 25% acetonitrile, pH 2.7 and buffer B was 5 mM phosphate, 350 mM KCL, 25% acetonitrile, pH 2.7. The dried iTRAQ-labelled sample was resuspended with loading buffer (buffer A) and loaded onto the SCX column. The flow through was discarded as this contained interfering chemicals for the second dimensional nanoLC and mass spectrometry. To elute peptides, buffer B gradient was increased from 10% to 45% in 70 minutes at a flow rate of 300 µl/min. 25 fractions were collected beginning from the start of the gradient.

RP HPLC: The sample was first cleaned up using Strong Anion Exchange resin (BioRad Macro-prep High Q Support) to remove neutral or negatively charged chemicals that would interfere with reverse phase HPLC separation and mass spectrometry data acquisition. The reverse phase HPLC fractionation used column Phenomenex Jupiter 5u C4 300A 150x2.00mm. Buffer A was 0.1% TFA in MilliQ water, Buffer B was 0.085% TFA in acetonitrile. After 10 minutes sample loading and desalting, Buffer B gradient was increased from 5% to 40% in 25 minutes and then increased to 90% in 5 minutes to elute peptides. The fractions were collected at one minute intervals.

NanoLC-ESI MS/MS mass spectrometry. The Agilent 1100 nanoLC system (Agilent) and the QStar XL MS/MS system (Applied Biosystems) were used for nanoLC-electrospray MS/MS. The peptide fractions from first dimensional HPLC were resuspended with loading/desalting solution (0.1% trifluoroacetic acid, 2% acetonitrile, 97.9% water). The resuspended sample was loaded onto a peptide Captrap column (Michrom Bioresources) and desalted with the desalting solution at 10 µl per minute for 13 minutes. After desalting, the trap was switched online with a 150 µm x 10 cm C18 3µm 300A ProteCol column (SGE). Buffer solution A was 99.9% water/0.1% formic acid, buffer solution B was 90% acetonitrile/9.9% water/0.1% formic acid. The buffer B concentration was increased from 5% to 90% in 120 minutes in three linear gradient steps to elute peptides. The RP nanoLC eluent was subjected to positive ion nanoflow ESI analysis in an information-dependant acquisition mode (IDA). In the IDA mode, a TOF-MS survey scan was acquired (m/z 380-1600, 0.5 second), with the three most intense multiply charged ions (counts >50) in the survey scan sequentially subjected to MS/MS analysis. MS/MS spectra were accumulated for 2 seconds in the mass range m/z 100-1600 with a modified Enhance All Q2 transition setting favouring low mass ions so that the reporting iTRAQ tag ion (114, 115, 116 and 117 Da) intensities were enhanced for quantification. After peptide elution, the nanoLC column was cleaned with 100% buffer B for 15 minutes and then equilibrated with buffer A for 30 minutes before the next sample injection.

Database processing. The experimental nanoLC-ESI MS/MS data were submitted to ProteinPilot (Applied Biosystems, version 1.0) for data processing. The Paragon method was used in thorough ID search effort with Biological modifications selected in ID Focus. The software correction factors provided in the iTRAQ kit were entered in the iTRAQ Isotope Correction Factors table. The detected protein threshold (unused ProtScore) was set as larger than 1.3 (better than 95% confidence). The database used was uniprot_sprot20051220 with *Mus musculus* specified as the searched species.

After ProteinPilot data processing, the protein summary which listed the identified proteins and their iTRAQ ratios was exported as tab delimited text file. To compare the runs, all identified proteins from all runs were aligned using an excel macro. To highlight differentially expressed proteins, iTRAQ ratios larger than 1.2 or smaller than 0.82 and a P-value smaller than 0.05 were used as threshold.

BN-Page and Tricine-SDS-Page. Sample preparation, Blue Native (BN) electrophoresis, 2D Tricine-SDS-PAGE were performed as described (5). Per lane, the *n*-dodecyl-ß-D-maltoside (7 g/ g mitochondrial protein) solubilized fraction of ~10 mg protein from isolated mouse brain mitochondria was separated in the first dimension (acrylamide gradient 4-13 %, sample gel 3.5%). The native lanes were cut and used for 2D SDS PAGE (16% acrylamide) to separate the subunits of the respiratory chain complexes. Finally the gels were visualized by silver staining as described (6).

Brain tissue preparation for mitochondrial analysis. Cellular preparations were obtained to determine the mitochondrial membrane potential (MMP) and mitochondria, to determine respiration rates as described previously (7, 8). For that, mice were sacrificed by decapitation and brains quickly dissected on ice. The cerebellum and one cortical hemisphere (the other hemisphere was directly used for preparation of isolated mitochondria for mitochondrial respiration and complex activities) were separately minced into 1 ml of medium I (138 mM NaCl, 5.4 mM KCl, 0.17 mM Na_2HPO_4, 0.22 mM K_2PO_4, 5.5 mM glucose, 58.4 mM sucrose, pH 7.35) with a scalpel and further dissociated by trituration through a nylon mesh (pore diameter 1 mm) with a pasteur pipette. The resulting suspension, which contained both neuronal (about 72%) and glial cells (about 26%), was filtered by gravity through a fresh nylon mesh with a pore diameter of 102 µm, and the dissociated cell aggregates were washed twice with medium II (110 mM NaCl, 5.3 mM KCl, 1.8 mM $CaCl_2*H_2O$, 1 mM $MgCl_2*6\ H_2O$, 25 mM glucose, 70 mM sucrose, 20 mM HEPES, pH 7.4) by centrifugation (400 x g for 3 min at 4°C). 100 µl of the suspension were used for protein determination. After centrifugation, cells were resuspended in 3 ml DMEM, and then aliquots of 100 µl were distributed per well in a 48 well plate for measurement of the mitochondrial membrane potential. The preparations of cerebellar and cortical cells from transgenic mice and WT littermate controls (cross-over design) were made within 2 hours under the same conditions and in parallel and maintained at 37°C in a humidified atmosphere of 5% CO_2/95% air. Viability was found to be > 90% using the MTT assay and Trypan blue stain exclusion test. Data are expressed as fluorescence units per mg/ml protein.

Determination of the mitochondrial membrane potential MMP. The membrane potential of the inner mitochondrial membrane was measured using the dye tetramethylrhodamine ethyl ester (TMRE, Molecular Probes, Leiden, Netherlands) added to the cell culture medium at a final concentration of 0.4 µM for 15 min. Cells were washed twice with HBSS (Hank's Balanced Salt Solution, Sigma, Germany), and fluorescence was determined with a Victor2 multiplate reader (Perkin Elmer, Rodgau-Jügesheim, Germany) at 535 nm/590 nm (Ex/Em) (7).

ATP levels. The ATP content of dissociated cells was determined with a bioluminescence photometer (ViaLightTM HT, Cambrex Bio Science) according to the instruction of the manufacturer. The enzyme luciferase which catalyzes the formation of light from ATP and luciferin is utilized. Dissociated brain cells were lysed before the addition of the reagent. The emitted light is linearly related to the ATP concentration and is measured using a luminometer (7).

Amount of mitochondria. The total amount of mitochondria was measured using the cell-permeable mitochondria-selective dye, MitoTracker Green FM (100 nM, 15 min) (7). This probe can accumulate in active mitochondria and then react with accessible thiol groups of proteins and peptides to form fluorescent aldehydic-fixable conjugates. Fluorescence was determined using a Victor2 multiplate reader (PerkinElmer Life Sciences) at 490 nm (excitation)/516 nm (emission).

ROS levels. The levels of ROS were measured using the fluorescent probe H2DCF-DA and the levels of superoxide anion radical were measured using DHE (9). The brain cells were loaded for 15 min with 10 µM H2DCF-DA or for 60 minutes with 10 µM DHE. After washing twice with Hank's balanced salt solution, the formation of the fluorescent product dichlorofluorescein was detected using the Victor2 multiplate reader (PerkinElmer Life

Sciences) at 485 nm (excitation)/535 nm (emission). DHE, which is oxidized to the fluorescent ethidium cation by $O2^{\cdot -}$ was detected using the Victor2 multiplate reader at 490 nm (excitation)/590 nm (emission).

Preparation of isolated mitochondria. Mitochondria were isolated from mouse brains as described previously (7). Briefly, mice were sacrificed by decapitation, and one brain hemisphere was rapidly dissected on ice and washed in an ice-cold buffer (210mM mannitol, 70mM sucrose, 10mM HEPES, 1mM EDTA, 0.45% bovine serum albumin, 0.5mM dithiothreitol, and Complete protease inhibitor mixture tablets (Roche Diagnostics)). After removing the cerebellum, the tissue sample was homogenized in 2ml of buffer with a glass homogenizer (10–15 strokes, 400 rpm), and the resulting homogenate was centrifuged at 1,400*g* for 7min at 4°C to remove nuclei and tissue particles. The low-speed centrifugation step was repeated once with the supernatant. Then, the supernatant fraction was centrifuged at 10,000 *g* for 5 min at 4°C to pellet mitochondria. The resulting pellet was resuspended in 1ml of ice-cold buffer and centrifuged again at 1,400*g* for 3 min at 4°C. Finally, the mitochondria-enriched supernatant was centrifuged at 10,000*g* for 5 min at 4°C to obtain a mitochondrial fraction. This fraction was resuspended in 100µl of ice-cold buffer and stored at 4°C until use, followed by determination of protein content (7).

Mitochondrial respiration. Mitochondrial oxygen consumption was measured at 37°C using an Oroboros Oxygraph-2k system. Isolated mitochondria (0.5mg) were added to 2ml of a mitochondrial respiration medium containing 65mM sucrose, 10mM potassium phosphate, 10mM Tris-HCl, 10mM $MgSO_4$, and 2mM EDTA (pH 7.0) (7). To measure the state 4 of the complex I, 10mM glutamate and 2mM malate were added. Then, 2mM ADP was added to measure state 3 respiration. After determining coupled respiration, 0.05µM FCCP (Carbonyl cyanide p-(trifluoro-methoxy) phenyl-hydrazone) was added and respiration was measured in the absence of a proton gradient. To check the integrity of the mitochondrial membrane 10µM cytochrome c was added. In order to inhibit complex I and III activities 0.5µM rotenone and 2.5µM antimycin A, respectively were added. Then, 2mM ascorbate and 0.5mM TMPD were added and respiration was measured. Finally, 10mM sodium azide was added to inhibit complex IV activity (10). Mitochondria from transgenic and control mice were measured in parallel pairs using the same conditions (crossover design).

Activity of complex I. 100µg of isolated mitochondria were solubilized in n-dodecyl β-D-maltoside (0.1mg). NADH:hexaammineruthenium(III)-chloride (HAR) activity was measured at 30 °C in a buffer containing 2mM Na^+/MOPS, 50mM NaCl, and 2mM KCN, pH 7.2, using 2mM HAR and 200µM NADH as substrates to estimate the complex I content. To determine NADH-ubiquinone oxidoreductase activity, 100µM *n*-decylubiquinone (DBQ) and 100µM NADH were used as substrates and 5µM rotenone as inhibitor, as described previously (7). Oxidation rates of NADH were recorded with a Shimadzu Multi Spec-1501 diode array spectrophotometer ($\varepsilon_{340\text{-}400nm}$ = 6.1 $mM^{-1}.cm^{-1}$). Complex I activity was normalized to the complex I content of the mitochondrial preparation and is given as DBQ/HAR ratio.

Activity of complex IV. Cytochrome *c* oxidase activity was determined in intact isolated mitochondria (50µg) using the Cytochrome *c* Oxidase Assay Kit. The colorimetric assay is based on the observation that a decrease in absorbance at 550 nm of ferrocytochrome *c* is caused by its oxidation to ferricytochrome *c* by cytochrome *c* oxidase. The Cytochrome *c* Oxidase Assay was performed as described previously (7). Activity was normalized to the corresponding citrate synthase.

Activity of citrate synthase. The reduction of 5,5'-dithiobis(2-nitrobenzoic acid) (DTNB) by citrate synthase at 412 nm (extinction coefficient of 13.6 $mM^{-1}.cm^{-1}$) was followed in a coupled reaction with coenzymeA and oxaloacetate as described previously (11). Briefly, a reaction mixture of 0.2M Tris-HCl, pH 8.0, 0.1mM acetyl-coenzymeA, 0.1mM DTNB, n-dodecyl-β-D-maltoside (20%) and 10µg of mitochondrial protein was incubated at 30°C for 5 min. The reaction was initiated by the addition of 0.5mM oxaloacetate, and the absorbance change was monitored for 5min with a Shimadzu Multi-Spec-1501 diode array spectrophotometer (10).

References

1. Gotz J, Chen F, Barmettler R, Nitsch RM (2001) Tau filament formation in transgenic mice expressing P301L tau. J Biol Chem 276:529-34.
2. Gotz J, Chen F, van Dorpe J, Nitsch RM (2001) Formation of neurofibrillary tangles in P301l tau transgenic mice induced by Abeta 42 fibrils. Science 293:1491-5.
3. Richards JG, Higgins GA, Ouagazzal AM, Ozmen L, Kew JN et al. (2003) PS2APP transgenic mice, coexpressing hPS2mut and hAPPswe, show age-related cognitive deficits associated with discrete brain amyloid deposition and inflammation. J Neurosci 23:8989-9003.

4. Grueninger F BB, Czech C, Ballard TM, Frey JR, Weidensteiner C et al. (2009) Phosphorylation of Tau at S422 is enhanced by Abeta in TauPS2APP triple transgenic mice. in press.
5. Schagger H (2006) Tricine-SDS-PAGE. Nat Protoc 1:16-22.
6. Wittig I, Braun HP, Schagger H (2006) Blue native PAGE. Nat Protoc 1:418-28.
7. David DC, Hauptmann S, Scherping I, Schuessel K, Keil U et al. (2005) Proteomic and functional analyses reveal a mitochondrial dysfunction in P301L tau transgenic mice. J Biol Chem 280:23802-14. Epub 2005 Apr 14.
8. Eckert A, Hauptmann S, Scherping I, Meinhardt J, Rhein V et al. (2008) Oligomeric and fibrillar species of beta-amyloid (A beta 42) both impair mitochondrial function in P301L tau transgenic mice. J Mol Med 86:1255-67.
9. Leutner S, Eckert A, Muller WE (2001) ROS generation, lipid peroxidation and antioxidant enzyme activities in the aging brain. J Neural Transm 108:955-67.
10. Rhein V, Baysang G, Rao S, Meier F, Bonert A et al. (2009) Amyloid-beta Leads to Impaired Cellular Respiration, Energy Production and Mitochondrial Electron Chain Complex Activities in Human Neuroblastoma Cells. Cell Mol Neurobiol.
11. Aleardi AM, Benard G, Augereau O, Malgat M, Talbot JC et al. (2005) *G*radual alteration of mitochondrial structure and function by beta-amyloids: importance of membrane viscosity changes, energy deprivation, reactive oxygen species production, and cytochrome c release. J Bioenerg Biomembr 37:207-25.

SUPPLEMENTARY FIGURES

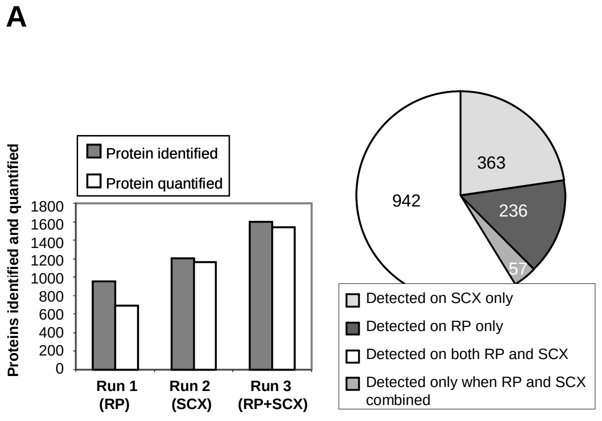

Accession	Name	pR5 vs triple AD	APP/PS2 vs triple AD
NUCM mouse (Q91WD5)	complex I, 49kDa subunit		0.90
COX2 mouse (P00405)	complex IV, subunit II	1.40	
COX41 mouse (P19783)	complex IV, subunit IV	1.20	

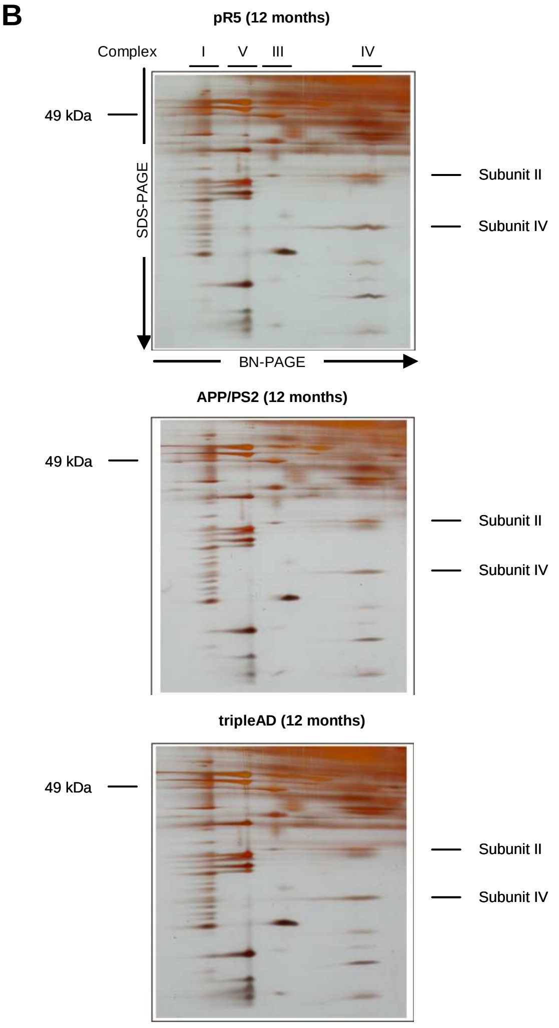
B
pR5 (12 months)
Complex
I
V
III
IV
49 kDa
SDS-PAGE
BN-PAGE
Subunit II
Subunit IV
APP/PS2 (12 months)
49 kDa
Subunit II
Subunit IV
tripleAD (12 months)
49 kDa
Subunit II
Subunit IV

SI Fig.1. Quantitative proteomic analyses and separation of dodecylmaltoside-solubilized mitochondrial complexes from mouse brain. (A) Total of proteins identified and quantified in each run and proteins identified in Run3 (Suppl. Table 1) by combined strong cation exchange (SCX) HPLC and reverse phase (RP) HPLC. (B) Solubilized brain mitochondrial complexes (I–III and V) from 12 months old mice with different genetic background (pR5; APP/PS; $^{\text{triple}}$AD) were separated on a linear 4-13% acrylamide gradient gel by BN-PAGE (not shown) and subsequently the individual subunits of the native complexes were separated by tricine-SDS-PAGE using a 16% T, 3% C gel type as detailed under Materials and Methods. Proteins were visualized by silver staining. The position of the 49 kDA subunit of complex I and the positions of the complex IV subunits II and IV are indicated.

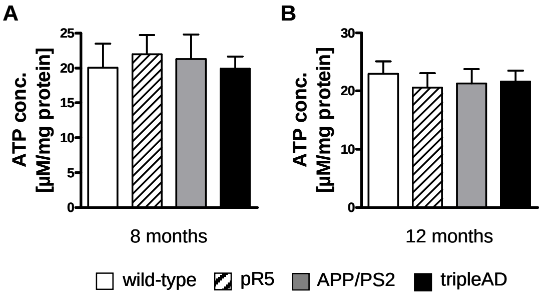

SI Fig.2. No drop of ATP synthesis in cerebellar cells. Decrease of ATP levels is brain region specific since no difference in ATP levels was observed between cerebellar cells from the different mouse models (A) at the age of 8 and (B) 12 months. Values represent the means ± S.E. from n= 7-12 animals/group.

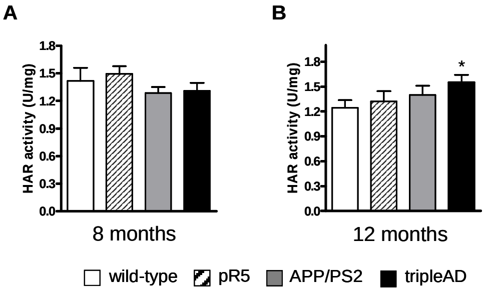

SI Fig.3. Increase of complex I content in cortical brain from ^{triple}AD mice. The complex I content (HAR activity) significantly increased in the mitochondria of ^{triple}AD mice (B) at the age of 12 months (*, $p<0.05$ vs wt, Student t-test). Values represent the means ± S.E. from n= 7-12 animals/group.

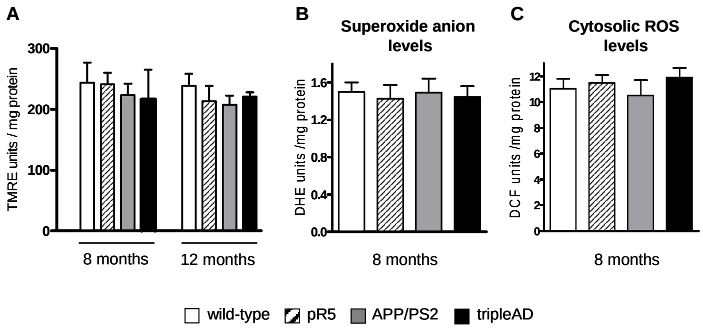

SI Fig.4. Unchanged MMP and levels of ROS in cerebellar cells at 8 months of age. (A) The decrease of the basal mitochondrial membrane potential is brain-region specific, since no difference was observed in cells from cerebellum. (B) Superoxide anions levels determined by DHE oxidation and (C) cytosolic ROS levels from cortical cells measured after incubation with DCF did not increase at 8 months. Values represent the means ± S.E. from n= 7-12 animals/group.

SUPPLEMENTARY TABLE

iTRAQ Runs	**2DLC**	**114**	**115**	**116**	**117**
Run1	RP-RP	A (1, 2, 3)	B (1, 2, 3)	C (1, 2, 3)	D (1, 2, 3)
Run2	SCX-RP	A (4, 5, 6)	B (4, 5, 6)	C (4, 5, 6)	D (4, 5, 6)
Run3	RP-RP	A (1, 2, 5)	B (2, 3, 4)	C (3, 5, 6)	D (2, 5, 6)

Supplementary Table 1. iTRAQ experiment runs and the mouse sample labelling. A: wild-type; B: pR5; C: APP/PS2; D: ^{triple}AD

3. Amyloid-beta leads to impaired cellular respiration, energy production and mitochondrial electron chain complex activities in human neuroblastoma cells

V. **Rhein**[1], G. Baysang[1], S. Rao[1], F. Meier[1], A. Bonert[2], F. Müller-Spahn[1], A. Eckert[1]

[1] Neurobiology Laboratory for Brain Aging and Mental Health, Psychiatric University Clinics, Univ. of Basel, Basel, Switzerland

[2] Dept. of Pharmacology, Biocenter, J.W. Goethe Univ. of Frankfurt, Frankfurt am Main, Germany

Cellular and Molecular Neurobiology (2009), 29 (6):1063-1071.

ABSTRACT

Aims: Evidence suggests that amyloid-beta (Aβ) protein is a key factor in the pathogenesis of Alzheimer's disease (AD) and it has been recently proposed that mitochondria are involved in the biochemical pathway by which Aβ can lead to neuronal dysfunction. Here we investigated the specific effects of Aβ on mitochondrial function under physiological conditions.

Methods: Mitochondrial respiratory functions and energy metabolism were analyzed in control and in human wild-type amyloid precursor protein (APP) stably-transfected human neuroblastoma cells (SH-SY5Y). Mitochondrial respiratory capacity of mitochondrial electron transport chain (ETC) in vital cells was measured with a high-resolution respirometry system (Oxygraph-2k). In addition, we determined the individual activities of mitochondrial complexes I-IV that compose ETC and ATP cellular levels.

Results: While activities of complexes I and II did not change between cell types, complex IV activity was significantly reduced in APP cells. In contrast, activity of complex III was significantly enhanced in APP cells, as compensatory response in order to balance the defect of complex IV. However, this compensatory mechanism could not prevent the strong impairment of total respiration in vital APP cells. As a result, the respiratory control ratio (state3/state4) together with ATP production decreased in the APP cells in comparison to control cells.

Conclusions: Chronic exposure to soluble Aβ protein may result in an impairment of energy homeostasis due to a decreased respiratory capacity of mitochondrial electron transport chain which, in turn, may accelerate neurons demise.

INTRODUCTION

Alzheimer's disease (AD) is the most frequent form of dementia among elderly individuals and is characterized by neuropathological hallmarks of extracellular amyloid plaques and intracellular neurofibrillary tangles in the brain of AD patients. Extensive evidences suggest that amyloid-beta (Aβ) protein, which is derived from its precursor protein APP, plays a pivotal role in the pathogenesis of AD. In addition, mitochondrial dysfunction and energy metabolism deficiencies have been recognized as earliest events in AD (Chagnon et al. 1995) and have been correlated with impairments of cognitive abilities in this clinical scenario (Blass 2003). The most consistent defect in mitochondrial electron transport chain enzymes in AD is the deficiency in cytochrome c oxidase (complex IV) activity in post-mortem brain tissues, as well as in other tissues, such as platelets from AD patients and AD cybrid cells (Cardoso et al. 2004a; Cardoso et al. 2004b). Although, the specific mechanisms leading to mitochondrial failure in AD still remain unknown, a substantial body of evidence indicates that Aβ promotes neuronal degeneration and death by enhancing neurons vulnerability to increases in levels of oxidative stress and impairments in cellular energy metabolism (Gibson and Huang 2002; Mattson and Liu 2002). Interestingly, enzyme activities in mitochondrial respiratory chain and citric acid cycle, which are reduced in AD, can be inhibited by Aβ in vitro. Furthermore, several findings have demonstrated Aβ-induced mitochondrial damage, e.g. Aβ inhibited cytochrome c oxidase (COX) activity, in isolated brain mitochondria (Canevari et al. 1999; Parker et al. 1994) However, results on how mitochondrial respiratory chain complexes and complex IV are affected by Aβ are rather inconsistent (Casley et al. 2002b; Cassarino and Bennett 1999; Swerdlow and Kish 2002). It has been recently proposed that toxic species of Aβ that intervene in molecular and biochemical abnormalities in AD may be intracellular oligomeric forms, instead of extracellular, insoluble deposits. According to this hypothesis, mitochondria could intervene in the mechanism by which intracellular Aβ triggers synaptic failure and neurodegeneration (Eckert et al. 2008). This idea is supported by *in vivo* evidence of Aβ accumulation within mitochondria in brain tissues of AD patients (Fernandez-Vizarra et al. 2004; Lustbader et al. 2004) and mitochondrial structural abnormalities (Hirai et al. 2001). Taken together, these data indicate that mitochondrial dysfunction can play a major role in AD pathophysiology (Eckert et al. 2003; Leuner et al. 2007; Rhein and Eckert 2007).

To unravel the direct impact of Aβ on mitochondrial respiratory functions, we established a new high resolution respiratory protocol to investigate the respiratory capacity of mitochondrial electron transport chain (ETC) under physiological conditions in control and in wild-type APP stably transfected human neuroblastoma cells (SH-SY5Y). By means of stably transfected APP SH-SY5Y cells, which represent a neuronal cell line of human origin widely used in studies testing the effect of Aβ *in vitro*, we circumvent the artificial experimental design of most of the other studies, where isolated mitochondria were treated with high concentrations of Aβ in the micromolar range (5-50µM). In addition, we determined the activities of mitochondrial complexes I-IV composing ETC, as well as the ATP levels.

RESULTS

APP expression and Aß levels of APP transfected SH-SY5Y cells. In our cell model, the overexpression of human wild-type APP lead to a significantly increased Aß secretion, as compared to control cells with the empty vector. The APP expression of APPwt cells was substantially increased in comparison to control cells (Fig.1b,d) confirming previous findings (Scheuermann et al. 2001). The strong expression of APP was not correlated with a change of the general morphological aspect of APP cells compared to control cells (Fig.1a). APP cells secreted Aß levels within pg/mL range, reflecting the physiological situation *in vivo* during cellular metabolism (Fig.1c). Using the APP SH-SY5Y cell line allows us to study effects of chronic stress of soluble forms Aß protein on cells and mitochondria, respectively, as it may occur in the brains of AD patients.

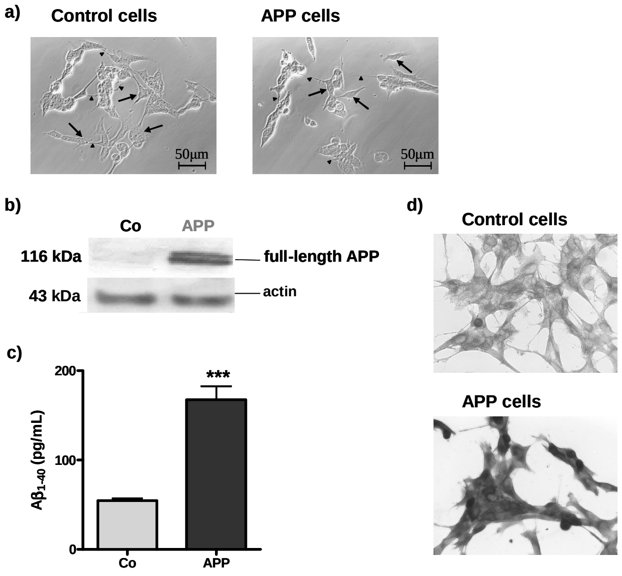

Fig.1 Human APP and secreted $A\beta_{1-40}$ levels of SY5Y cells. a) Morphological analysis of native and transfected SH-SY5Y cells showed neuroblast-like morphology with differentiated perikaria (arrows) and occasional short neurites (arrowheads). Transfection of SH-SY5Y cells with cDNAs (pCEP4 vector) containg the vector alone or containing the entire coding region of human APP (APP695) did not significantly change the general morphological aspect of the cells. Scale bars: 50µm b) Human APP expression levels of SH-SY5Y cells detected by Western Blotting using W02 antibody indicating strong expression of APP in APP transfected cells compared to control cells. c) Cell culture supernatants of 5 x 10^6 SH-SY5Y cells (APPwt, Co) were collected and assayed for $A\beta_{1-40}$ by ELISA. $A\beta_{1-40}$ levels were significantly enhanced in APP cells compared to control cells (***$p<0.001$, n=6, Student’s t-test). d) Human APP detected by immunochemistry using a monoclonal anti-APP antibody indicating stronger presence of APP in the APP cells compared to the endogenous APP expression in control cells.

Amyloid beta leads to mitochondrial respiratory defects. To investigate mitochondrial capacity and function of mitochondria in both control and APP cells, we initially focused on the activity of the citrate synthase (CS) in both cell types, which was similar in control and APP cells (Fig.2a). Given the direct inhibitory effect of extracellular Aß on complex I (10% inhibition) (Aleardi et al., 2005), we conducted direct measurements of the complex I activity. NADH-ubiquinone oxidoreductase (NADH:DBQ) activity in the mitochondria APP cells did not alter, the same occurring for NADH:HAR activity, indicating that the complex I content was similar in both cell types. APP mitochondria did not exhibit any loss in complex I activity, as indicated by normalization of complex I activity with complex I content expressed as DBQ/HAR ratio (Fig. 2b). After normalization of complex I activity with the content of mitochondria, complex I / CS ratio did not modify between controls and APP cells (Fig.2c). Moreover, activity of respiratory chain complexes II, III and IV were also normalized to the corresponding CS activity. Accodingly, we found an unchanged complex II (Fig.2d), although there was a significantly up-regulated activity of complex III in APP cells compared to control cells (Fig.2e). Similarly we observed a significantly reduced cytochrome c oxidase activity between control and APP mitochondria (Fig. 2f), which is consistent with reduced complex IV activity in platelets from AD patients (Cardoso et al. 2004a) and the direct interaction of Aß with mitochondrial membranes, which results in the inhibition of complex IV *in vivo* (Canevari et al. 1999; Hauptmann et al. 2008).

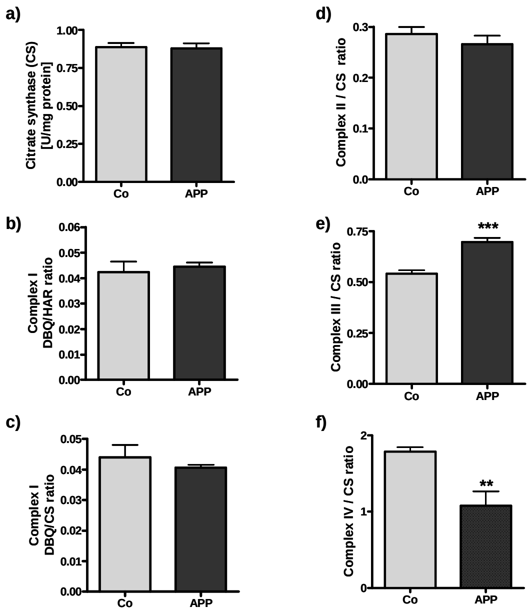

Fig.2 Mitochondrial enzymes activities in control and APP cells. a) Unaltered citrate synthase activity between control and APP cells. b) complex I activity (DBQ activity) normalized to the complex I content (HAR activity) of the mitochondrial preparation is shown as DBQ/HAR ratio. Complex I activity is unaltered. c) unaltered complex I / CS ratio. d) unaltered complex II / CS ratio. e) complex III / CS ratio was significantly increased in the APP cells (***, p<0.001 versus control cells, Student's t test). f) Complex IV / CS ratio was significantly decreased in the APP cells (**, p<0.01 versus control cells, Student's t test). All values represent the means ± S.E. from n= 4-6 independent experiments.

In order to evaluate the functionality of the respiratory chain, we determined the physiological cell respiration in vital control and APP cells (Fig.3). We used the NADH generating substrates pyruvate and malate to determine state 4 of respiration (Fig. 3). State 3 respiration measures the capacity of the mitochondria to metabolize oxygen and the selected substrate in the presence of a defined amount of ADP, which is a substrate for the ATP synthase (complex V). State 4 respiration represents a “basal-coupled” rate of respiratory chain activity and reflects activities of respiratory chain complexes and proton leakage across the inner mitochondrial membrane. We observed a significantly reduced state 3 and state 4 respirations in the APP cells (Fig. 3c). The addition of another substrate of complex I, glutamate was not able to further increase cellular respiration driven by complex I in both cell types. Afterwards, succinate was added as a substrate for complex II. In control cells, addition of succinate substantially increase total cell respiration, while in APP cells only a minor increase was observed (Fig.3a). In addition, after uncoupling with FCCP, the respiratory rate increased in the absence of a proton gradient, which indicates the maximum capacity of electron transport chain. This maximum capacity was significantly enhanced in the control cells in relation to the APP cells (Fig.3a).

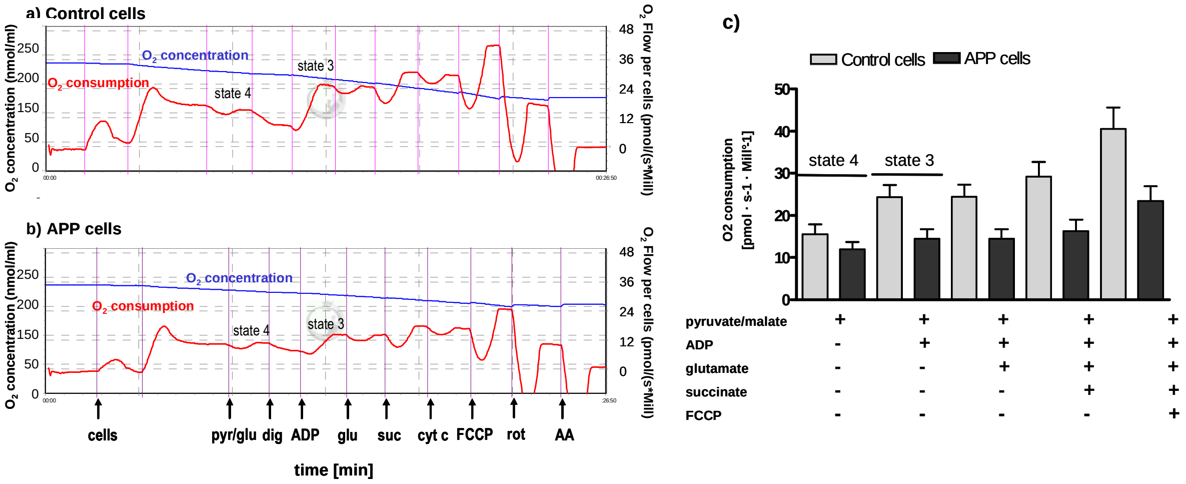

Fig.3 High-resolution respirometry revealed a reduction of oxygen consumption in APP cells. Representative diagrams of measurement of oxygen (O_2) consumption in control cells a) and in APP cells b) demonstrating a decrease in the total O_2 concentration with time . O_2 flux and consumption by vital cells was measured after addition of different agents: pyruvate/glutamate *(pyr/glu)*, digitonin (*dig*), ADP, glutamate (*glu*), succinate (*suc*), cytochrome c *(cyt c)*, FCCP, rotenone *(rot)*, antimycine A *(AA)*. C) O_2 consumption in control and APP cells. Two-way ANOVA revealed a significant difference between the cellular respiration of the two cell types ($p<0.001$). The respiratory rates of mitochondria were significantly reduced in APP cells. Values represent the means ± S.E. from n= 5 assays (cell type).

The respiratory control ratio (RCR) revealed a significant effect of Aβ on the coupling of mitochondrial respiration, indicating that the relative efficiency of metabolic coupling of electron chain complexes is impaired under conditions of chronic stress evoked by soluble forms of Aß in our APP cell model (Fig. 4a). ATP levels were significantly reduced in APP cells (Fig. 4b). Taken together, these results suggest that soluble species of Aß exhibit an initial defect in mitochondrial function with reduced complex IV activity that is translated into a mitochondrial respiration deficiency with diminished ATP synthesis, which cannot be compensated by an increased activity of complex III.

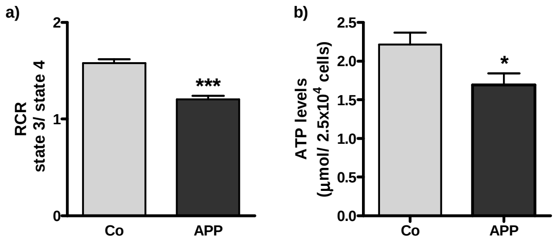

Fig.4 Reduced respiratory control ratio (state3/state4) (RCR) and impaired ATP synthesis in APP cells. a) Significantly reduced RCR in APP cells (***, $p < 0.001$ versus control cells, Student’s t test), indicating an impaired efficiency of electron transport. Values represent means +/- S.E. from n=5. b, in accordance, ATP levels are significantly reduced in APP cells (*, $p < 0.05$ versus control cells, Student’s t test).Values represent means ± S.E. from n=5 (measurements of control and APP cells were performed in parallel).

DISCUSSION

A priori our findings support a toxic role of Aβ in respiration. Although the specific pathways that lead to energy deprivation in AD remain unclear, there is evidence in favour of Aβ- induction of cell loss and synaptic failure by energy deprivation and oxidative stress (Gibson and Huang 2002; Mattson and Liu 2002). Recently, the focus on toxic species of Aβ has switched from its extracellular and fibrillar forms to its soluble species, e.g. oligomers, that can be detected ntracellularly and may represent the primary toxic Aβ correlate (Fernandez-Vizarra et al. 2004; Lustbader et al. 2004). Accoding to this novel hypothesis, mitochondrial dysfunction may play a crucial role in the biochemical pathway, by which Aβ can lead to neuronal dysfunction in AD (Eckert et al. 2008).

To unravel the effects of soluble species of Aβ on the mitochondrial respiratory capacity under physiological conditions, we established for the first time a high resolution respiratory protocol to perform whole cell recording of total cellular respiration in control and with wild-type APP stably transfected human neuroblastoma cells (SH-SY5Y). We observed an impairment of oxygen consumption rate and a decrease of respiratory control ratio (state3/state4) in the APP that might be induced by the chronic over expression of Aβ within the low nanomolar range. This defect of the whole mitochondrial respiratory chain may be explained by the accumulated dysfunctions of one or several mitochondrial chain complexes. To test this hypothesis, we measured individual activities of mitochondrial complexes I-IV as well as the ATP levels. Our results clearly show a decrease in complex IV activity in the APP cells, which is in accordance to previous findings (Cardoso et al. 2004a; Caspersen et al. 2005; Hauptmann et al. 2008). Interestingly, the activity of the complex III significantly increased, most probably as a compensatory mechanism in response to the toxic effect of Aβ on complex IV. Nevertheless, this compensatory response could not entirely balance or avoid the impairment of cellular respiration. This finding is in contrast to Caspersen et al. (2005). Accordingly, a decrease of complex III activity was revealed, together with a decrease of complex IV activity in brain tissues from APP transgenic mice at the age of 12 months. It is likely that in our cell model, we were able to detect a premature intervention mechanism in response to soluble forms of Aβ as a compensatory increase of complex III activity, whereas the strong Aβ load might have lead to a breakdown of that response thus decreasing complex III activity. Moreover, we could show that complexes I and II were not affected by Aβ, which is in accordance with findings on APP transgenic mice (Caspersen et al. 2005; Hauptmann et al. 2008). However, it contrasts to *in vitro* findings on isolated mitochondria, which were acutely treated with rather high concentrations of aggregated and fibrillar forms of Aβ (5-50µM), which in turn can induce defects in nearly all complexes (Aleardi et al. 2005; Casley et al. 2002a; Casley et al. 2002b). Thus, nearly all other studies used synthetic Aß peptides in the micromolar range, many orders of magnitude over physiological levels, and cells or even isolated mitochondria were exposed only to synthetic Aß fragments. By contrast, our neuroblastoma cell model represents a very valuable approach to investigate AD-specific cell death pathways by studying Aß levels within the picomolar range. This cell model attempts to mimic physiological conditions studying chronic effects of rather low concentrations of Aß that are relevant for AD patients. The fact that the mitochondrial dysfunction in our APP cell model, especially the decrease in complex IV activity, is already observed at picomolar concentrations and higher amounts of synthetic Aß are needed to achieve a comparable mitochondrial impairment highlights also the potential role of other APP fragments, e.g. the carboxy-terminal APP fragments (CTFs), which may accelerate the Aß-induced mitochondrial failure (Jin et al., 2002; Chang and Su, 2005). This is of special interest, since both, Aß and CTFs, can accumulate intraneuronally. The neuronal loss and synaptic transmission deficit in AD may therefore depend on intraneuronal accumulation of Aß and CTFs (Jin et al., 2002; Chang and Su, 2005). Similarly, we showed that energy production was impaired in the APP cells, which is corroborated with other findings (Hauptmann et al., 2008; Keil et al., 2004).

One can speculate that in humans increased accumulation and associated mitochondrial toxicity can be underlying factors in the pathogenesis of AD. Initially, the damaging effects of low physiological concentrations of Aß may be partly compensated by an adaptive response, e.g. increased complex III activity. However, when age-related secondary stress occurs, pronounced mitochondrial impairment might lead to the induction of cell death processes, while in familial AD, high Aß load might be directly responsible for mitochondrial and cellular dysfunction. In summary, we show novel and distinct actions of Aß on mitochondria that may contribute to the pathogenic outcome.

MATERIAL AND METHODS

Cell culture. Stably expressing cell lines were obtained by transfecting the human neuroblastoma SH-SY5Y with cDNAs (pCEP4 vector) containing either vector alone (control cells) or the entire coding region of human APP (APP695) (Scheuermann et al. 2001). Stably transfected cell clones were selected with hygromycin (Scheuermann et al. 2001). Cells were grown at 37^{o}C in DMEM medium supplemented with 10% calf serum, 2mM L-glutamine, and 0.3µg/ml hygromycin.

Detection of Aß levels. For the detection of secreted Aß$_{1-40}$, we used a specific sandwich enzyme-linked immunosorbent assay employing monoclonal antibodies (Keil et al. 2004). The ELISA was performed in accordance to the Abeta-ELISA Kit by Biosource. The assay principle is that of a standard sandwich ELISA, which utilizes a monoclonal mouse anti-human Abeta$_{1-16}$ capture antibody, a cleavage-site-specific rabbit anti-human Abeta$_{1-40}$ C-terminal detection antibody and anti-rabbit IgG peroxidase-conjugated secondary antibody.

Western blot. Equal amounts (10-20 µg) of protein were loaded on a 4-20% acryamide gel (Invitrogen, Germany) to perform SDS-PAGE at 200 V for 50mn. The probes were transferred to a PVDF membrane (Amersham Biosciences, Germany). Equal protein loading was confirmed by Ponceau Red staining (Sigma, Germany). Membranes were saturated with 5% nonfat dry milk for one hour, washed three times with TBST and incubated with the primary antibody (monoclonal anti-APP/Aß W02, Stratech, UK, or anti-actin, Santa Cruz, Germany), overnight at 4°C. After washing with TBST, PVDF membranes were treated with anti-IgG, horseradish-coupled secondary antibody (Calbiochem, Germany), for one hour at room temperature. The bands were specifically detected by enhanced chemiluminescence reaction (ECL, Amersham, Germany).

Immunohistochemical staining. Cells were plated at a density of 4x10^{5} cells on collagen treated coverslips. After two days growing, coverslips were fixed in PBS with 4% PFA at 37° for 30mn, then permeabilized with 0.1% Triton for 15mn and blocked with PBS 10% goat serum for 1h at 37°C. The coverslips were incubated for 1h at 37°C with the primary antibody (monoclonal mouse anti-APP MAB348, Chemicon International, Switzerland, which recognizes amino acids 66-81 of the N-terminal of APP). After washing with PBS, they were incubated for 30mn at 37°C with the secondary antibody anti-mouse IgG biotinylated (Sigma, Switzerland). Then, they were incubated with Vectastain ABC reagent (Vector Laboratories Inc., Burlingame) containing avidin and horseradish peroxidase reagents for immunoperoxidase staining. Finally, slides were incubated with AEC substrate solution (Sigma, Switzerland) containing 3-amino-9-ethyl carbazole for localizing peroxidase in the cells by producing a red reaction product. Staining was assessed using a Zeiss Axiolab microscope. Black-and-white photographs were taken.

Phase contrast microscopy and morphological anlysis. For the morphological analysis, cells were seeded at a density of $4x10^4$ cells/ml on coverslips previously coated with 0.05 mg/mL collagen. Phase contrast pictures were taken from living neuroblastoma cells using a Zeiss Axiolab microscope equipped with a digital camera Zeiss AxioCam MRc.

Preparation of isolated mitochondria. Cells were incubated for 15mn in an ice-cold lysis buffer (75mM NaCl, 1mM NaH_2PO_4, 8mM Na_2HPO_4, 250mM sucrose, 1mM Pefabloc, 0.05% digitonine, complete protease inhibitor mixture tablets® (Roche Diagnostics). Then, the cells were homogenized with a glass homogenizer (10 strokes at 400rpm and 5 strokes at 700rpm), and the resulting homogenate was centrifuged at 800 *x g* for 10mn at 4°C to remove nuclei and tissue particles. The supernatant 1 (S1) was saved and the pellet resuspended in the lysis buffer. The homogenization step as well as the low-speed centrifugation step was repeated. The supernatant 2 (S2) was saved and added to the supernatant 1. The combined mitochondria-enriched supernatants (S1+S2) were centrifuged at 20,000 *x g* for 15mn at 4°C to obtain the mitochondrial fraction. The pellet was resuspended in PBS and stored at 4°C until use, followed by determination of protein content (Lowry et al. 1951).

Complex I activity. A total of 300μg of isolated mitochondria was solubilized in n-dodecyl β-D-maltoside (20%). NADH:hexaammineruthenium(III)-chloride (HAR) activity was measured at 30 °C in a buffer containing 2mM Na^+/MOPS, 50mM NaCl, and 2mM KCN, pH 7.2, using 2mM HAR and 200μM NADH, as substrates to estimate the complex I content. To determine NADH-ubiquinone oxidoreductase activity, 100μM *n*-decylubiquinone (DBQ) and 100μM NADH were used as substrates and 5μM rotenone as inhibitor, as described previously (David et al. 2005; Djafarzadeh et al. 2000; Hauptmann et al. 2008). Oxidation rates of NADH were recorded with a Shimadzu Multi Spec-1501 diode array spectrophotometer ($\varepsilon_{340\text{-}400nm}$ = 6.1 $mM^{-1}.cm^{-1}$). Complex I activity was normalized to the complex I content of the mitochondrial preparation and is given as DBQ/HAR ratio.

Complex II activity. The assay was performed by following the decrease in absorbance at 600 nm, which results in the reduction of 2,6-dichlorophenolindo-phenol (DCIP) in 1ml of medium containing 60mM KH_2PO_4 (pH 7.4), 3mM KCN, 20µg/mL rotenone, 20mM succinate, and 20µg mitochondrial protein. The reaction was initiated by the addition of 1.3mM phenazine methasulfate (PMS) and 0.18mM DCIP as described previously (Aleardi et al. 2005).The extinction coefficient used for DCIP was $21mM^{-1}$ $.cm^{-1}$.

Complex III activity. The oxidation of 50µM decylubiquinol obtained by complex III was determined using cytochrome *c* as an electron acceptor as described previously (Krahenbuhl et al. 1991). Briefly, decylubiquinol is prepared by dissolving decylubiquinone (10mM) in ethanol acidified to pH 2. The quinone is reduced with excess solid sodium borohydride. Decylubiquinol is extracted into diethylether:cyclohexane (2:1, v/v) and evaporated to dryness under nitrogen gas, dissolved in ethanol acidified to pH 2. The assay was carried out in a medium containing 35mM KH_2PO_4, 5mM $MgCl_2$, 2mM KCN (pH 7.2), supplemented with 2.5mg/mL BSA, 15µM cytochrome *c*, 0,6mM n-dodecyl β-D-maltoside and 5µg/mL rotenone. The reaction was started with 10µg of mitochondrial protein and the enzyme activity was measured at 550 nm. The extinction coefficient used for cytochrome *c* was $18.5mM^{-1}.cm^{-1}$.

Complex IV activity. Cytochrome *c* oxidase activity was determined in intact isolated mitochondria (100µg) using Cytochrome *c* Oxidase Assay Kit. The colorimetric assay is based on the observation that a decrease in absorbance at 550 nm of ferrocytochrome *c* is caused by its oxidation to ferricytochrome *c* by cytochrome *c* oxidase. The Cytochrome *c* Oxidase Assay was performed as described previously (Rasmussen and Rasmussen 2000).

Mitochondrial respiration in vital cells. Mitochondrial oxygen consumption was measured at 37°C using an Oroboros Oxygraph-2k system. Five millions of cells were added to 2ml of a mitochondrial respiration medium containing 0.5mM EGTA, 3mM $MgCl_2$, 60mM K-lactobionate, 20mM Taurine, 10mM KH_2P0_4, 20mM HEPES, 110mM Sucrose, 1g/l BSA (pH 7.1). To measure the state 4 (= state 2) of the complex I, 5mM pyruvate and 2mM malate were added and cells were permeabilised with 15µg/ml digitonin. Afterwards, 2mM ADP is added to measure state 3 respiration, and, in order to increase the respiratory capacity, 10mM glutamate was added. To study the effect of the convergent complex I+II electron input on the respiration, 10mM of succinate was added. The integrity of the mitochondrial membrane was checked through the addition of 10uM cytochrome c. After determining coupled respiration, 0.4µM FCCP (Carbonyl cyanide p-(trifluoro-methoxy) phenyl-hydrazone) was added and respiration was measured in the absence of a proton gradient. In order to inhibit complex I and III activities 0.5uM rotenone and 2.5uM antimycine A, respectively were added. Mock and APP cells were measured in parallel pairs using the same conditions (crossover design).

Citrate synthase activity. The reduction of 5,5'-dithiobis(2-nitrobenzoic acid) (DTNB) by citrate synthase at 412 nm (extinction coefficient of 13.6mM-1.cm-1) was followed in a coupled reaction with coenzyme A and oxaloacetate (Aleardi et al. 2005). Briefly, a reaction mixture of 0.2M Tris-HCl, pH 8.0, 0.1mM acetyl-coenzymeA, 0.1mM DTNB, n-dodecyl-β-D-maltoside (20%) and 10g of mitochondrial protein was incubated at 30°C for 5 min. The reaction was initiated by adding 0.5mM oxaloacetate, and the absorbance change was monitored for 5min with a Shimadzu Multi-Spec-1501 diode array spectrophotometer.

Determination of ATP levels. Cells were plated one day before at a density of 2.5 x 10^4 cells/ well in a white 96 well plate. The kit is based on the bioluminescent measurement of ATP. The bioluminescent method utilizes the enzyme luciferase, which catalyses the formation of light from ATP and luciferin. The emitted light was linearly related to the ATP concentration and was measured using a luminometer (David et al. 2005; Keil et al. 2004).

Statistical Analysis. Data are presented as mean ± S.E.M. For all statistical comparison, Student's *t*-test or Two-way ANOVA was used. P values less than 0.05 were considered statistically significant.

ACKNOWLEDGEMENTS

This research was supported by grant from the SNSF (Swiss National Science Foundation) #310000-108223 to A.E.

REFERENCES

Aleardi, A. M., Benard, G., Augereau, O., Malgat, M., Talbot, J. C., Mazat, J. P., Letellier, T., Dachary-Prigent, J., Solaini, G. C., and Rossignol, R. (2005) Gradual alteration of mitochondrial structure and function by beta-amyloids: importance of membrane viscosity changes, energy deprivation, reactive oxygen species production, and cytochrome c release. J Bioenerg Biomembr 37:207-25.

Blass, J. P. (2003) Cerebrometabolic abnormalities in Alzheimer's disease. Neurol Res. 25:556-66.

Canevari, L., Clark, J. B., and Bates, T. E. (1999) beta-Amyloid fragment 25-35 selectively decreases complex IV activity in isolated mitochondria. FEBS Lett 457:131-4.

Cardoso, S. M., Proenca, M. T., Santos, S., Santana, I., and Oliveira, C. R. (2004a) Cytochrome c oxidase is decreased in Alzheimer's disease platelets. Neurobiol Aging 25:105-10.

Cardoso, S. M., Santana, I., Swerdlow, R. H., and Oliveira, C. R. (2004b) Mitochondria dysfunction of Alzheimer's disease cybrids enhances Abeta toxicity. J Neurochem 89:1417-26.

Casley, C. S., Canevari, L., Land, J. M., Clark, J. B., and Sharpe, M. A. (2002a) Beta-amyloid inhibits integrated mitochondrial respiration and key enzyme activities. J Neurochem 80:91-100.

Casley, C. S., Land, J. M., Sharpe, M. A., Clark, J. B., Duchen, M. R., and Canevari, L. (2002b) Beta-amyloid fragment 25-35 causes mitochondrial dysfunction in primary cortical neurons. Neurobiol Dis 10:258-67.

Caspersen, C., Wang, N., Yao, J., Sosunov, A., Chen, X., Lustbader, J. W., Xu, H. W., Stern, D., McKhann, G., and Yan, S. D. (2005) Mitochondrial Abeta: a potential focal point for neuronal metabolic dysfunction in Alzheimer's disease. Faseb J 19:2040-1.

Cassarino, D. S., and Bennett, J. P., Jr. (1999) An evaluation of the role of mitochondria in neurodegenerative diseases: mitochondrial mutations and oxidative pathology, protective nuclear responses, and cell death in neurodegeneration. Brain Res Brain Res Rev 29:1-25.

Chagnon, P., Betard, C., Robitaille, Y., Cholette, A., and Gauvreau, D. (1995) Distribution of brain cytochrome oxidase activity in various neurodegenerative diseases. Neuroreport. 6:711-5.

Chang, K. A., Suh, Y. H. (2005) Pathophysiological roles of amyloidogenic carboxy-terminal fragments of the beta-amyloid precursor protein in Alzheimer's disease. J Pharmacol Sci 97:461-71.

David, D. C., Hauptmann, S., Scherping, I., Schuessel, K., Keil, U., Rizzu, P., Ravid, R., Drose, S., Brandt, U., Muller, W. E., Eckert, A., and Gotz, J. (2005) Proteomic and functional analyses reveal a mitochondrial dysfunction in P301L tau transgenic mice. J Biol Chem 280:23802-14.

Djafarzadeh, R., Kerscher, S., Zwicker, K., Radermacher, M., Lindahl, M., Schagger, H., and Brandt, U. (2000) Biophysical and structural characterization of proton-translocating NADH-dehydrogenase (complex I) from the strictly aerobic yeast Yarrowia lipolytica. Biochim Biophys Acta 1459:230-8.

Eckert, A., Hauptmann, S., Scherping, I., Meinhardt, J., Rhein, V., Drose, S., Brandt, U., Fandrich, M., Muller, W. E., and Gotz, J. (2008) Oligomeric and fibrillar species of beta-amyloid (Abeta42) both impair mitochondrial function in P301L tau transgenic mice. J Mol Med 86:1255-67.

Eckert, A., Keil, U., Marques, C. A., Bonert, A., Frey, C., Schussel, K., and Muller, W. E. (2003) Mitochondrial dysfunction, apoptotic cell death, and Alzheimer's disease. Biochem Pharmacol 66:1627-34.

Fernandez-Vizarra, P., Fernandez, A. P., Castro-Blanco, S., Serrano, J., Bentura, M. L., Martinez-Murillo, R., Martinez, A., and Rodrigo, J. (2004) Intra- and extracellular Abeta and PHF in clinically evaluated cases of Alzheimer's disease. Histol Histopathol. 19:823-44.

Gibson, G. E., and Huang, H. M. (2002) Oxidative processes in the brain and non-neuronal tissues as biomarkers of Alzheimer's disease. Front Biosci 7:d1007-15.

Hauptmann, S., Scherping, I., Drose, S., Brandt, U., Schulz, K. L., Jendrach, M., Leuner, K., Eckert, A., and Muller, W. E. (2008) Mitochondrial dysfunction: An early event in Alzheimer pathology accumulates with age in AD transgenic mice. Neurobiol Aging.

Hirai, K., Aliev, G., Nunomura, A., Fujioka, H., Russell, R. L., Atwood, C. S., Johnson, A. B., Kress, Y., Vinters, H. V., Tabaton, M., Shimohama, S., Cash, A. D., Siedlak, S. L., Harris, P. L., Jones, P. K., Petersen, R. B., Perry, G., and Smith, M. A. (2001) Mitochondrial abnormalities in Alzheimer's disease. J Neurosci. 21:3017-23.

Jin, L. W., Hua, D. H., Shie, F. S., Maezawa, I., Sopher, B., Martin, G. M. (2002) Novel tricyclic pyrone compounds prevent intracellular APP C99-induced cell death. J Mol Neurosci 19:57-61.

Keil, U., Bonert, A., Marques, C. A., Scherping, I., Weyermann, J., Strosznajder, J. B., Muller-Spahn, F., Haass, C., Czech, C., Pradier, L., Muller, W. E., and Eckert, A. (2004) Amyloid beta-induced changes in nitric oxide production and mitochondrial activity lead to apoptosis. J Biol Chem 279:50310-20.

Krahenbuhl, S., Chang, M., Brass, E. P., and Hoppel, C. L. (1991) Decreased activities of ubiquinol:ferricytochrome c oxidoreductase (complex III) and ferrocytochrome c:oxygen oxidoreductase (complex IV) in liver mitochondria from rats with hydroxycobalamin[c-lactam]-induced methylmalonic aciduria. J Biol Chem 266:20998-1003.

Leuner, K., Hauptmann, S., Abdel-Kader, R., Scherping, I., Keil, U., Strosznajder, J. B., Eckert, A., and Muller, W. E. (2007) Mitochondrial dysfunction: the first domino in brain aging and Alzheimer's disease? Antioxid Redox Signal 9:1659-75.

Lowry, O. H., Rosebrough, N. J., Farr, A. L., and Randall, R. J. (1951) Protein measurement with the Folin phenol reagent. J. Biol. Chem. 193, 265–275.

Lustbader, J. W., Cirilli, M., Lin, C., Xu, H. W., Takuma, K., Wang, N., Caspersen, C., Chen, X., Pollak, S., Chaney, M., Trinchese, F., Liu, S., Gunn-Moore, F., Lue, L. F., Walker, D. G., Kuppusamy, P., Zewier, Z. L., Arancio, O., Stern, D., Yan, S. S., and Wu, H. (2004) ABAD directly links Abeta to mitochondrial toxicity in Alzheimer's disease. Science. 304:448-52.

Mattson, M. P., and Liu, D. (2002) Energetics and oxidative stress in synaptic plasticity and neurodegenerative disorders. Neuromolecular Med 2:215-31.

Parker, W. D., Jr., Parks, J., Filley, C. M., and Kleinschmidt-DeMasters, B. K. (1994) Electron transport chain defects in Alzheimer's disease brain. Neurology 44:1090-6.

Rasmussen, U. F., and Rasmussen, H. N. (2000) Human quadriceps muscle mitochondria: a functional characterization. Mol Cell Biochem 208:37-44.

Rhein, V., and Eckert, A. (2007) Effects of Alzheimer's amyloid-beta and tau protein on mitochondrial function - role of glucose metabolism and insulin signalling. Arch Physiol Biochem 113:131-41.

Scheuermann, S., Hambsch, B., Hesse, L., Stumm, J., Schmidt, C., Beher, D., Bayer, T. A., Beyreuther, K., and Multhaup, G. (2001) Homodimerization of amyloid precursor protein and its implication in the amyloidogenic pathway of Alzheimer's disease. J Biol Chem 276:33923-9.

Swerdlow, R. H., and Kish, S. J. (2002) Mitochondria in Alzheimer's disease. Int Rev Neurobiol 53:341-85.

4. Ginkgo biloba extract ameliorates oxidative phosphorylation performance and rescues Aβ-induced failure

Rhein V, Baysang G, Rao S, Meier F, Tripodi T, Giese M, Schulz K, Müller-Spahn F, Eckert A.

Neurobiology Laboratory for Brain Aging and Mental Health, Psychiatric University Clinics, Univ. of Basel, Basel, Switzerland

Manuscript submitted

ABSTRACT

Background: Energy deficiency and mitochondrial failure have been recognized as a prominent, early event in Alzheimer's disease (AD). Recently, we demonstrated that chronic exposure to amyloid-beta (Aβ) in human neuroblastoma cells over-expressing human wild-type amyloid precursor protein (APP) resulted in (i) activity changes of complexes III and IV of the oxidative phosphorylation system (OXPHOS) and in (ii) a drop of ATP levels which may finally instigate loss of synapses and neuronal cell death in AD. Therefore, the aim of the present study was to investigate whether standardized Ginkgo biloba extract LI 1370 (GBE) is able to rescue Aβ-induced defects in energy metabolism.

Methodology: We used a high-resolution respiratory protocol to investigate OXPHOS respiratory capacity and metabolic states under physiological condition in vital control and APP cells after treatment with GBE. In addition, oxygen consumption of isolated mitochondria, activities of mitochondrial enzymes (complexes I-IV and citrate synthase), ATP levels, mitochondria amount, and mitochondrial DNA content were determined.

Principal Findings: We observed a GBE-induced increase of the coupling state of mitochondria resulting in an improvement of the OXPHOS efficiency in both cell lines, with the strongest enhancing effect in APP cells. GBE effect on OXPHOS was even preserved in mitochondria after isolation from treated cells. The GBE-induced amelioration of oxygen consumption most likely arose from the modulation and respective normalization of the activity of mitochondrial complexes I, III and IV that are markedly disturbed in APP cells finally yielding a rise in ATP levels. Of note, these functional data were paralleled by an up-regulation of mitochondrial DNA in GBE-treated cells.

Conclusions/Significance: Although the underlying molecular mechanisms of the mode of action of GBE remain to be determined, our study clearly highlights the beneficial effect of GBE on the cellular OXPHOS performance leading to retrieval of Aβ-induced mitochondrial dysfunction.

INTRODUCTION

Standardized Ginkgo biloba extract (GBE) derived from dried leaves of Ginkgo tree is a valuable therapeutic drug for the treatment of memory impairment and dementia including Alzheimer's disease (AD). Double-blind, placebo-controlled studies showed the improvement of cognitive symptoms in the elderly and in AD patients [1-5]. GBE exhibits a complex mode of action. Notably, multiple effects on mitochondrial function and on the apoptotic pathway that seems to be crucial for its beneficial effects in AD were reported: stabilization of mitochondrial membrane potential, improvement of energy metabolism, up-regulation of anti-apoptotic Bcl-2 protein and down-regulation of pro-apoptotic Bax protein, inhibition of cytochrome c release, reduction of caspase 9 and caspase 3 activity after oxidative stress and reduction of apoptotic cell death [6-12]. However, evidence how GBE influences the mitochondrial oxidative phosphorylation system (OXPHOS) in neuronal cells is lacking.

AD is characterized by amyloid-beta (Aβ)-containing plaques, neurofibrillary tangles, as well as synapse and neuron loss. Aβ which represents with tau the main neuropathological hallmarks of AD is supposed to play a pivotal role in the pathogenesis of the disease. Within the Aβ toxicity cascade, mitochondrial dysfunction and energy metabolism deficiencies have been recognized as earliest events [8, 13] and have been correlated with impairments of cognitive abilities in AD clinical scenario [14]. The most consistent defect in mitochondrial electron transport chain enzymes in AD is the deficiency in cytochrome c oxidase (complex IV) activity in post-mortem brain tissues of AD patients [15-17] and APP transgenic mice [18], as well as in other tissues, such as platelets from AD patients and AD cybrid cells [19, 20]. Interestingly, few years ago, the target of interest of Aβ toxic species switched from its extracellular, fibrillar form to its soluble, oligomeric form [21, 22] emphasising the important early role of mitochondria in AD pathogenic pathways [8, 23-25].

In line with these findings, we recently reported that chronic exposure to Aβ in human neuroblastoma cells (SH-SY5Y) over-expressing human wild-type APP (APP cells) resulted in an impairment of the respiratory capacity of OXPHOS and a drop in ATP generation by complex V which in turn may initiate cell death pathway [26].

Therefore, the aim of the present study was to investigate the potential effect of standardized GBE LI 1370 on Aβ-induced mitochondrial dysfunction in APP cells. In addition to the measurement of oxygen consumption in whole cells as well as of isolated mitochondria, we examined activities of mitochondrial enzymes assembling the electron transport system (ETS) that are the complexes I to IV, the activity of citrate synthase, an enzyme located in the mitochondrial matrix those activity is reported to be very proportional to the content of ETS enzymes within mitochondria [27], ATP levels and mitochondria mass. Finally, we studied the mitochondrial DNA / nuclear DNA ratio using real-time PCR to determine changes at the genetic level.

RESULTS

GBE did not modify cells morphology but decreased amount of mitochondria. As described in our previous study [26], transfection of SH-SY5Y cells with cDNAs (pCEP4 vector) containing the vector alone or the entire coding region of human APP (APP695) did not significantly change the general morphological aspect of cells (Fig 1A). Similarly, vector control as well as APP cells conserved their neuroblast-like morphology with differentiated perikaria and short neurites after treatment with GBE (Fig 1B). However, using a MitoTracker Green^{TM}, we observed a decrease of mitochondria amount in GBE-treated control and APP cells, with the strongest effect in APP cells (Fig. 1C). In accordance with this result, citrate synthase (CS) activity, which is commonly used as a quantitative measure of the content of mitochondria and ETS enzymes [27], was also reduced in GBE-treated control and APP cells (Fig. 1D).

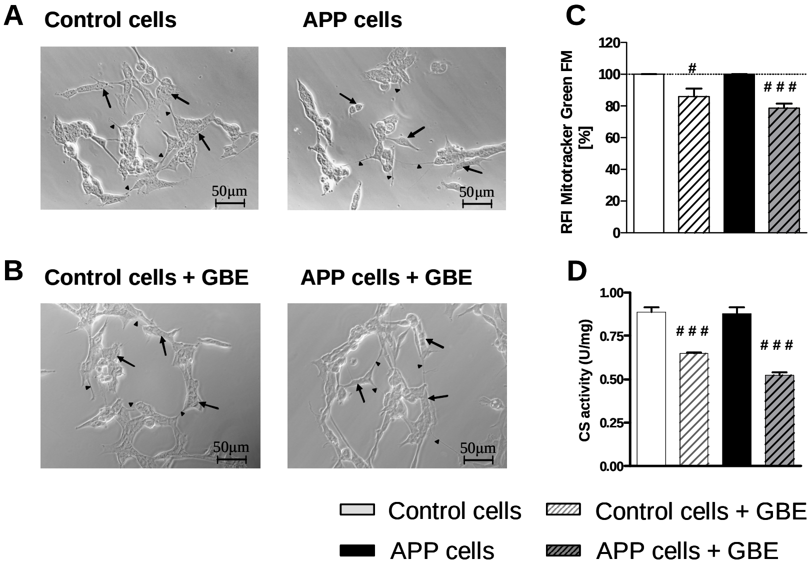

Fig.1 GBE did not modify cell morphology but mitochondrial amount. Morphological analysis of vector control and APP cells showed neuroblast-like morphology with differentiated perikaria (*arrows*) and occasional short neurites (*arrowheads*). **A)** Transfection of SH-SY5Y cells with cDNAs (pCEP4 vector) containing the vector alone or the entire coding region of wild-type human APP (APP cells) and **B)** GBE treatment (0.1mg/ml; 24h) did not significantly change general cell morphology. Scale bars: 50µm. **C)** A decrease of mitochondria amount was measured in GBE-treated cells using MitoTracker Green^{TM}. **D)** A decrease of citrate synthase activity (CS) was observed in GBE-treated cells. Values represent the means ± S.E. from n= 5 assays, student's t-test: #, $p<0.05$; ###, $p<0.001$ versus corresponding untreated cells.

GBE ameliorated OXPHOS capacity and restored Aβ-induced deficits in vital cells. To investigate the protective effect of GBE against Aβ toxicity at the mitochondrial level, we used a high-resolution respiratory protocol established lately by our group [26]. Thus, physiological substrate combinations (pyruvate, glutamate and malate as substrates for complex I and succinate for complex II) were used to obtain mitochondrial bioenergetics approaching the most of physiological states (Fig. 2A). We compared OXPHOS that is the whole ETS composed of the four mitochondrial enzymes (complex I to complex IV) and the F_1F_0ATP synthase of vital control and APP cells after pre-treatment with GBE for 24h. As previously observed [26], APP cells exhibited an impairment of OXPHOS capacity (Fig, 2B). Of note, GBE was able to significantly ameliorate the global failure of mitochondrial respiration in APP cells and increased oxygen consumption in control cells as well (Fig. 2B). Importantly, GBE-treated control and APP cells presented comparable mitochondrial respiratory rate validating the protective role of GBE on stabilization and normalization of mitochondrial capacity, respectively (Fig. 2B).

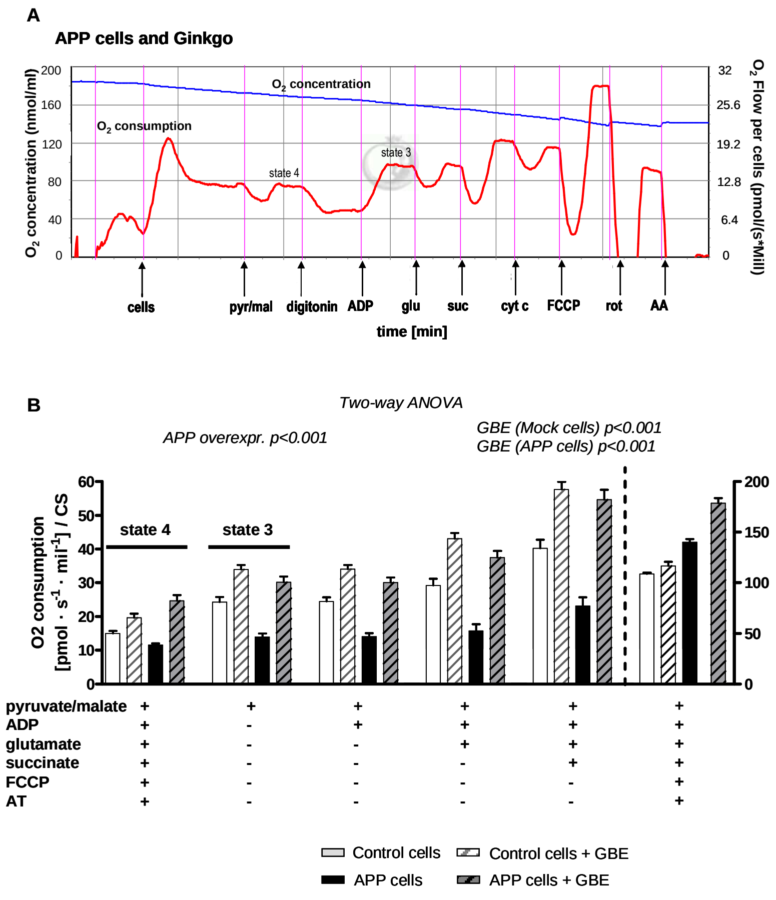

Fig.2 High-resolution respirometry revealed an improvement of mitochondrial capacity of vital cells after GBE treatment. A) Representative diagram of measurement of oxygen (O_2) consumption in GBE-treated APP cells. O_2 flux and O_2 consumption by vital cells were measured after addition of different agents: pyruvate/glutamate *(pyr/glu)*, digitonin (*dig*), ADP, glutamate (*glu*), succinate (*suc*), cytochrome c *(cyt c)*, FCCP, rotenone *(rot)*, antimycine A *(AA)*. **B)** Two-way ANOVA revealed a significant Aβ-induced decrease of the cellular respiration in APP cells compared to that of control cells ($p<0.001$). Two-way ANOVA revealed also a significant effect of GBE on O_2 consumption. Indeed, respiratory rates of mitochondria were increase in GBE-treated control and APP cells corresponding to that of their respective cell type ($p<0.001$). Values represent the means ± S.E. from n= 5 assays (measurements of control and APP cells were performed in parallel).

To analyse the impact of GBE on metabolic states of mitochondrial respiration, two flux control ratios have been evaluated. First, the respiratory control ratio (RCR3/4) which is an indicator of the coupling state of mitochondria was determined. State 3 is the rate of phosphorylating respiration in the presence of exogeneous ADP, when mitochondria are actively making ATP, whereas state 4 is the rate of resting respiration, when all ADP has been consumed. State 4 is associated with proton leakage across the inner mitochondrial membrane, when mitochondria exhibit basal activity, i.e. they are respiring but not making ATP. Therefore, RCR3/4 represents the ADP-activated flux to measure coupled OXPHOS capacity (state3) divided by leak flux (state4). Whereas increased Aβ levels led to a decrease of RCR3/4 in APP cells, treatment with GBE significantly increased the ratio in both cell types (Fig. 3A). Secondly, ROX/ETS yields an index of the magnitude of residual oxygen consumption relative to maximum oxygen consumption capacity. This ratio was decreased in both cell types after treatment with GBE with the strongest effect in APP cells (Fig. 3B). Both flux control ratio changes indicate an increase of the coupling state of mitochondria leading to a better efficiency of OXPHOS. Consistent with this result, we observed a rise of ATP levels produced by complex V, the final OXPHOS enzyme, in GBE-treated control and APP cells (Fig. 3C).

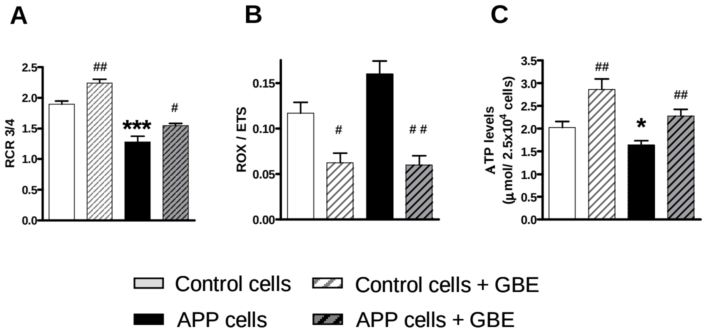

Fig.3 GBE modulated mitochondrial flux control ratios and rose ATP synthesis. A) Respiratory control ratio (RCR3/4) represents the mitochondrial coupling state. RCR3/4 was decreased in APP cells and increased in GBE-treated control and APP cells. **B)** ROX/ETS yields an index of the magnitude of residual oxygen consumption relative to the maximum oxygen consumption capacity. This ratio was decreased in GBE-treated control and APP cells. **C)** ATP levels were decreased in APP cells and increased in GBE-treated control and APP cells. Values represent the means ± S.E. from n= 5 assays, student's t-test: *, $p<0.05$; ***, $p<0.001$ versus control cells; #, $p<0.05$; ##, $p<0.01$ versus corresponding untreated cells.

Taken together, respiratory analyses showed that GBE enhanced metabolic pathways by increasing the coupling state of OXPHOS promoting finally a rise of ATP synthesis in both cell types but with the strongest effects on APP cells. As a consequence, GBE-treated control and APP cells presented comparable mitochondrial respiratory system capacity suggesting a complete restoration of Aβ-induced deficits in energy metabolism.

GBE improved oxygen consumption in isolated mitochondria from APP cells and led to an up-regulation of mitochondrial DNA. To confirm the improvement of mitochondrial performance observed in whole cells, we investigated oxygen consumption of mitochondria that were isolated form APP cells after 24h treatment with GBE. In isolated mitochondria, the GBE-induced enhancement of oxygen consumption was still significantly present (Fig. 4A) suggesting a regulatory effect of GBE at the mitochondrial level even after its removal. Of note, this functional enhancement can be associated with an increase of the mitochondrial DNA / nuclear DNA ratio after treatment with GBE (Fig. 4B).

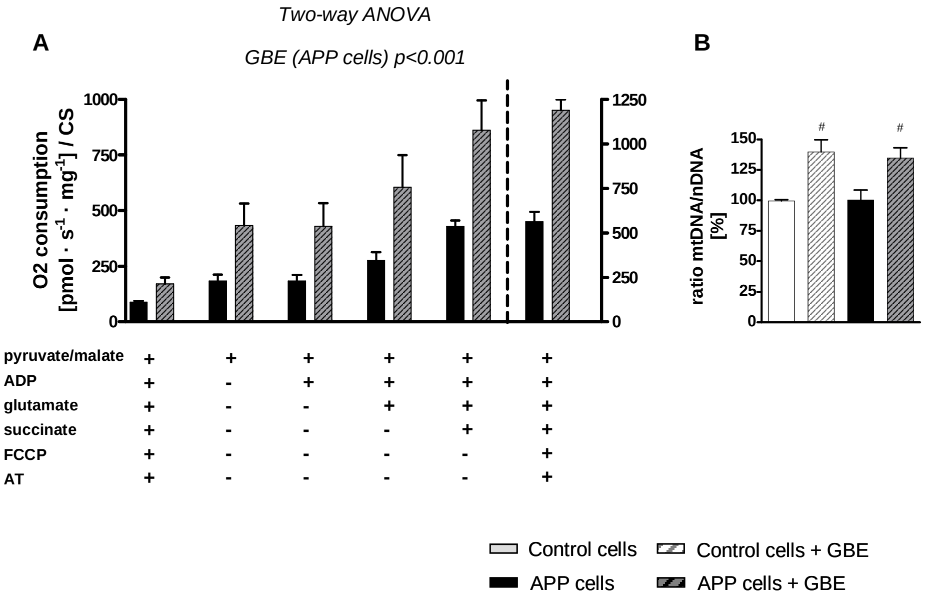

Fig.4 GBE enhanced oxygen consumption of isolated mitochondria from APP cells and led to an up-regulation of mitochondrial DNA. A) Two-way ANOVA revealed a significant effect of GBE on respiratory rates of isolated mitochondria from APP cells. The oxygen consumption was increased in mitochondria isolated from GBE-treated APP cells when compared to that of untreated APP cells ($p<0.001$). **B)** RT-PCR analyses revealed an increase of the mitochondrial DNA / nuclear DNA ratio from GBE-treated control and APP cells compared to their corresponding untreated cells (#, $p<0.05$). Values represent means ± S.E. from n=5 assays.

GBE modulated the activity of respiratory complexes. To improve the mitochondrial respiratory capacity, GBE may act on one or several mitochondrial enzyme. To study this hypothesis, the activities of individual respiratory complexes have been investigated. Complex I activity was significantly increased in GBE-treated APP cells (Fig 5A). Complex III activity which is markedly increased in APP cells was normalized to the level of control cells after treatment with GBE (Fig. 5B). Complex IV activity which is decreased in APP cells, significantly increased in control and APP cells after treatment with GBE (Fig. 5C).

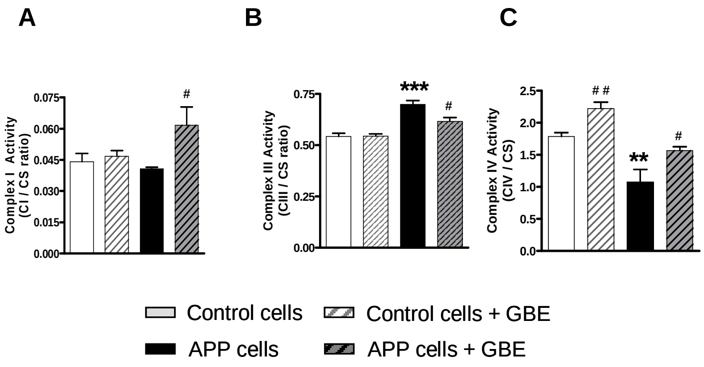

Fig.5 GBE modulated activities of mitochondrial ETS enzymes. A) Complex I activity (CI/CS ratio) was increased in GBE-treated APP. **B)** Complex III activity (CIII/CS ratio) was increased in APP cells and decreased in GBE-treated APP cells. **C)** Complex IV activity (CIV/CS ratio) was decreased in APP cells and increased in GBE-treated control and APP cells. All values represent the means ± S.E. from n= 4-6 assays, student's t-test: **, p<0.01, ***, p<0.001 versus control cells; #, p<0.05, ##, p<0.01 versus corresponding untreated cells.

DISCUSSION

To pinpoint the mode of action of GBE on mitochondrial function as well as on Aβ-induced OXPHOS failure, we first measured oxygen consumption in vital cells. This approach facilitates the determination of the capacity of the whole OXPHOS as well as flux control ratios (RCR3/4 and ETS/ROX) widely recognized as indicators of metabolic states of mitochondrial respiration [28]. In the present study, we present for the first time clear evidence that under physiological conditions mimicked in our respiratory whole cell protocol, GBE improved metabolic energy pathways by increasing the coupling state of mitochondria. Importantly, the comparability of the mitochondrial energetic capacity in both cell types after treatment with GEB indicates a recovery of the disturbed bioenergetics homeostasis found in APP cells. Notably, GBE-enhancing effect on OXPHOS was still present in mitochondria after removal of mitochondria from the cells suggesting possible continuing, regulatory actions of GEB at the mitochondrial level. These results corroborate findings showing an increase of the coupling state of isolated mitochondria by GBE in ischemia models [29] and findings demonstrating that GBE ameliorated oxygen consumption of mitochondria from rat heart mainly driven by effects of GBE on complex I and III [30]. The capacity of mitochondria to re-phosphorylate ADP in state 3 is positively dependent on the degree of coupling. In accordance with this assumption, we also observed an enhancement of ATP levels in both cell types after treatment with GBE. Moreover, the respiration rate in state 3 is determined by the activity of mitochondrial enzymes of the whole ETS and ATP-synthase [30, 31]. Thus, the global improvement of mitochondria functionality may be explained by the action of GBE on one or several mitochondrial enzymes. To test this hypothesis, we measured individual activities of mitochondrial enzymes belonging to the ETS. The increased activity of complex III in APP cells that can be interpreted as a compensatory mechanism to rescue Aβ-induced mitochondrial defects [26] normalized after treatment with GBE. This effect can be taken as a back to a physiological functionality, i.e. the over-activity of complex III in untreated APP cells was down-regulated in the presence of GBE which in turn up-regulated complex IV activity and ATP synthesis, both markedly reduced in our AD cell model. Interestingly, complex I activity was increased in APP cells after treatment with GBE while it was unchanged in APP cells per se. GBE by increasing the coupling mitochondrial state may improve complex I activity. Moreover, complex I due to its first position in ETS plays a crucial role in energy metabolism and oxidative phosphorylation. Indeed, a partial decrease of its activity (about 25%) is sufficient to alter severely the mitochondrial respiration [32].

Complex I as a main ROS producer may also be a key element in GBE efficacy. In an ischemic model, the increase of coupling state of mitochondria was also associated with a protection of the activities of complexes I and III by GBE [33]. Our study is further in line with recent findings studying the effect of GBE after in vivo treatment on mitochondrial membrane potential in dissociated brain cells from aged mice after inhibiting OXPHOS using specific inhibitors of complexes [9]. Here, GEB showed protective effects on mitochondrial membrane potential at the complexes I, IV and V [9]. Even if the exact molecular mechanisms by which GBE stabilizes mitochondrial enzymes is not yet clear, it can be speculated that besides other regulatory effects on mitochondria components: (i) GBE may act as an antioxidant scavenging superoxide anion generated by electron leakage which occurs mainly at complexes I and III. (ii) GBE may also scavenge nitric oxide leading to an increase of complex IV activity which is the main target of NO [34]. Consequently, the protection of mitochondrial complexes by GBE may not only lead to an increase of mitochondrial performance (coupling state) but also to a decrease of ROS production. In accordance with this idea, some authors proposed that GBE provides anti-apoptotic effects [6, 7, 35]. Thus, GBE significantly attenuated mitochondria-initiated apoptosis and decreased the activity of caspase 3, a key enzyme in the apoptosis cell signalling cascade, in neuroblastoma cells stably expressing an AD-associated double mutation in APP [10]. In addition, GBE inhibited formation of Aβ-fibrils [10] either by a direct interaction with Aβ [36, 37] or by activating α-secretase pathway [38].

Of note, we observed an up-regulation of mitochondrial DNA in cells treated with GBE, but at the same time, a decrease of mitochondria mass in GBE-treated cells suggesting that GBE may act not only at a functional level but also at a genetic one. The number of mitochondrial DNA copies per mitochondrion as well as mitochondria per cell is exquisitely calibrated on cellular energy demand. The fact that an increased content of mitochondrial DNA encoding for important core subunits of the OXPHOS is associated with an increased OXPHOS performance suggest that possibly the assembly of mitochondrial super complexes is facilitated coupled to an increased activity. Accordingly, Tendi and colleagues [35] showed that GBE up-regulated mitochondrial gene expression of a mtDNA encoded subunit of complex I (ND1) in PC12 cells which may perfectly correspond to the increase of complex I activity detected in GBE-treated APP cells. Moreover, the transcript level of the anti-apoptotic Bcl-2-like protein was found to be elevated, whereas the transcript level of the pro-apoptotic caspase 12 was decreased in PC12 cells after treatment with GBE [7, 10]. Although further studies are necessary, we can speculate that a GBE treatment may not only enhance mtDNA but may modulate mitochondria biogenesis after chronic exposure. In line with this idea, a recent study showed that GBE induced hippocampal neurogenesis, a very energy demanding process, in young and old transgenic AD mouse model (TgAPP/PS1) after receiving a diet supplemented with GBE for 1 month [39].

In total, our findings and the findings of others indicate substantial mitochondria modulating properties of GBE. We could clearly show that GBE improved OXPHOS performance and was able to restore Aβ-induced mitochondria failure. Hereby, the increase in mitochondrial content might represent an important early event. Taking into account the increasing interest in mitochondrial stabilization as intervention strategy in AD, the regulating mechanisms of GBE on mitochondria function suggested by this study qualifies this drug as therapeutic candidate.

MATERIAL AND METHODS

Cell culture. Stably expressing cell lines were obtained by transfecting human neuroblastoma SH-SY5Y with cDNAs (pCEP4 vector) containing either the vector alone (control cells) or the entire coding region of human wild-type APP (APP695) [40]. APP cells secreted Aβ levels within pg/mL range (around 150 pg/mL Aβ1-40 compared to approximately 50 pg/mL Aβ1-40 secreted by vector control cells) [26]. Stably transfected cell clones were selected with hygromycin [40]. Cells were grown at 37^{o}C in DMEM medium supplemented with 10% calf serum, 2mM L-glutamine, and 0.3µg/ml hygromycin. Cells were pre-treated with 0.1mg/ml of standardized Ginkgo biloba extract LI 1370 (Vifor SA, Switzerland), for 24h before analyzing the cells. In pre-experiments, we excluded effects of the vehicle.

Phase contrast microscopy and morphological anlysis. For the morphological analysis, cells were seeded at a density of $4x10^{4}$ cells/ml on coverslips previously coated with 0.05 mg/mL collagen. Phase contrast pictures were taken from living neuroblastoma cells using a Zeiss Axiolab microscope equipped with a digital camera Zeiss AxioCam MRc.

Preparation of isolated mitochondria. Cells were incubated for 15min in an ice-cold lysis buffer (75mM NaCl, 1mM NaH_2PO_4, 8mM Na_2HPO_4, 250mM sucrose, 1mM Pefabloc, 0.05% digitonine, complete protease inhibitor mixture tablets® (Roche Diagnostics). Then, cells were homogenized with a glass homogenizer (10 strokes at 400rpm and 5 strokes at 700rpm), and the resulting homogenate was centrifuged at 800*g* for 10min at 4°C to remove nuclei and tissue particles. The supernatant 1 (S1) was saved and the pellet resuspended in the lysis buffer. The homogenization step as well as the low-speed centrifugation step was repeated. The supernatant 2 (S2) was saved and added to the supernatant 1. Combined mitochondria-enriched supernatants (S1+S2) were centrifuged at 20,000*g* for 15min at 4°C to obtain the mitochondrial fraction. The mitochondrial pellet was resuspended in PBS and stored at 4°C until use, followed by determination of protein content [41].

Citrate synthase activity. The reduction of 5,5'-dithiobis(2-nitrobenzoic acid) (DTNB) by citrate synthase at 412 nm (extinction coefficient of $13.6mM^{-1}.cm^{-1}$) was followed in a coupled reaction with coenzyme A and oxaloacetate [26, 27]. Briefly, a reaction mixture of 0.2M Tris-HCl, pH 8.0, 0.1mM acetyl-coenzymeA, 0.1mM DTNB, n-dodecyl-β-D-maltoside (20%) and 10µg of mitochondrial protein was incubated at 30°C for 5 min. The reaction was initiated by adding 0.5mM oxaloacetate, and the absorbance change was monitored for 5min with a Shimadzu Multi-Spec-1501 diode array spectrophotometer. CS activity is given as units per mg mitochondrial protein [U/mg]. CS is commonly used as a quantitative marker enzyme for the content of mitochondria and ETS, respectively. In the following experiments, mitochondrial respiration and complex raw activities, therefore, are expressed per CS activity to take into account variations in the amount of mitochondrial and non-mitochondrial protein contamination between the samples [26, 27].

Complex I activity. A total of 240µg of isolated mitochondria was solubilized in n-dodecyl β-D-maltoside (20%). NADH-ubiquinone oxidoreductase activity was measured at 30 °C in a buffer containing 2mM Na^+/MOPS, 50mM NaCl, and 2mM KCN, pH 7.2, using 100µM *n*-decylubiquinone (DBQ) and 100µM NADH as substrates and 5µM rotenone as inhibitor [18, 26, 42, 43]. Oxidation rate of NADH were recorded with a Shimadzu Multi-Spec-1501 diode array spectrophotometer ($\varepsilon_{340\text{-}400nm}$ = 6.1$mM^{-1}.cm^{-1}$). Complex I activity was normalized to citrate synthase activity and is given as CI/CS ratio.

Complex III activity. The oxidation of 50µM decylubiquinol obtained by complex III was determined using cytochrome *c* as an electron acceptor as described previously [26, 44]. Briefly, decylubiquinol was prepared by dissolving decylubiquinone (10mM) in ethanol acidified to pH 2. The quinone was reduced with excess solid sodium borohydride. Decylubiquinol was extracted into diethylether:cyclohexane (2:1, v/v) and evaporated to dryness under nitrogen gas, dissolved in ethanol acidified to pH 2. The assay was carried out in a medium containing 35mM KH_2PO_4, 5mM $MgCl_2$, 2mM KCN (pH 7.2), supplemented with 2.5mg/mL BSA, 15µM cytochrome *c*, 0,6mM n-dodecyl β-D-maltoside and 5µg/mL rotenone. The reaction was started with 10µg of mitochondrial protein and the enzyme activity was measured at 550nm. The extinction coefficient used for cytochrome *c* was 18.5$mM^{-1}.cm^{-1}$. Complex III activity was normalized to citrate synthase activity and is given as CIII/CS ratio.

Complex IV activity. Cytochrome *c* oxidase activity was determined in intact isolated mitochondria (100µg) using the Cytochrome *c* Oxidase Assay Kit. The colorimetric assay was based on the observation that a decrease in absorbance at 550nm of ferrocytochrome *c* was caused by its oxidation to ferricytochrome *c* by cytochrome *c* oxidase. The Cytochrome *c*

Oxidase Assay was performed as described previously [26, 43, 45]. Complex IV activity was normalized to citrate synthase activity and is given as CIV/CS ratio.

Mitochondrial respiration in vital cells. Mitochondrial oxygen consumption was measured at 37°C using an Oroboros Oxygraph-2k system. Five millions of cells were added to 2ml of a mitochondrial respiration medium containing 0.5mM EGTA, 3mM $MgCl_2$, 60mM K-lactobionate, 20mM Taurine, 10mM KH_2P0_4, 20mM HEPES, 110mM Sucrose, 1g/l BSA (pH 7.1). To measure state 4 (= state 2) of complex I, 5mM pyruvate and 2mM malate were added and cells were permeabilised with 15µg/ml digitonin. Afterwards, 2mM ADP was added to measure state 3, and in order to increase the respiratory capacity, 10mM glutamate was added. To study the effect of convergent complex I+II electron input on respiration, 10mM of succinate was added [28]. The integrity of mitochondrial membrane was checked through the addition of 10uM cytochrome c. After determining coupled respiration, 0.4µM FCCP (Carbonyl cyanide p-(trifluoro-methoxy) phenyl-hydrazone) was added and respiration was measured in the absence of a proton gradient. In order to inhibit complex I and III activities 0.5uM rotenone and 2.5uM antimycine A, respectively were added. Then, 2mM ascorbate and 0.5mM TMPD were added to have access to complex IV activity. Finally, 100mM sodium azide was added to inhibit the mitochondrial respiration. Mock and APP cells untreated or treated with GBE were measured in parallel pairs using same conditions (crossover design).

Oxygen consumption of isolated mitochondria. The respiratory protocol used for mitochondria was the same than this for whole cells except for the following points: (i) isolated mitochondria (0.5mg) were added to 2ml of a mitochondrial respiration medium containing 65mM sucrose, 10mM potassium phosphate, 10mM Tris-HCl, 10mM $MgSO_4$, and 2mM EDTA (pH 7.0), (ii) digitonin was not added and (iii) 0.05µM of FCCP was sufficient to obtain the maximal mitochondrial respiration [43].

Determination of ATP levels. Cells were plated one day before at a density of 2.5 x 10^4 cells/well in a white 96 well plate. The assay kit is based on the bioluminescent measurement of ATP. The bioluminescent method utilizes the enzyme luciferase, which catalyses the formation of light from ATP and luciferin. The emitted light was linearly related to ATP concentration and was measured using a luminometer [43, 46].

Amount of mitochondria. Cells were plated at a density of 100 000 cells/well in a 48 well plate. The total amount of mitochondria was measured using the cell-permeable mitochondria-selective dye MitoTracker Green^{TM} (400nM, 15min). This probe can accumulate in active mitochondria independently of mitochondrial membrane potential and then react with accessible thiol groups of proteins and peptides [47]. Fluorescence was determined using a Fluoroskan Ascent FL multiplate reader (Labsystems) at 490nm (excitation) / 516nm (emission).

Quantitative real-time PCR for determination of mitochondrial DNA / nuclear DNA ratio. Total DNA was extracted with the Qiagen FlexiGen Kit (Qiagen, Basel, Switzerland) according the manufactors protocol. For standard curves, the peripheral venous blood was taken from a volunteer to extract genomic DNA (the platelet enriched plasma was removed) to amplify genes of interest. After amplification DNA templates were purified with the Qiagen QIAquick PCR Purification Kit (Qiagen, Basel, Switzerland) and the absorption at 260nm was measured to determine the gene copy number and produce serial standard dilutions.

Primers for the RT Q-PCR analysis of mitochondrial DNA (mtDNA)-tRNAleu [48] are mtF3212 (5`CACCAAGAACAGGGTTTGT3`) and mtR3319 (5`TGGCCATGGGTATGTT GTTAA3`) [49], those for nuclear DNA (nDNA), human polymerase γ accessory subunit gene (ASPOLG) are ASPG3F 5`GAGCTGTTGACGGAAAGGAG3` and ASPG4R (5`CAG AAGAGAATCCCGGCTAAG3`) [50]. For each DNA extract, the nDNA and mtDNA gene respectively were quantified separately in triplicates and/or duplicates by real-time quantitative PCR in the presence of SYBR-green with the use of the Applied Biosystems StepOne^{TM} cycler (Applied-Biosystems). PCR reactions contained 1x Power SYBR Green Master Mix (ABI P/N 4367659, Rotkreuz, Switzerland), 1µM of each primer and 1ng of DNA extract. The PCR amplification consisted of a single denaturation-enzyme-activation step of 10min at 95°C, followed by 40 cycles of 15sec denaturation at 95°C and 60sec of annealing / extension at 60°C. Fluorescence was measured at the end of each extension step. A standard curve of corresponding mtDNA and nDNA template equivalents with defined copy numbers were included in each run to quantify the content of mtDNA and nDNA in each sample. Data thus obtained were analyzed by using the cycle threshold (C_T) of each amplification reaction relating it to its respective standard curve. Results from the quantitative PCR were expressed as the ratio of the mean mitochondrial DNA to the mean nuclear DNA content.

Statistical Analysis. Data were presented as mean ± S.E.M. For statistical comparisons, unpaired Student's *t*-test or Two-way ANOVA was used. P values less than 0.05 were considered statistically significant.

ACKNOWLEDGEMENTS

This research was supported by a grant from the SNSF (Swiss National Science Foundation) #310000-108223 to A.E. and an unrestricted research grant from Vifor SA, Switzerland.

REFERENCES

1. Kanowski, S., et al., *Proof of efficacy of the ginkgo biloba special extract EGb 761 in outpatients suffering from mild to moderate primary degenerative dementia of the Alzheimer type or multi-infarct dementia.* Pharmacopsychiatry, 1996. **29**(2): p. 47-56.
2. Le Bars, P.L., et al., *A placebo-controlled, double-blind, randomized trial of an extract of Ginkgo biloba for dementia. North American EGb Study Group.* Jama, 1997. **278**(16): p. 1327-32.
3. Napryeyenko, O. and I. Borzenko, *Ginkgo biloba special extract in dementia with neuropsychiatric features. A randomised, placebo-controlled, double-blind clinical trial.* Arzneimittelforschung, 2007. **57**(1): p. 4-11.
4. Yancheva, S., et al., *Ginkgo biloba extract EGb 761(R), donepezil or both combined in the treatment of Alzheimer's disease with neuropsychiatric features: a randomised, double-blind, exploratory trial.* Aging Ment Health, 2009. **13**(2): p. 183-90.
5. Mix, J.A. and W.D. Crews, Jr., *A double-blind, placebo-controlled, randomized trial of Ginkgo biloba extract EGb 761 in a sample of cognitively intact older adults: neuropsychological findings.* Hum Psychopharmacol, 2002. **17**(6): p. 267-77.
6. Schindowski, K., et al., *Age-related increase of oxidative stress-induced apoptosis in mice prevention by Ginkgo biloba extract (EGb761).* J Neural Transm, 2001. **108**(8-9): p. 969-78.
7. Smith, J.V., et al., *Anti-apoptotic properties of Ginkgo biloba extract EGb 761 in differentiated PC12 cells.* Cell Mol Biol (Noisy-le-grand), 2002. **48**(6): p. 699-707.
8. Leuner, K., et al., *Mitochondrial dysfunction: the first domino in brain aging and Alzheimer's disease?* Antioxid Redox Signal, 2007. **9**(10): p. 1659-75.
9. Abdel-Kader, R., et al., *Stabilization of mitochondrial function by Ginkgo biloba extract (EGb 761).* Pharmacol Res, 2007. **56**(6): p. 493-502.
10. Luo, Y., et al., *Inhibition of amyloid-beta aggregation and caspase-3 activation by the Ginkgo biloba extract EGb761.* Proc Natl Acad Sci U S A, 2002. **99**(19): p. 12197-202.
11. Eckert, A., et al., *Stabilization of Mitochondrial Membrane Potential and Improvement of Neuronal Energy Metabolism by Ginkgo Biloba Extract EGb 761.* Ann N Y Acad Sci., 2005. **1056**: p. 474-85.
12. Eckert, A., et al., *Effects of EGb 761 Ginkgo biloba extract on mitochondrial function and oxidative stress.* Pharmacopsychiatry, 2003. **36 Suppl 1**: p. S15-23.
13. Chagnon, P., et al., *Distribution of brain cytochrome oxidase activity in various neurodegenerative diseases.* Neuroreport., 1995. **6**(5): p. 711-5.
14. Blass, J.P., *Cerebrometabolic abnormalities in Alzheimer's disease.* Neurol Res., 2003. **25**(6): p. 556-66.
15. Kish, S.J., et al., *Brain cytochrome oxidase in Alzheimer's disease.* J Neurochem, 1992. **59**(2): p. 776-9.
16. Valla, J., J.D. Berndt, and F. Gonzalez-Lima, *Energy hypometabolism in posterior cingulate cortex of Alzheimer's patients: superficial laminar cytochrome oxidase associated with disease duration.* J Neurosci, 2001. **21**(13): p. 4923-30.
17. Gibson, G.E., K.F. Sheu, and J.P. Blass, *Abnormalities of mitochondrial enzymes in Alzheimer disease.* J Neural Transm, 1998. **105**(8-9): p. 855-70.
18. Hauptmann, S., et al., *Mitochondrial dysfunction: An early event in Alzheimer pathology accumulates with age in AD transgenic mice.* Neurobiol Aging, 2008.
19. Cardoso, S.M., et al., *Cytochrome c oxidase is decreased in Alzheimer's disease platelets.* Neurobiol Aging, 2004. **25**(1): p. 105-10.

20. Cardoso, S.M., et al., *Mitochondria dysfunction of Alzheimer's disease cybrids enhances Abeta toxicity.* J Neurochem., 2004. **89**(6): p. 1417-26.
21. Fernandez-Vizarra, P., et al., *Intra- and extracellular Abeta and PHF in clinically evaluated cases of Alzheimer's disease.* Histol Histopathol., 2004. **19**(3): p. 823-44.
22. Lustbader, J.W., et al., *ABAD directly links Abeta to mitochondrial toxicity in Alzheimer's disease.* Science., 2004. **304**(5669): p. 448-52.
23. Rhein, V. and A. Eckert, *Effects of Alzheimer's amyloid-beta and tau protein on mitochondrial function - role of glucose metabolism and insulin signalling.* Arch Physiol Biochem, 2007. **113**(3): p. 131-41.
24. Eckert, A., et al., *Oligomeric and fibrillar species of beta-amyloid (A beta 42) both impair mitochondrial function in P301L tau transgenic mice.* J Mol Med, 2008. **86**(11): p. 1255-67.
25. Rhein V, S.X., Wiesner A, Ittner LM, Baysang G, Meier F, Ozmen L, Bluethmann H, Dröse S, Brandt U, Savaskan E, Czech C, Götz J, Eckert A, *Amyloid-beta and tau synergistically impair the oxidative phosphorylation system in triple transgenic Alzheimer's disease mice.* PNAS, in press.
26. Rhein, V., et al., *Amyloid-beta Leads to Impaired Cellular Respiration, Energy Production and Mitochondrial Electron Chain Complex Activities in Human Neuroblastoma Cells.* Cell Mol Neurobiol, 2009.
27. Aleardi, A.M., et al., *Gradual alteration of mitochondrial structure and function by beta-amyloids: importance of membrane viscosity changes, energy deprivation, reactive oxygen species production, and cytochrome c release.* J Bioenerg Biomembr., 2005. **37**(4): p. 207-25.
28. Gnaiger, E., *Capacity of oxidative phosphorylation in human skeletal muscle New perspectives of mitochondrial physiology.* Int J Biochem Cell Biol, 2009.
29. Janssens, D., et al., *Protection of hypoxia-induced ATP decrease in endothelial cells by ginkgo biloba extract and bilobalide.* Biochem Pharmacol, 1995. **50**(7): p. 991-9.
30. Trumbeckaite, S., et al., *Effect of Ginkgo biloba extract on the rat heart mitochondrial function.* J Ethnopharmacol, 2007. **111**(3): p. 512-6.
31. Doussiere, J., et al., *Control of oxidative phosphorylation in rat heart mitochondria. The role of the adenine nucleotide carrier.* Biochim Biophys Acta, 1984. **766**(2): p. 492-500.
32. Davey, G.P., S. Peuchen, and J.B. Clark, *Energy thresholds in brain mitochondria. Potential involvement in neurodegeneration.* J Biol Chem., 1998. **273**(21): p. 12753-7.
33. Janssens, D., et al., *Protection of mitochondrial respiration activity by bilobalide.* Biochem Pharmacol, 1999. **58**(1): p. 109-19.
34. Cleeter, M.W., et al., *Reversible inhibition of cytochrome c oxidase, the terminal enzyme of the mitochondrial respiratory chain, by nitric oxide. Implications for neurodegenerative diseases.* FEBS Lett, 1994. **345**(1): p. 50-4.
35. Tendi, E.A., et al., *Ginkgo biloba extracts EGb 761 and bilobalide increase NADH dehydrogenase mRNA level and mitochondrial respiratory control ratio in PC12 cells.* Neurochem Res, 2002. **27**(4): p. 319-23.
36. Bastianetto, S., et al., *The Ginkgo biloba extract (EGb 761) protects hippocampal neurons against cell death induced by beta-amyloid.* Eur J Neurosci, 2000. **12**(6): p. 1882-90.
37. Yao, Z., K. Drieu, and V. Papadopoulos, *The Ginkgo biloba extract EGb 761 rescues the PC12 neuronal cells from beta-amyloid-induced cell death by inhibiting the formation of beta-amyloid-derived diffusible neurotoxic ligands.* Brain Res, 2001. **889**(1-2): p. 181-90.

38. Colciaghi, F., et al., *Amyloid precursor protein metabolism is regulated toward alpha-secretase pathway by Ginkgo biloba extracts.* Neurobiol Dis, 2004. **16**(2): p. 454-60.
39. Tchantchou, F., et al., *EGb 761 enhances adult hippocampal neurogenesis and phosphorylation of CREB in transgenic mouse model of Alzheimer's disease.* Faseb J, 2007. **21**(10): p. 2400-8.
40. Scheuermann, S., et al., *Homodimerization of amyloid precursor protein and its implication in the amyloidogenic pathway of Alzheimer's disease.* J Biol Chem, 2001. **276**(36): p. 33923-9.
41. Lowry, O.H., et al., *Protein measurement with the Folin phenol reagent.* J Biol Chem, 1951. **193**(1): p. 265-75.
42. Djafarzadeh, R., et al., *Biophysical and structural characterization of proton-translocating NADH-dehydrogenase (complex I) from the strictly aerobic yeast Yarrowia lipolytica.* Biochim Biophys Acta, 2000. **1459**(1): p. 230-8.
43. David, D.C., et al., *Proteomic and functional analyses reveal a mitochondrial dysfunction in P301L tau transgenic mice.* J Biol Chem., 2005. **280**(25): p. 23802-14. Epub 2005 Apr 14.
44. Krahenbuhl, S., et al., *Decreased activities of ubiquinol:ferricytochrome c oxidoreductase (complex III) and ferrocytochrome c:oxygen oxidoreductase (complex IV) in liver mitochondria from rats with hydroxycobalamin[c-lactam]-induced methylmalonic aciduria.* J Biol Chem, 1991. **266**(31): p. 20998-1003.
45. Rasmussen, U.F. and H.N. Rasmussen, *Human quadriceps muscle mitochondria: a functional characterization.* Mol Cell Biochem, 2000. **208**(1-2): p. 37-44.
46. Keil, U., et al., *Amyloid beta-induced changes in nitric oxide production and mitochondrial activity lead to apoptosis.* J Biol Chem, 2004. **279**(48): p. 50310-20.
47. Pendergrass, W., N. Wolf, and M. Poot, *Efficacy of MitoTracker Green and CMXrosamine to measure changes in mitochondrial membrane potentials in living cells and tissues.* Cytometry A, 2004. **61**(2): p. 162-9.
48. Bai, R.K. and L.J. Wong, *Simultaneous detection and quantification of mitochondrial DNA deletion(s), depletion, and over-replication in patients with mitochondrial disease.* J Mol Diagn, 2005. **7**(5): p. 613-22.
49. Bai, R.K., et al., *Quantitative PCR analysis of mitochondrial DNA content in patients with mitochondrial disease.* Ann N Y Acad Sci, 2004. **1011**: p. 304-9.
50. Cote, H.C., et al., *Changes in mitochondrial DNA as a marker of nucleoside toxicity in HIV-infected patients.* N Engl J Med, 2002. **346**(11): p. 811-20.

5. Conclusion

Reduced energy metabolism together with mitochondrial failure and oxidative stress has been recognized as prominent and early events in AD. However, the pathogenic mechanisms underlying these defects are far to be resolved. The aim of the present thesis was to gain new insights into the contribution of the two unquestionable AD-related proteins, Aβ and tau, on one hand, and the mode of action of GBE on the other hand, toward mitochondrial modulation.

Combining transgenesis[3-5], quantitative proteomics and functional assays, our findings support first of all that Aβ and tau acting synergistically heighten mitochondrial respiration deficits. Thereby, hyperphosphorylated tau may drive a vicious cycle within the Aβ cascade. We found also that age-related oxidative stress may exaggerate the dysfunctional energy homeostasis and in turn, take part in the vicious cycle finally leading to cell death (Figure 11). Our results are in line with recent studies associating Aβ and tau with oxidative stress[6-9] as well as axonal traffic inhibition, synapse starvation and neurodegeneration[7, 10]. A crucial role for mitochondria in AD is further underpinned by findings linking maternal inheritance of mtDNA to both AD predisposition and glucose hypometabolism[11] that may reflect energy disturbances as found, e.g., in our $^{\text{triple}}$AD model.

In line with the recent “intracellular hypothesis”[12-15], soluble oligomers appear to interfere with hippocampal synaptic function and memory[16]. Interestingly, in this new paradigm, mitochondria sound as key features in the pathological mechanisms leading to synaptic failure and cell loss. Our group reported a direct impact of Aβ oligomeric on $\Delta\psi$ and ATP levels in APP transgenic mice model[17]. We also showed first evidence for an increased vulnerability of P301L tau mitochondria towards oligomers Aβ insult *in vitro*[18]. These findings were confirmed in our $^{\text{triple}}$AD study demonstrating an interplay between Aβ and tau at the mitochondrial level *in vivo*. In the second part of the thesis, we ripened our understanding of the specific actions of soluble Aβ on mitochondrial respiration. For this approach, a novel high-resolution respiratory protocol was established and an APP cell model mimicing relevant conditions of AD patients by secreting Aβ within a picomolar range was used. We observed that Aβ oligomers caused serious impairments of the total cellular respiration with main impacts on complexes III, IV and V.

The crucial role of mitochondrial dysfunction in the biochemical pathways by which Aβ can lead to neuronal dysfunction in AD[17, 18] is particularly challenging in order to establish therapeutic treatments. To test this idea we investigated the potential effect of a natural antioxidant, GBE, on Aβ-induced mitochondrial deficits. Although the precise molecular mechanisms inside cells as well as on mitochondria stay unknown yet, the findings of the thesis and the findings of others[19-23] indicate substantial mitochondria modulating properties of GBE. We could clearly show that GBE improved OXPHOS performance and was able to restore Aβ-induced mitochondria failure. Hereby, the increase in mitochondrial content might represent an important early event. Thus, we observed an up-regulation of mtDNA in cells treated with GBE, but at the same time, a decrease of mitochondria mass in GBE-treated cells suggesting that GBE may act not only at a functional level but also at a genetic one[24-26]. Although further studies are necessary, we can speculate that a GBE treatment may not only enhance mtDNA but may modulate mitochondria biogenesis after chronic exposure. Taking into account the increasing interest in mitochondrial stabilization as intervention strategy in AD, the regulating mechanisms of GBE on mitochondria function suggested by this study qualifies this drug as a therapeutic candidate.

In total, our results strengthen the key role of mitochondria in the pathogenesis of AD demonstrating close relationship with the two indisputable hallmarks of the disease acting independently as well as synergistically on the vital organelle. Consequently, besides the treatment and/or removal of both Aβ and tau pathology, strategies involving efforts to protect cells at the mitochondrial level by stabilizing or restoring mitochondrial function or to interfere with the energy metabolism appear to be promising in order to prevent AD. Moreover, the better understanding of the biochemical pathways by which mitochondria-protecting substances such as GBE act may not only optimize our therapeutic options but also clarify the role of mitochondria in the pathogenesis of AD (Figure 11). Our age-related Aβ and tau transgenic mouse model ($^{\text{triple}}$AD) may be very valuable in order to monitor therapeutic interventions at the mitochondrial level and the impact to prevent the progression of Aβ deposits and tau hyperphosphorylation at early stages of the disease.

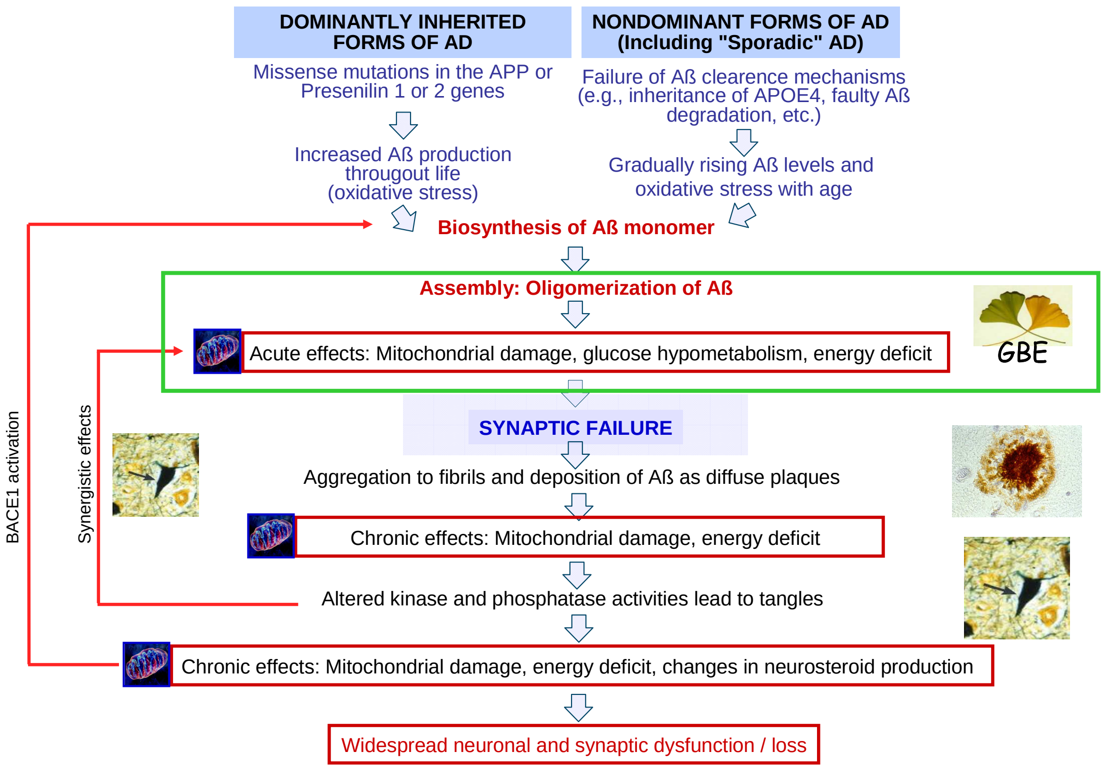
DOMINANTLY INHERITED FORMS OF AD
NONDOMINANT FORMS OF AD (Including "Sporadic" AD)
Missense mutations in the APP or Presenilin 1 or 2 genes
Failure of Aß clearence mechanisms (e.g., inheritance of APOE4, faulty Aß degradation, etc.)
Increased Aß production througout life (oxidative stress)
Gradually rising Aß levels and oxidative stress with age
Biosynthesis of Aß monomer
Assembly: Oligomerization of Aß
Acute effects: Mitochondrial damage, glucose hypometabolism, energy deficit
GBE
SYNAPTIC FAILURE
Aggregation to fibrils and deposition of Aß as diffuse plaques
Chronic effects: Mitochondrial damage, energy deficit
Altered kinase and phosphatase activities lead to tangles
Chronic effects: Mitochondrial damage, energy deficit, changes in neurosteroid production
Widespread neuronal and synaptic dysfunction / loss
BACE1 activation
Synergistic effects

Figure 12. A hypothetical sequence of the pathogenic steps linking amyloid-beta peptide (Aβ) and tau pathologies with mitochondrial dysfunction as well as early use of *Ginkgo biloba* extract (GBE). Aβ and tau may act synergistically on mitochondria inducing strong failure in mitochondrial respiration und function thereby triggering a vicious cycle. In addition, defects in energy metabolism may increase BACE1 activity[1] which, in turn, increases the production of Aβ. Thus, a comprehensive vision of the neuropathophysiologic mechanisms that result in AD reveals several vicious cycles within a larger vicious cycle. All of them, once set in motion, amplify their own processes, thus accelerating the development of AD. GBE used at early stage of the disease could be promising for AD prevention and treatment (adapted from *Rhein and Eckert*, 2007[2]).

References

1. Velliquette, R.A., T. O'Connor, and R. Vassar, *Energy inhibition elevates beta-secretase levels and activity and is potentially amyloidogenic in APP transgenic mice: possible early events in Alzheimer's disease pathogenesis.* J Neurosci., 2005. **25**(47): p. 10874-83.
2. Rhein, V. and A. Eckert, *Effects of Alzheimer's amyloid-beta and tau protein on mitochondrial function -- role of glucose metabolism and insulin signalling.* Arch Physiol Biochem, 2007. **113**(3): p. 131-41.
3. Gotz, J., et al., *Tau filament formation in transgenic mice expressing P301L tau.* J Biol Chem, 2001. **276**(1): p. 529-34.
4. Richards, J.G., et al., *PS2APP transgenic mice, coexpressing hPS2mut and hAPPswe, show age-related cognitive deficits associated with discrete brain amyloid deposition and inflammation.* J Neurosci, 2003. **23**(26): p. 8989-9003.
5. Grueninger F, B.B., Czech C, Ballard TM, Frey JR, Weidensteiner C, von Kienlin M, Ozmen L, *Phosphorylation of Tau at S422 is enhanced by Abeta in TauPS2APP triple transgenic mice.* in press, 2009.
6. Melov, S., et al., *Mitochondrial oxidative stress causes hyperphosphorylation of tau.* PLoS ONE, 2007. **2**(6): p. e536.
7. Mandelkow, E.M., et al., *Clogging of axons by tau, inhibition of axonal traffic and starvation of synapses.* Neurobiol Aging, 2003. **24**(8): p. 1079-85.
8. Moreira, P.I., et al., *Alzheimer disease and the role of free radicals in the pathogenesis of the disease.* CNS Neurol Disord Drug Targets, 2008. **7**(1): p. 3-10.
9. Su, B., et al., *Oxidative stress signaling in Alzheimer's disease.* Curr Alzheimer Res, 2008. **5**(6): p. 525-32.
10. Ittner, L.M., et al., *Parkinsonism and impaired axonal transport in a mouse model of frontotemporal dementia.* Proc Natl Acad Sci U S A, 2008. **105**(41): p. 15997-6002.
11. Mosconi, L., et al., *Maternal family history of Alzheimer's disease predisposes to reduced brain glucose metabolism.* Proc Natl Acad Sci U S A, 2007. **104**(48): p. 19067-72.
12. Hartley, D.M., et al., *Protofibrillar intermediates of amyloid beta-protein induce acute electrophysiological changes and progressive neurotoxicity in cortical neurons.* J Neurosci, 1999. **19**(20): p. 8876-84.
13. Necula, M., et al., *Small molecule inhibitors of aggregation indicate that amyloid beta oligomerization and fibrillization pathways are independent and distinct.* J Biol Chem, 2007. **282**(14): p. 10311-24.
14. Fernandez-Vizarra, P., et al., *Intra- and extracellular Abeta and PHF in clinically evaluated cases of Alzheimer's disease.* Histol Histopathol, 2004. **19**(3): p. 823-44.
15. Lustbader, J.W., et al., *ABAD directly links Abeta to mitochondrial toxicity in Alzheimer's disease.* Science, 2004. **304**(5669): p. 448-52.
16. Selkoe, D.J., *Alzheimer's disease is a synaptic failure.* Science, 2002. **298**(5594): p. 789-91.
17. Eckert, A., et al., *Soluble beta-amyloid leads to mitochondrial defects in amyloid precursor protein and tau transgenic mice.* Neurodegener Dis, 2008. **5**(3-4): p. 157-9.
18. Eckert, A., et al., *Oligomeric and fibrillar species of beta-amyloid (A beta 42) both impair mitochondrial function in P301L tau transgenic mice.* J Mol Med, 2008. **86**(11): p. 1255-67.
19. Abdel-Kader, R., et al., *Stabilization of mitochondrial function by Ginkgo biloba extract (EGb 761).* Pharmacol Res, 2007. **56**(6): p. 493-502.

20. Leuner, K., et al., *Mitochondrial dysfunction: the first domino in brain aging and Alzheimer's disease?* Antioxid Redox Signal, 2007. **9**(10): p. 1659-75.
21. Luo, Y., et al., *Inhibition of amyloid-beta aggregation and caspase-3 activation by the Ginkgo biloba extract EGb761.* Proc Natl Acad Sci U S A, 2002. **99**(19): p. 12197-202.
22. Tendi, E.A., et al., *Ginkgo biloba extracts EGb 761 and bilobalide increase NADH dehydrogenase mRNA level and mitochondrial respiratory control ratio in PC12 cells.* Neurochem Res, 2002. **27**(4): p. 319-23.
23. Chen, F., et al., *Role for glyoxalase I in Alzheimer's disease.* Proc Natl Acad Sci U S A, 2004. **101**(20): p. 7687-92.
24. Hoerndli, F.J., et al., *Reference genes identified in SH-SY5Y cells using custom-made gene arrays with validation by quantitative polymerase chain reaction.* Anal Biochem, 2004. **335**(1): p. 30-41.
25. David, D., F. Hoerndli, and J. Gotz, *Functional Genomics meets neurodegenerative disorders Part I: Transcriptomic and proteomic technology.* Prog Neurobiol, 2005. **76**(3): p. 153-68.
26. Hoerndli, F., D. David, and J. Gotz, *Functional genomics meets neurodegenerative disorders. Part II: Application and data integration.* Prog Neurobiol, 2005. **76**(3): p. 169-88.

Abbreviations

Aβ	Amyloid-beta peptide
ABAD	Aβ binding protein alcohol dehydrogenase
AD	Alzheimer’s disease
ADAM	A disintegrin and metalloproteinase
A2M	Alpha-2-macroglobulin
AICD	Aβ intracellular cytoplasmic domain
AIF	Apoptosis-inducing factor
APH1	Anterior pharynx-defective 1
APOE	Apolipoprotein E
APP	Amyloid precursor protein
CAA	Cerebral amyloid angiopathy
CaMKII	Calcium-calmodulin dependent protein kinase II
CAT	Catalase
cdk5	Cyclin-dependent kinase 5
C83	83-amino-acid Ct APP fragment
C99	99-amino-acid Ct APP fragment
COX	Cytochrome c oxidase
Ct	Carboxy-terminal
Cu/Zn SOD	Copper/zinc superoxide dismutase
$\Delta\psi$	Mitochondrial membrane potential
ERK2	Extracellular signal-regulated kinase 2
ETC	Electron transport chain
FAD	Familial Alzheimer’s disease form
$FADH_2$	Flavin adenine dinucleotide
4R	Four microtubule binding repeats
FTDP-17	Fronto-temporal dementia with Parkinsonism linked to chromosome 17
GAB2	Growth factor receptor-bound protein associated binding-protein 2
GBE	Ginkgo biloba extract
GPX	Glutathione peroxidase
GSH	Glutathione
GSK-3β	Glycogen synthase kinase-3β
H_2O_2	Hydrogen peroxide

HNE	4-hydroxynonenal
IDE	Insulin-degrading enzyme
IMM	Inner mitochondrial membrane
IMS	Intermembrane space
iTRAQ	Isobaric tags for relative and absolute quantitation
LRP	Low-density lipid receptor-related protein
LTP	Long-term potentiation
MAOA	Monoamine oxidase A
MAOB	Monoamine oxidase B
MAP1	Microtubule-associated protein 1
MAP2	Microtubule-associated protein 2
MARK	Mitogen-associated protein affinity-regulating kinases
MCI	Mild cognitive impairment
MDA	Malondialdehyde
MMP	Mitochondrial membrane permeabilization
MnSOD	Manganese superoxide dismutase
mtDNA	Mitochondrial DNA
mtNOS	Mitochondrial nitric oxide synthase
NADH	Nicotine adenine dinucleotide
nDNA	Nuclear DNA
NFTs	Neurofibrillay tangles
NMDA	N-methyl-D-aspartate
$NO^{\cdot}$	Nitric oxide
NOS	Nitric oxide synthase
Nt	Amino-terminal
$O_2^{-\cdot}$	Superoxide anion
$OH^{\cdot}$	Hydroxyl radical
OMM	Outer mitochondrial membrane
$ONOO^{-}$	Peroxynitrite
OXPHOS	Oxidative phosphorylation system
PAF	Platelet activating factor
PDGF	Platelet-derived growth factor
PEN-2	Presenilin enhancer 2
PET	Positron emission tomography

PHFs	Paired helical filaments
pR5	P301L mutant tau transgenic pR5 mice
PSEN1	Presenelin 1
PSEN2	Presenelin 2
RNS	Reactive nitrogen species
ROS	Reactive oxygen species
SAD	Sporadic Alzheimer’s disease form
TCA	Tricarboxylic acid cycle
TM	Transmembrane
3R	Three microtubule binding repeats
TOM	Translocator outer membrane
^{triple}AD	mutated Tau (P301L), PS2 (N141l) and APP^{Swe} (KM670/671NL) triple transgenic mouse model
UCPs	Uncoupling proteins
VDAC	Voltage-dependant anion channels
VLDL-R	Very low-density lipoprotein receptor

CURRICULUM VITAE

Personal Data

Name	Virginie Françoise RHEIN
Place and date of birth	Strasbourg, February 1st, 1981
Citizenship	French
e-mail	virginie.rhein@upkbs.ch

Education

2005-present	**PhD student** in the group of Prof. Anne Eckert, Neurobiology Laboratory for Brain Aging and Mental Health, Associated Research Group, Dept. Biomedecine Psychiatric University Clinic, University of Basel, Switzerland
2005	**Master's degree II in Neuroscience** Diploma thesis in the laboratory "Psychopathology and pharmacology of cognition" INSERM 666 under the supervision of Dr. Anne Giersch (Title: Physiopathology of Schizophrenia: relationship between attentional, visual and memory troubles). University Louis Pasteur, Strasbourg, France
2004	**Master's degree I in Neuroscience** Training in the laboratory "Psychopathology and pharmacology of cognition" INSERM 666 under the supervision of Dr. Didier Pinault (Title: Morpho-functional study of Zona Incerta neurons in adult rats). University Louis Pasteur, Strasbourg, France

2003	**Bachelor’s degree in Cell biology and Physiology** Training in the laboratory “Steroïds and Nociceptive System”, CNRS / ULP 7519 under the supervision of Pr. Guy Mensah-Nyagan (Title: Detection of the P450scc cytochrom’s activity by the techniques of Pulse-chase and HPLC in the spinal chord of rats), University Louis Pasteur, Strasbourg, France
1999	**High School Diploma:** Graduation in Sciences Strasbourg, France

PUBLICATIONS

1- Original Papers (Peer Reviewed)

Giersch A, **Rhein V**. Lack of flexibility in visual grouping in patients with schizophrenia. J Abnorm Psychol 117(1):132-42 (2008).

Eckert A, Hauptmann S, Scherping I, **Rhein V**, Mueller-Spahn F, Goetz J, Mueller W.E. Soluble amyloid-beta leads to mitochondrial defects in APP and Tau transgenic mice. Neurodegener Dis 5(3-4):157-9 (2008).

Eckert A, Hauptmann S, Scherping I, **Rhein V**, Droese S, Brandt U, Mueller W.E, Goetz J. Oligomeric and fibrillar species of β-amyloid (Aβ42) both impair mitochondrial function in P301L tau transgenic mice. J Mol Med 86(11):1255-67 (2008).

Rhein V, Baysang G, Rao S, Meier F, Bonert A, Müller-Spahn F, A. Eckert. Amyloid-beta leads to impaired cellular respiration, energy production and mitochondrial electron chain complex activities in human neuroblastoma cells. Cell Mol Neurobiol 29 (6):1063-1071 (2009).

Under revision

Rhein V, Song X, Wiesner A, Ittner LM, Baysang G, Meier F, Ozmen L, Bluethmann H, Dröse S, Brandt U, Savaskan E, Muller-Spahn, Czech C, Götz J, Eckert A. Amyloid-beta and tau synergistically impair the oxidative phosphorylation system in triple transgenic Alzheimer's disease mice *(Proceedings of the National Academy of Sciences of the United States of America).*

Submitted

Rhein V, Baysang G, Rao S, Meier F, Tripodi T, Giese M, Schulz K, Müller-Spahn F, Eckert A. Ginkgo biloba extract ameliorates oxidative phosphorylation performance and rescues Aβ-induced failure.

Kulic L, Wollmer MA, **Rhein V**, Pagani L, Kuehnle K, Cattepoel S, Tracy J, Götz J, Eckert A & Nitsch RM. Combined expression of tau and the Harlequin mouse mutation leads to increased mitochondrial dysfunction, tau pathology and neurodegeneration.

Schulz K L, **Rhein V**, Mai S, Haase W, Reichert A S., Eckert A, Jendrach M, Müller W E, Leuner K. A Novel Mechanism of Mitochondrial Impairment in Tauopathies.

Lim YA, **Rhein V**, Baysang G, Meier F, Plojak A, Raftery M, Ittner L, Guilhaus M, Eckert A, Gotz J. Aβ and human amylin share a common toxicity pathway via mitochondrial dysfunction.

2- Reviews (Peer Reviewed)

Rhein V, Eckert A. Effects of Alzheimer's amyloid-beta and tau protein on mitochondrial function – Role of glucose metabolism and insulin signalling. Arch Physiol Biochem 113(3):131-41 (2007).

3- Abstracts

Giersch A, & **Rhein V**. *Relationship between top-down control, binding processes, and memory in patients with schizophrenia*. XXth international congress on schizophrenia research, Schizophrenia Bulletin, 31, pp356, Savannah, Georgia, USA, April 2-6, 2005.

Rhein V, Baysang G, Meier F, Ozmen L, Savaskan E, Müller-Spahn F, Czech C, Götz J and Eckert A. *Mitochondrial failure in the pathogenesis of Alzheimer's disease.* Joint Meeting Swiss Society for Neuroscience NCCR « Neural Plasticity and Repair » Swiss Multiple Sclerosis Society, Poster n°J11, Session: Disorders of the nervous systems: Basic mechanisms (p44), Bern, Switzerland, March 9-10, 2007.

Rhein V, Baysang G, Meier M, Ozmen L, Bluethmann H, Savaskan E, Müller-Spahn F, Czech C, Götz J and Eckert A. *A Triple transgenic mice model of Alzheimer's disease with plaques and tangles.* 27th Annual Meeting of the Swiss Society of Biological Psychiatry "Sleep in Psychiatry-State of the Art", Basel, Switzerland, March 15, 2007.

Rhein V, Baysang G, Meier M, Ozmen L, Bluethmann H, Savaskan E, Müller-Spahn F, Czech C, Götz J and Eckert A. *Effects of Alzheimer's amyloid-beta and tau proteins on mitochondrial dysfunction in the brain of transgenic mice.* 8th International Conference Alzheimer's and Parkinson's Diseases, Neurodegenerative Dis 2007; 4 (suppl 1):1-350 Abstract n°455 (p153) Poster n°116, Salzburg, Austria, March 14-18, 2007.

Rhein V, Baysang G, Meier M, Ozmen L, Bluethmann H, Savaskan E, Müller-Spahn F, Czech C, Götz J and Eckert A. *A Triple transgenic mice model of Alzheimer's disease with plaques and tangles.* Neurex / BCCN Annual Meeting, Freiburg, Germany, June 22-23, 2007.

Rhein V, Baysang G, Meier M, Ozmen L, Bluethmann H, Savaskan E, Müller-Spahn F, Czech C, Götz J and Eckert A. *Changes in mitochondrial respiration in brain cells of transgenic mice models of Alzheimer's disease.* 1st MIPsummer School on Mitochondrial Respiratory Physiology, Schröcken, Austria, 12-18 July, 2007.

Rhein V, Baysang G, Meier M, Ozmen L, Savaskan E, Müller-Spahn F, Czech C, Götz J and Eckert. *Mitochondrial failure in a transgenic mice model of Alzheimer's disease with plaques and tangles.* 25th Symposium der AGNP, Pharmacopsychiatry 40:234, 2007. München, Germany, October 3-6, 2007.

Rhein V, Baysang G, Meier M, Ozmen L, Bluethmann H, Savaskan E, Müller-Spahn F, Czech C, Götz J and Eckert A. *Mitochondrial failure in a transgenic mice model of Alzheimer's disease with plaques and tangles.* Society for Neuroscience, Annual Meeting, Poster n° 688.14, San Diego, USA, November 3-7, 2007.

Rhein V, Baysang G, Meier M, Ozmen L, Bluethmann H, Savaskan E, Müller-Spahn F, Czech C, Götz J and Eckert A. *Mitochondrial dysfunction as an emerging preclinical concept of Alzheimer's disease*. ECNP Workshop on Neuropsychopharmacology for Young Scientists in Europe, Abstract S92-P4.09, Nice, France, 6-9 March, 2008.

Rhein V, Baysang G, Meier M, Ozmen L, Bluethmann H, Savaskan E, Müller-Spahn F, Czech C, Götz J and Eckert A. *Transgenic mouse models of Alzheimer's disease: from proteomics to functional assays of mitochondria.* Swiss Society of Neuropathology, XXIInd International Winter Meeting "Growth and Death in the Nervous system", St-Moritz, Switzerland, March 27-30, 2008.

Rhein V, Baysang G, Meier M, Ozmen L, Bluethmann H, Savaskan E, Müller-Spahn F, Czech C, Götz J and Eckert A. *Altered mitochondrial respiration and energy metabolism in brain cells from transgenic Alzheimer's disease mice.* Ebec, 15th European Bioenergetics Conference, Biochemica and Biophysica Acta (BBA)-Bioenergetics, Volume 1777 (Suppl 1):S85-S86, Dublin, Ireland, July 19-24, 2008.

Rhein V, Baysang G, Meier M, Ozmen L, Bluethmann H, Savaskan E, Müller-Spahn F, Czech C, Götz J and Eckert A. *Mitochondrial failure in a transgenic mice model of Alzheimer's disease with plaques and tangles.* International Conference on Alzheimer's disease, Abstract P2-140, Chicago, USA, 26-31 July, 2008.

Rhein V, Baysang G, Meier M, Ozmen L, Bluethmann H, Savaskan E, Müller-Spahn F, Czech C, Götz J and Eckert A. *Transgenic mouse models of Alzheimer's disease: From proteomics to functional assays of mitochondria*. Joint Meeting of the SGN / SGPP / SGBP "La neurologie et la psychiatrie au fil du temps" (poster n°80) Basel, Switzerland, October 30 – November 1, 2008.

Rhein V, Rao S, Baysang G, Meier F, Tripodi T, Eckert A. *Protective effects of Ginkgo biloba extract on mitochondrial abnormalities in APP overexpressing human neuroblastoma cells.* 9th International Conference – AD/PD, p358, Prague, Czech Republic, March 11-15, 2009.

Rhein V, Baysang G, Meier M, Ozmen L, Bluethmann H, Savaskan E, Müller-Spahn F, Czech C, Götz J and Eckert A. *Transgenic mouse models of Alzheimer's disease: From proteomics to functional assays of mitochondria.* 9th International Conference – AD/PD, p352, Prague, Czech Republic, March 11-15, 2009.

Travel Fellowships / Honors

Travel grant from *Reisefonds für den Akademischen Nachwuchs der Universität Basel* in order to attend the Annual Meeting of the Society for Neuroscience, from 03.11.2007 to 07.11.2007 in San Diego, USA.

Selection by the ecnp Committee for the ecnp Workshop on Neuropsychopharmacology for young Scientists in Europe from 6 to 9 March 2008 in Nice, FRANCE.

Travel Fellowship from the *Alzheimer's Association-ICAD* for the International Conference on Alzheimer's Disease Annual Meeting, from the 26 to the 31 July 2008 in Chicago, USA.

Selection by the ecnp Committee to become an associate membership of the European College of Neuropsychopharmacology (ECNP) for a period of 4 years.

Invited oral presentations

ECNP, Workshop on Neuropsychopharmacology for Young Scientists in Europe, March 6-9, 2008, Nice, France. Junior speakers, Session: *Dementia: towards new drug targets*. *Mitochondrial dysfunction as an emerging preclinical concept of Alzheimer's disease*.

Swiss Society of Neuropathology, XXIInd International Winter Meeting *Growth and Death in the Nervous system*, March 27-30, 2008, St-Moritz, Switzerland. *Transgenic mouse models of Alzheimer's disease: from proteomics to functional assays of mitochondria***.**

Ebec, 15th European Bioenergetics Conference, July 19-24, Dublin, Ireland.
Selected for a talk, Symposium on "*Mitochondria and Disease*" among 13 postgraduate students out of over 150. *Altered mitochondrial respiration and energy metabolism in brain cells from transgenic Alzheimer's disease mice.*